Alzheimer's & Dementia 15 (2019) 106-152

Review Article

Understanding disease progression and improving Alzheimer's disease clinical trials: Recent highlights from the Alzheimer's Disease Neuroimaging Initiative

Dallas P. Veitch[a,b], Michael W. Weiner[a,c,d,e,f,*], Paul S. Aisen[g], Laurel A. Beckett[h], Nigel J. Cairns[i,j], Robert C. Green[k], Danielle Harvey[h], Clifford R. Jack, Jr.[l], William Jagust[m], John C. Morris[i], Ronald C. Petersen[n], Andrew J. Saykin[o,p], Leslie M. Shaw[q], Arthur W. Toga[r], John Q. Trojanowski[q,s,t,u], Alzheimer's Disease Neuroimaging Initiative

[a]*Department of Veterans Affairs Medical Center, Center for Imaging of Neurodegenerative Diseases, San Francisco, CA, USA*
[b]*Northern California Institute for Research and Education (NCIRE), Department of Veterans Affairs Medical Center, San Francisco, CA, USA*
[c]*Department of Radiology, University of California, San Francisco, CA, USA*
[d]*Department of Medicine, University of California, San Francisco, CA, USA*
[e]*Department of Psychiatry, University of California, San Francisco, CA, USA*
[f]*Department of Neurology, University of California, San Francisco, CA, USA*
[g]*Alzheimer's Therapeutic Research Institute, University of Southern California, San Diego, CA, USA*
[h]*Division of Biostatistics, Department of Public Health Sciences, University of California, Davis, CA, USA*
[i]*Knight Alzheimer's Disease Research Center, Washington University School of Medicine, Saint Louis, MO, USA*
[j]*Department of Neurology, Washington University School of Medicine, Saint Louis, MO, USA*
[k]*Division of Genetics, Department of Medicine, Brigham and Women's Hospital and Harvard Medical School, Boston, MA, USA*
[l]*Department of Radiology, Mayo Clinic, Rochester, MN, USA*
[m]*Helen Wills Neuroscience Institute, University of California Berkeley, Berkeley, CA, USA*
[n]*Department of Neurology, Mayo Clinic, Rochester, MN, USA*
[o]*Department of Radiology and Imaging Sciences, Indiana University School of Medicine, Indianapolis, IN, USA*
[p]*Department of Medical and Molecular Genetics, Indiana University School of Medicine, Indianapolis, IN, USA*
[q]*Department of Pathology and Laboratory Medicine, Perelman School of Medicine, University of Pennsylvania, Philadelphia, PA, USA*
[r]*Laboratory of Neuroimaging, Institute of Neuroimaging and Informatics, Keck School of Medicine, University of Southern California, Los Angeles, CA, USA*
[s]*Institute on Aging, Perelman School of Medicine, University of Pennsylvania, Philadelphia, PA, USA*
[t]*Alzheimer's Disease Core Center, Perelman School of Medicine, University of Pennsylvania, Philadelphia, PA, USA*
[u]*Udall Parkinson's Research Center, Perelman School of Medicine, University of Pennsylvania, Philadelphia, PA, USA*

Dr. Aisen has no conflicts of interest to declare. Dr. Beckett has no conflicts of interest to declare. Dr. Cairns has no conflicts of interest to declare. Dr. Green receives compensation for consultation from AIA, Helix, Ohana, Prudential, and Veritas and is a cofounder, advisor, and equity holder in Genome Medical, Inc. Dr. Harvey has no conflicts of interest to declare. Dr. Jack has no conflicts of interest to declare. Dr. Jagust serves as a consultant to BioClinica, Novartis, and Genentech. Dr. Saykin received flortaucipir precursor from Avid Radiopharmaceuticals, collaborative research support from Eli Lilly and support from Springer-Nature as an editor-in-chief of *Brain Imaging and Behavior*. Dr. Shaw provides quality control oversight for the Roche Electrosys immunoassay platform as part of the ADNI-3 study. Dr. Toga has no conflicts of interest to declare. Dr. Trojanowski has no conflicts of interest to declare. Dr. Veitch has no conflicts of interest to declare. Dr. Weiner has served on the Scientific Advisory Boards for Alzheon, Inc., Accera, Merck, Nestle (Nolan), PCORI (PPRN), Eli Lilly, Delfino Logic Ltd. (for Merck), Dolby Ventures, Brain Health Registry, and ADNI. He served on the editorial boards for Alzheimer's & Dementia and MRI. He has provided consulting and/or acted as a speaker/lecturer to Synarc, Pfizer, Accera, Inc., Alzheimer's Drug Discovery Foundation (ADDF), Merck, BioClinica, Eli Lilly, Howard University, Guidepoint, Denali Therapeutics, Nestle/Nestec, GLG Research, Atheneum Partners, BIONEST Partners, American Academy of Neurology (AAN), and Society for Nuclear Medicine and Molecular Imaging (SNMMI). He holds stock options with Alzheon, Inc.

*Corresponding author. Tel.: 415-221-4810 x 3642; Fax: 415-668-2864.
E-mail address: michael.weiner@ucsf.edu

https://doi.org/10.1016/j.jalz.2018.08.005

Abstract

Introduction: The overall goal of the Alzheimer's Disease Neuroimaging Initiative (ADNI) is to validate biomarkers for Alzheimer's disease (AD) clinical trials. ADNI is a multisite, longitudinal, observational study that has collected many biomarkers since 2004. Recent publications highlight the multifactorial nature of late-onset AD. We discuss selected topics that provide insights into AD progression and outline how this knowledge may improve clinical trials.

Methods: We used standard methods to identify nearly 600 publications using ADNI data from 2016 and 2017 (listed in Supplementary Material and searchable at http://adni.loni.usc.edu/news-publications/publications/).

Results: (1) Data-driven AD progression models supported multifactorial interactions rather than a linear cascade of events. (2) β-Amyloid (Aβ) deposition occurred concurrently with functional connectivity changes within the default mode network in preclinical subjects and was followed by specific and progressive disconnection of functional and anatomical networks. (3) Changes in functional connectivity, volumetric measures, regional hypometabolism, and cognition were detectable at subthreshold levels of Aβ deposition. 4. Tau positron emission tomography imaging studies detailed a specific temporal and spatial pattern of tau pathology dependent on prior Aβ deposition, and related to subsequent cognitive decline. 5. Clustering studies using a wide range of modalities consistently identified a "typical AD" subgroup and a second subgroup characterized by executive impairment and widespread cortical atrophy in preclinical and prodromal subjects. 6. Vascular pathology burden may act through both Aβ dependent and independent mechanisms to exacerbate AD progression. 7. The *APOE* ε4 allele interacted with cerebrovascular disease to impede Aβ clearance mechanisms. 8. Genetic approaches identified novel genetic risk factors involving a wide range of processes, and demonstrated shared genetic risk for AD and vascular disorders, as well as the temporal and regional pathological associations of established AD risk alleles. 9. Knowledge of early pathological changes guided the development of novel prognostic biomarkers for preclinical subjects. 10. Placebo populations of randomized controlled clinical trials had highly variable trajectories of cognitive change, underscoring the importance of subject selection and monitoring. 11. Selection criteria based on Aβ positivity, hippocampal volume, baseline cognitive/functional measures, and *APOE* ε4 status in combination with improved cognitive outcome measures were projected to decrease clinical trial duration and cost. 12. Multiple concurrent therapies targeting vascular health and other AD pathology in addition to Aβ may be more effective than single therapies.

Discussion: ADNI publications from 2016 and 2017 supported the idea of AD as a multifactorial disease and provided insights into the complexities of AD disease progression. These findings guided the development of novel biomarkers and suggested that subject selection on the basis of multiple factors may lower AD clinical trial costs and duration. The use of multiple concurrent therapies in these trials may prove more effective in reversing AD disease progression.

Keywords: Alzheimer's disease; Mild cognitive impairment; Amyloid; Tau; Biomarker; Disease progression

1. Introduction

Thirteen years after its inception in October 2004, ADNI has had a profound impact on many aspects of science beyond its core mandate of "validation of biomarkers for AD therapeutic trials" [1]. The initial five-year study (ADNI-1), was extended for two years (ADNI-GO), and then by a further five years (ADNI-2) [2]. On August 1, 2016, a five-year renewal of ADNI, termed ADNI-3 began, featuring the use of a number of innovative technologies [2]. These include longitudinal tau positron emission tomography (PET) imaging using the radioligand, flortaucipir ([^{18}F]AV1451), which aims to clarify the role of tau in Alzheimer's disease (AD) progression, and the use of the β-amyloid (Aβ) tracer, florbetaben, to longitudinally evaluate new ADNI-3 participants. A fully automated Roche Electrosys immunoassay platform improves the accuracy of cerebrospinal fluid (CSF) biomarker measurements, and MRI sequences for connectivity analysis aim to elucidate the role of brain connectivity in AD. A Systems Biology approach aims to yield polygenic risk scores and identify novel genetic risk variants using gene pathway- and network-based metrics. The Brain Health Registry and Cogstate are online tools used for recruitment, assessment, and longitudinal monitoring of ADNI-3 participants. At the time of submission of this manuscript, 360 participants have continued from ADNI-2 (174 cognitively normal [CN], 97 mild cognitive impairment [MCI], and 35 AD), and 172 new subjects have been enrolled (115 CN, 26 MCI, 9 AD). Enrollment is expected to be completed in late 2018 or early 2019.

In part, the success of this "landmark imaging and omics study in AD" [3] can be measured by the number of publications and institutions that have used the freely available ADNI data. Using systematic science mapping methods,

Yao et al. [3] reported 996 ADNI papers until 5/12/2015 arising from 814 affiliated institutions worldwide, published in over 233 journals and conference proceedings. Both ADNI publications and institutions have increased linearly by year since 2008 (Fig. 1).

Successive comprehensive reviews [4–6] covered ADNI publications to the end of 2013 using the same modality-based format (magnetic resonance imaging [MRI], PET, Genetics, etc.). However, the evolution of techniques and ideas, and the increasingly interdisciplinary nature of publications, informed a subsequent review of 2014–2015 ADNI publications using a thematic-based approach focusing on advances in our understanding of AD disease progression, and how this translates to improving clinical trials [7]. The changes in research focus over time until 2014 are graphically represented by temporal profiles of selected keywords of ADNI papers; some terms, such as "white matter" and "genetics," increase over time, others such as "FDG" and "atrophy" peak and decline in different years (Fig. 2). Over the last 3 years, research topics have continued to evolve, and the number of ADNI publications has increased annually. By the end of 2017, ADNI publications numbered over 1500, almost 600 of them from 2016–2017 alone, testament to the outstanding success of the study. All ADNI publications can be searched online at http://adni.loni.usc.edu/news-publications/publications/ and a complete list of ADNI publications from 2016 to 2017 can be found in Supplementary Material.

The present study is not an exhaustive review of recent ADNI publications, but rather a collection of "hot topics" in the field, each centered around key ADNI papers published in 2016–2017 that have significantly advanced progress toward the ultimate goal of ADNI, the improvement of clinical trials for AD-modifying or AD-preventive therapies. The topics selected reflect the evolution of research in AD, and include progress on understanding the complexities of AD disease progression and its underlying genetics, how advanced methodologies have supported critical discoveries and improvements to clinical trials such as the development of novel biomarkers, and selection strategies and outcome measures that increase power to detect treatment effects. Findings of ADNI papers are briefly discussed in the context of non-ADNI findings where applicable.

2. Data-driven models of AD disease progression

The development of effective disease-modifying therapeutic agents depends on an understanding of late-onset AD disease progression. Observational models such as the hypothetical model for the ordering of AD biomarkers by Jack et al. [8,9] were dependent on available neuroimaging modalities and other biomarkers as biological factors influencing AD disease progression. Factors beyond those involved in the amyloid cascade hypothesis have been incorporated into less subjective data-driven models (e.g., [10]) which then have hinted at highly complex multifactorial mechanisms underlying AD disease progression [7].

The ordering of AD biomarkers posited by Jack et al. [8,9] was largely recapitulated in a data-driven model [11], based on changes in the magnitude and spatiotemporal distribution of multiple factors. One exception was the positioning of vascular dysregulation as the earliest identifiable pathological event followed in turn by Aβ deposition, glucose hypometabolism, impairment of neuronal function, and gray matter (GM) atrophy. However, the 2D arterial spin labeling data from ADNI-GO/2 used to measure the vascular component in the study are thought to be unreliable (C. Jack, personal communication), and therefore, this aspect of the model must be viewed with caution [2]. Changes in functional connectivity may also precede detectable Aβ accumulation. The optimum temporal order of AD biomarkers estimated using an event-based probabilistic model [12] placed functional connectivity changes in the hippocampus and posterior cingulate cortex (PCC) as occurring before CSF Aβ42 became abnormal.

A subsequent multifactorial causal model [13] additionally accounted for interactions between causal mechanisms, considering the interrelationship of six neuroimaging modalities and cognitive measures. This study quantified the degree of regional changes in a given biological factor caused by the direct influence of any other factor (Fig. 3A, B), and how much each biological factor is directly influenced by, and directly influences, other biological factors (Fig. 3C

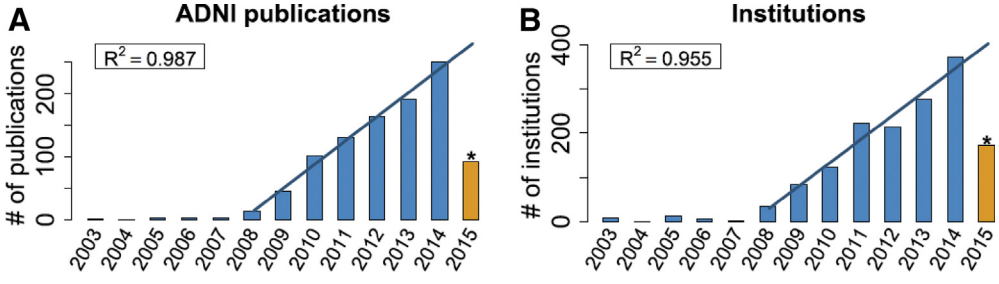

Fig. 1. Statistics for ADNI publications between 01/01/2003 and 05/12/2015. (A) Growth of ADNI publications on a year-by-year basis; line indicates linear regression prediction for 2015 using data from 2008 to 2014. (B) Growth of institutions involved in ADNI publications; line indicates linear regression prediction for 2015 using data from 2008 to 2014. *Marked orange bar corresponds to the actual collected data from 1/1/2015 to 5/12/2015. Abbreviation: ADNI, Alzheimer's Disease Neuroimaging Initiative. Reproduced with permission from Weiner et al. [3].

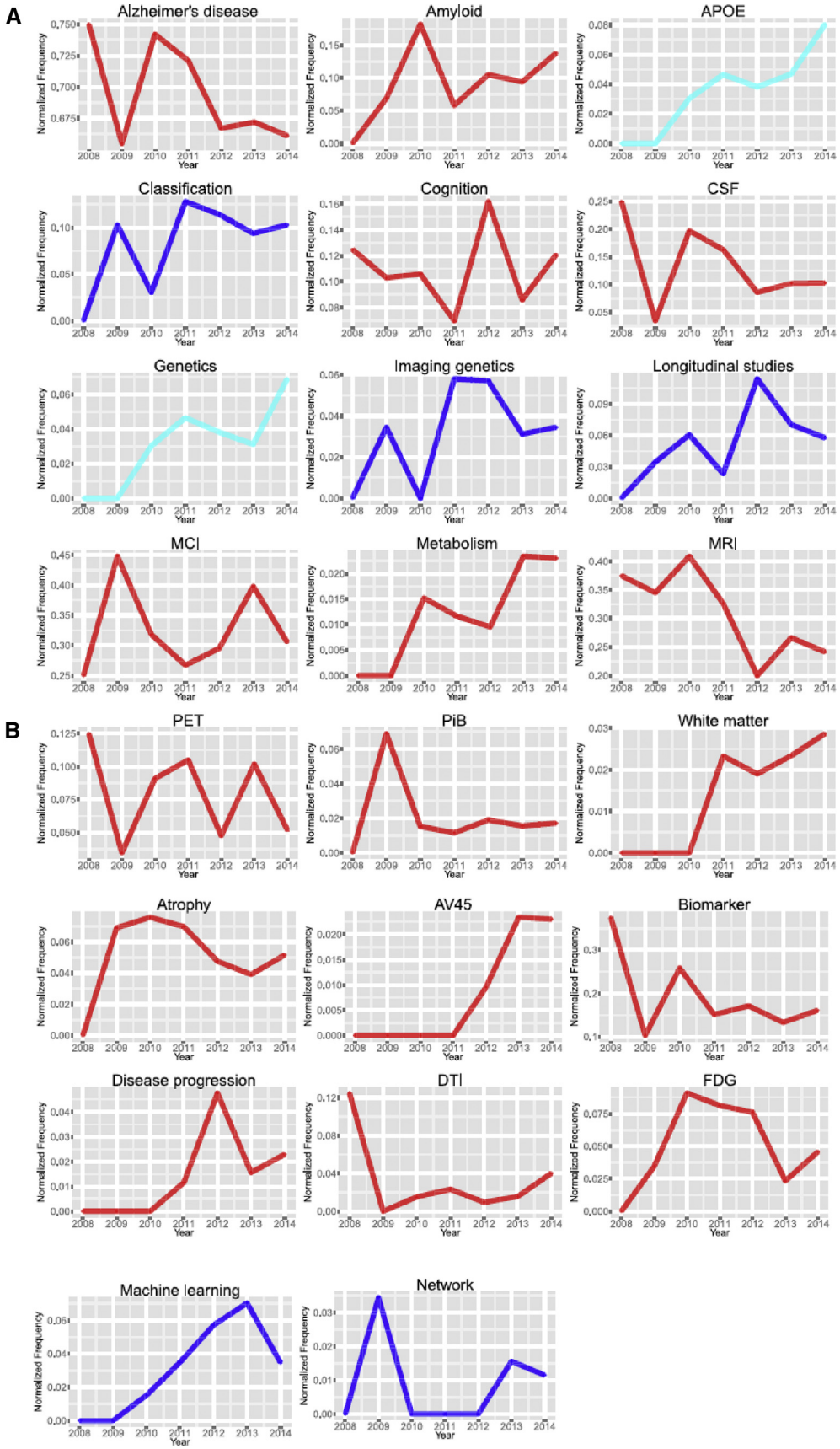

Fig. 2. Temporal profiles of selected keywords from 2008 to 2014. Plots show keyword frequency normalized to the number of publications. Red: phenotype, blue: analysis, aqua: genotype. Abbreviations: CSF, cerebrospinal fluid; FDG, ^{18}F-fluorodeoxyglucose; MCI, mild cognitive impairment; MRI, magnetic resonance imaging; PET, positron emission tomography. Reproduced with permission from Weiner et al. [3].

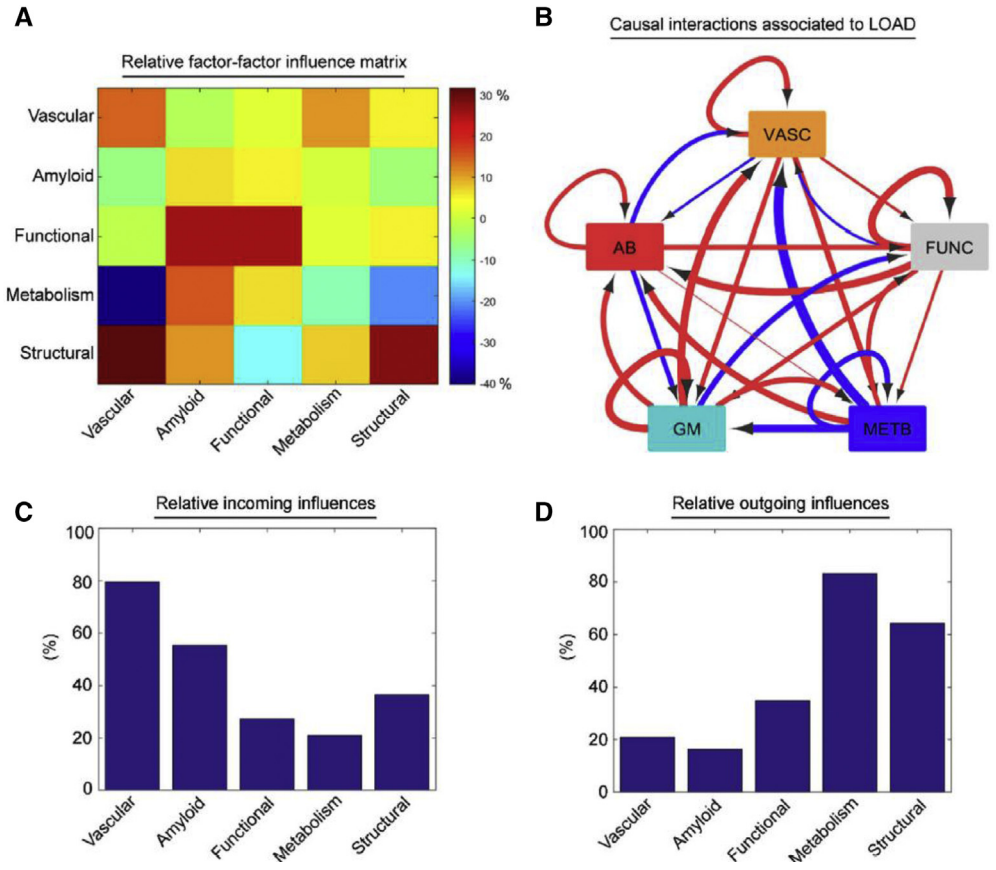

Fig. 3. Direct interactions associated with LOAD progression. (A) Relative factor-factor influence matrix quantifying the percent of regional changes in a biological factor caused by the direct influence of any other factor. (B) Associated causal diagram. Red and blue links correspond to positive and negative direct relationships, respectively, and link thickness corresponds to strength of relationship. (C) Relative incoming influences quantifying the degree to which each biological factor is directly influenced by other biological factors. (D) Relative outgoing influences quantifying the degree to which each biological factor influences other biological factors. Abbreviation: LOAD, late-onset Alzheimer's disease. Reproduced with permission from Iturria-Medina et al. [13].

and D, respectively). The model predicted spatiotemporal spread of Aβ, glucose hypometabolism, vascular flow, abnormal neuronal activity, and atrophy across anatomical and vascular brain networks and pinpointed vascular dysregulation in the hippocampus and entorhinal cortex as the most likely initial pathologic event. Neurodegeneration appeared to result from the complex interaction of multiple factors involving positive and negative feedback loops, rather than a linear cascade of events after Aβ deposition.

Structural brain networks may also play an early role in AD disease progression. Previous ADNI studies proposed frameworks that accounted for the observed patterns of regional atrophy and metabolism [14,15] and Aβ spread [16]. These were based on a trans-synaptic "prion-like" diffusive progression in which initial misfolding of pathological proteins induces misfolding of adjacent same species proteins, which in turn cascade along the brain's connectivity network. More recently, Pandya et al. [17] developed a data-driven model that considered relationships between connectivity networks, regional metabolism, and Aβ deposition, which found that regional Aβ deposition was related to both the healthy metabolism of that region, and the healthy metabolism of remote regions structurally connected to it. These data supported initial enhancement of Aβ deposition in areas of high metabolism such as the default mode network (DMN), followed by the spread of Aβ deposition along the connectome mediated by metabolic load in remote regions (Fig. 4). A probabilistic graphical model found that observed patterns of Aβ deposition, glucose metabolism, and GM atrophy were best accounted for by initial Aβ deposition in the highly interconnected PCC hub region induced by high metabolic demands followed by transneuronal spread of pathological Aβ. These studies are consistent with a combination of the "wear and tear" hypothesis in which brain regions with high metabolic demands, usually highly interconnected hubs, are more vulnerable to Aβ deposition leading to neuronal dysfunction and death [18], and with the transneuronal hypothesis [14,16].

These models should be considered with the caveat that associations and even sequential order of changes do not necessarily mean cause effect. They are limited by the use of cross-sectional, or limited longitudinal data to infer

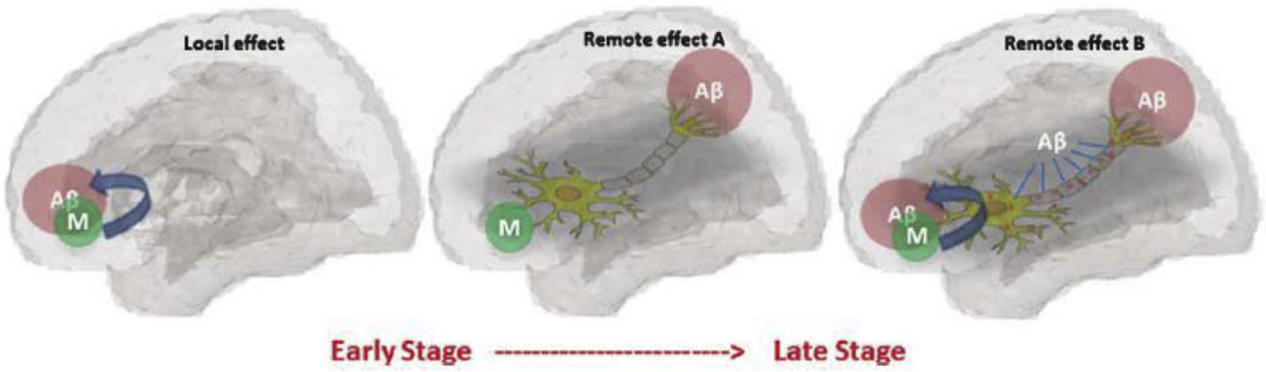

Fig. 4. Proposed model of stage-dependent connectome mediation. Local amyloid deposition occurs in proportion to local metabolic load in the early stages of disease (left). Remote, connectome-mediated effects emerge as the disease progresses. Two potential mechanisms for the relationship between metabolic load and amyloid deposition are as follows: (1) remote effect A that may operate along and within axonal projections or (2) remote effect B in which the relationship might be strictly local, but in which connectivity mediation occurs as a result of the physical transport of amyloid oligomers followed by transneuronal transmission into the remote site. Abbreviation: Aβ, β-amyloid. Reproduced with permission from Pandya et al. [17].

longitudinal progression, the number of biological factors considered, and by the ability to accurately measure these factors. It is possible that factors not currently being measured, such as genetic factors, are responsible for the observed sequence of events. However, these studies do suggest that Aβ deposition may not be the earliest pathological event. Pathological changes may be accounted for by a combination of the influence of high regional metabolism in hub

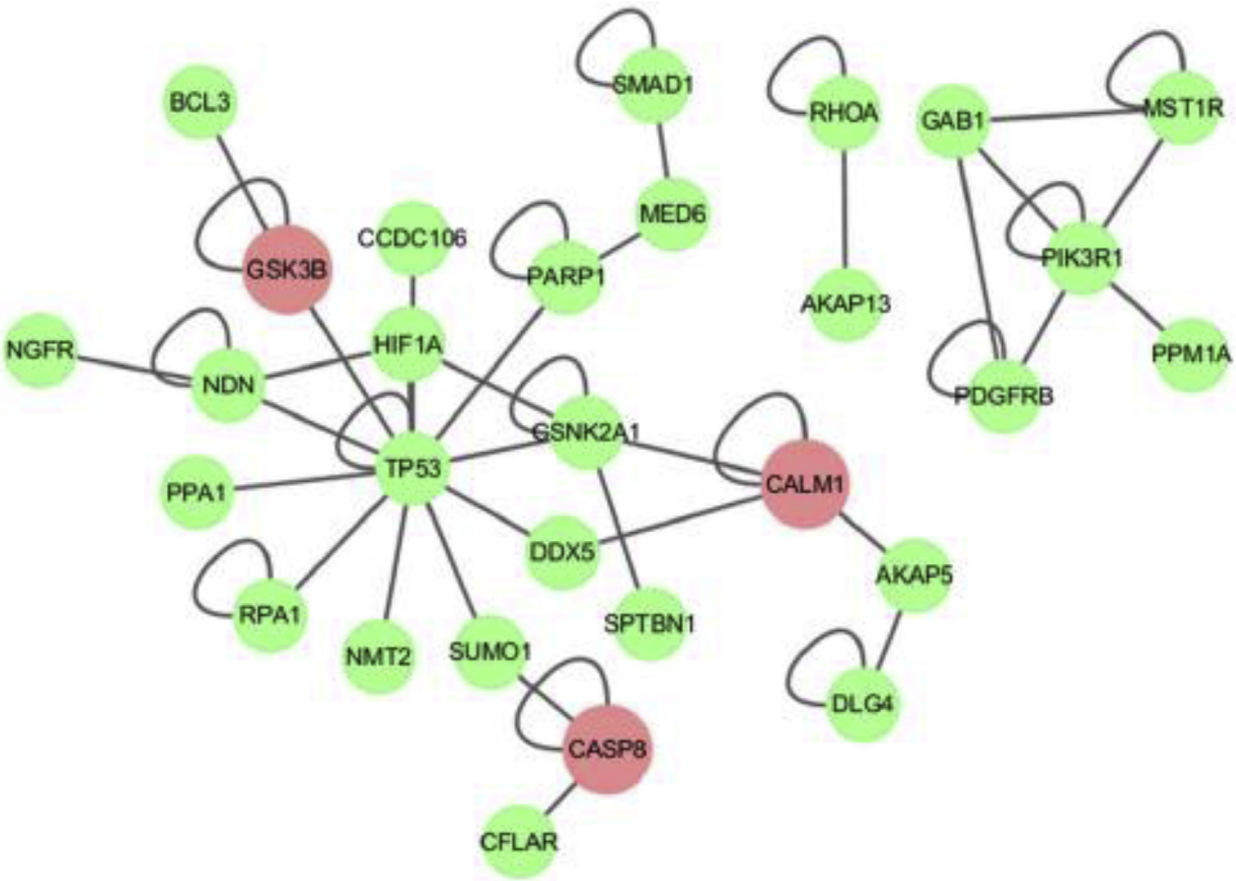

Fig. 5. The common subnetwork of genes identified from a genome-wide association study of t-tau and Aβ42. The subnetwork consists of only overlapping genes of all consensus modules. The reddish color indicates genes belonging to the Kyoto Encyclopedia of Genes and Genomes Alzheimer's Pathway. Reproduced with permission from Cong et al. [20].

regions such as the PCC on Aβ deposition, and the subsequent spread of pathological Aβ in a characteristic manner along the structural connectome by prion-like propagation, guided by high metabolism in remote regions. This process likely reflects the complex interplay of multiple factors.

3. Genetic approaches for understanding AD pathophysiology

The complex genetic etiology of AD involves polygenic inheritance, allelic and locus heterogeneity, and epistasis. In the post–genome-wide association study (GWAS) era, new genetic strategies have augmented our understanding of pathological mechanisms underlying AD. These include investigations of genes involved with established AD pathology as well as the identification of pathways beyond those traditionally associated with AD pathology. Short-term silencing of protein coding genes using siRNA was used to assess which of the 123 genes located within the 19 identified AD susceptibility loci affect amyloid precursor protein (APP) metabolism [19]. A novel genetic risk factor, *FERM2*, was significantly associated with CSF levels of Aβ42, and further analysis suggested that it may act via the modulation of APP metabolism and Aβ peptide generation. A protein-protein interaction network analysis of genes identified in a GWAS of t-tau and Aβ42 levels identified as subnetwork of 29 genes not only related to tau phosphorylation (*GSK3B, SUMO1, AKAP5, CALM1,* and *DLG4*) and Aβ production (*CASP8, PIK3R1, PPA1, PARP1, CSNK2A1, NGFR,* and *RHOA*) but also in Kyoto Encyclopedia of Genes and Genomes pathways for AD, Huntington's disease, and several cancers [20] (Fig. 5). Similarly, a novel method that explored higher level associations between sets of genes in the pathway and brain circuits from Aβ PET imaging identified 12 gene set–brain circuit modules relevant to calcium signaling, oxidative stress, other neurodegenerative disorders, and cancers [21]. The results from these studies attest to a biological complexity of AD involving multiple contributing factors.

APOE and other genetic loci identified by GWAS account for only around half of the disease heritability for AD [22]. ADNI multimodal quantitative phenotypes have enabled a variety of approaches in the hunt for the remaining heritability. Two studies targeted rare variants (defined as having a minor allele frequency of less than 0.05) in or near known AD risk genes. Rare variants in or near *PSEN1* (early-onset familial AD) were associated with bilateral entorhinal cortical thickness, and *APOE* ε4 carriers with the exonic. E319G variant had an increased risk of AD, lower CSF Aβ42, and higher CSF tau [23]. Similarly, a gene-based association analysis of rare variants in the vicinity of *APOE* with CSF and neuroimaging biomarkers identified rare nonsynonymous variants in *CBLC*, *BCAM*, *RELB*, and *APOE* associated with CSF Aβ42 levels [24]. The rare variants in *CBLC* were additionally associated with temporal and frontal lobe atrophy, and the rare variants in *RELB* were associated with cortical Aβ burden in the frontal and parietal lobes.

Biological knowledge-driven approaches have identified a series of epistatic interactions that likely account for some of the missing heritability. An interaction study of SNPs identified using CSF t-tau/Aβ42 ratio as a quantitative phenotype identified seven pairs of SNPs whose interactions explained significant variance in the t-tau/Aβ42 ratio despite marginal dominance effects of the individual variants [25]. A genome-wide interaction study of five risk variants in *APOE*, *BIN1*, *CR1, PICALM,* and *MS4A6A* identified interactions with SNPs in the gene pathways involved in gonadotropin-releasing hormone signaling and vascular smooth muscle contraction (*APOE* and *MS4A6A*) and dilated cardiomyopathy (*MS4A6A*) among others [26]. Novel gene-gene interactions between three gene pairs (*SIRT1* × *ABCB1, PSAP* × *PEBP4, GRIN2B* × *ADRA1A*) were identified using meta-analytic knowledge-driven approach to identify consistent SNP × SNP interactions associated with AD [22]. These interactions may modify AD risk directly through alterations in Aβ clearance (*SIRT1* × *ABCB1)*, or via other genes such as *CDH23* (*PSAP* × *PEBP4)*, suggesting the involvement of cell adhesion, and *NMDA* (*GRIN2B* × *ADRA1A*), a gene implicated in memory. The study also confirmed the genetic interaction between *RYR3* and *CACNA1C*, suggesting a role for calcium homeostasis in AD pathogenesis.

These ADNI studies underscore the biological complexity of AD suggested by AD disease progression models. Genetic risk for late-onset AD may involve not only multiple gene pathways underlying calcium signaling, oxidative stress, cancers, and other neurodegenerative disorders, but epistatic interactions and rare variants in known AD risk alleles.

4. Building a bridge between genetics and biochemistry: Biological effects of confirmed AD risk alleles

Large GWASs have identified and confirmed a number of AD risk loci, but these studies shed little light on how these loci increase risk from a biological perspective. Recent ADNI studies have analyzed the associations between variants at these loci and AD biomarkers and investigated the biological effects of specific coding and noncoding variants. Again, we caution about ascribing cause-effect to associations.

Variants in *CLU* (clusterin), a major susceptibility gene, were associated with primarily Aβ deposition in the cingulate and frontal cortex and with hippocampal volume, but not with glucose metabolism or CSF biomarkers [27]. By contrast, several variants in *PICALM* were associated with larger baseline thickness of the posterior cingulate in CN participants, and slower atrophy of the same region in both CN and MCI participants, suggesting that they act by increasing brain reserve capacity [28]. Similar studies fleshed out the effects of other risk variants, primarily in

pooled samples of patients spanning the disease spectrum (Table 1). However, a study of the effects of the top 20 AD genes on posterior cingulate hypometabolism and medial temporal GM found specific genes to be associated at successive disease stages and that these genes differed in their effect on GM density and on hypometabolism [29]. Significant predictors of hypometabolism (*SLC4A4/RIN3, NME8, CD2AP*) were found only in CN participants, whereas there were no significant predictors of GM density in this group; by contrast, significant predictors of GM density were found in MCI (*SLC4A4/RIN3, ZCWPW1*) and AD (*ABCA7, EPHA1, INPP5D*) participants only. This study suggests that hypometabolism may be an early neurodegenerative change that precedes GM atrophy, consistent with models for AD disease progression described in Section 2, and that stage-specific genes underlie these pathological changes.

Specific AD risk alleles may also have stage-dependent effects. For example, the Val66Met variant of *BDNF* (brain-derived neurotrophic factor) was suggested to be associated with aggregation of brain-derived neurotrophic factor which negatively affected medial temporal lobe

Table 1
Association studies of known AD risk variants

Gene	Number of variants	Association	Region	Reference	Conclusion
ABCA7	3	Amyloid deposition	Widespread	[179]	Increases amyloid deposition
BIN1	2	CSF t-tau, p-tau181	-	[180]	Alters neuronal degeneration
	3	Atrophy	Hippocampus, parahippocampus		
	3	Glucose metabolism	Right angular, temporal cortex		
	1	Atrophy	Left parahippocampal gyrus, right inferior parietal	[181]	
CD33	1	Baseline volume	Left parahippocampal gyrus	[182]	Affects volume of parahippocampal and hippocampal gyrus
	3	Baseline volume	Left hippocampal gyrus		
CLU	5	Amyloid deposition	Cingulate, frontal cortex	[27]	Affects amyloid load and hippocampal volume
	1	Baseline volume	Left hippocampus		
CR1	1	Amyloid deposition	Cingulate, frontal, parietal, temporal lobes	[183]	Widespread effects on amyloid deposition, brain structure, and glucose metabolism
	3	Atrophy	Middle temporal lobe		
	1	Glucose uptake (negative association)	Right temporal lobe		
	1	Baseline volume	Right temporal lobe	[181]	
HLA-A2	4	Atrophy (one protective variant)	Left parahippocampus, right hippocampus	[184]	Affects hippocampal volume
HLA-DRB1/DQB1	4	Baseline volume (one protective variant)	Left posterior cingulate	[185]	Affects left posterior cingulate volume
HLA-TNFα	2	Baseline volume	Left middle temporal lobe	[186]	Affects AD-related brain structures
HLA-HFE	1	Atrophy (protective)	Right middle temporal lobe		
HLA-RAGE	1	Atrophy	Hippocampal CA-1 subregion		
HMGCR	1	Decreased atrophy	Right entorhinal, left hippocampus	[187]	Protective effect via influence on brain structure and metabolism
	1	Increased glucose metabolism	Right temporal		
IL-6R	1	Age of onset in *APOE* ε4 carriers	-	[188]	Neuroinflammatory changes influence age of onset
MS4A4	2	Atrophy	Left middle temporal	[189]	Affects AD-related brain structures
	1	Atrophy	Precuneus		
	1	Atrophy	Entorhinal cortex		
MS4A46A	1	Volume increase	Left inferior temporal	[181]	Affects temporal lobe volumes
	1	Baseline volume	Right middle temporal		
PICALM	1	Baseline thickness (protective)	Posterior cingulate	[27]	Protective effect via increase in brain reserve
	2	Slower atrophy rate in MCI			
	7	Slower atrophy rate in CN			
PICALM × *CLU*	2	Atrophy	Hippocampus	[190]	Interaction affects hippocampal degeneration
SORL1	2	Atrophy	Right parahippocampal gyrus	[191]	Affects AD-related brain structures
	1	Volume increase	Left inferior parietal	[181]	
	1	Atrophy	Left parahippocampal, right inferior parietal		

Abbreviations: AD, Alzheimer's disease; CN, cognitively normal; MCI, mild cognitive impairment.

structural and functional integrity early in AD disease progression, and cognition in later disease stages [30]. When CN and MCI/AD participants were stratified by both *APOE* and *BDNF* genotypes, carriers of both *APOE* ε4 and *BDNF* Val66Met alleles had greater atrophy in the posterior cingulate and precuneus in CN participants and greater atrophy in the entorhinal cortex in MCI and AD participants than carriers of only one allele or ε3/ε3 and V/V homozygotes. The greater deleterious effect of Val66Met on an *APOE* ε4 background suggests that their interaction may impact stage-dependent AD brain regions via a mechanism involving Aβ deposition, given the effect of the *APOE* ε4 allele on CSF Aβ42.

The data-driven models of AD progression described in Section 2 suggest that Aβ clearance deficiencies may contribute to Aβ deposition and the following cascade of pathological events. One ADNI study found that a protective effect of SNP rs11014002 in the precursor for the intronic micro RNA, miR-603 in the *KIAA1217* gene [31]. The putative effect of this SNP was to promote miR-603 biogenesis that increases low-density lipoprotein receptor–related protein 1 expression, while also downregulating LRP-associated protein 1 mRNA and protein levels, promoting Aβ clearance in the brain. Data-driven models also predict a role for vascular disease in AD, and this is supported by genetic studies. The C677 T variant of *MTHFR* has been linked to increased susceptibility for cardiovascular diseases and in turn to cognitive decline and depressive symptoms in old age. The association of this variant with increased medial orbitofrontal atrophy was mediated by elevated plasma homocysteine levels, which are associated with vascular risk factors for AD such as cardiovascular disease and stroke (Fig. 6A) [32]. Furthermore, medial orbitofrontal cortical volumes mediated the association between cognition and depression (Fig. 6B) [32]. These findings offer a mechanistic model linking homocysteine metabolism, medial orbitofrontal atrophy, cognition, and depression.

These recent ADNI studies of established risk AD alleles have begun to bridge the gap between genetics and underlying biology and suggest a wide influence of these alleles that may differ depending on disease stage and that may affect multiple biochemical pathways, consistent with the complex interplay of multiple factors suggested by data-driven AD disease progression models.

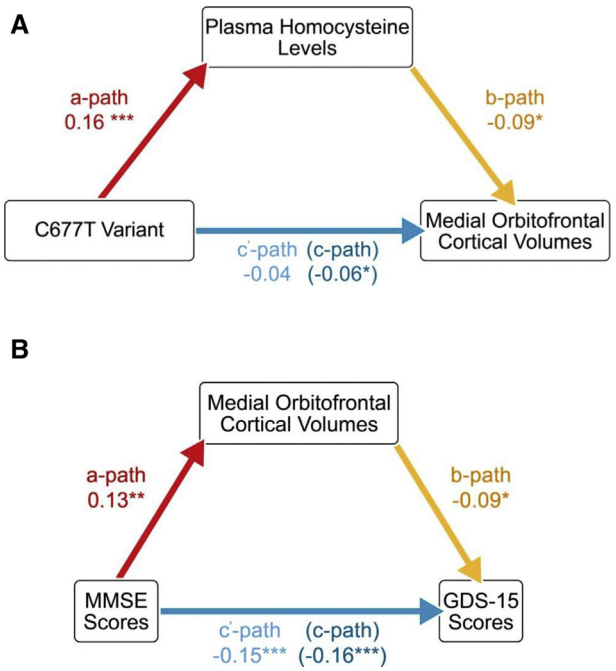

Fig. 6. Mediation analyses of the effect of the C677 T variant. (A) Mediation of the association between genotype and medial orbitofrontal volumes by plasma homocysteine levels ($n = 634$). The *a*-path represents the association between genotype and plasma homocysteine levels. The *b*-path denotes the relationship between plasma homocysteine levels and medial orbitofrontal volumes while also controlling for genotype. The *c*′-path and *c*-path represent the associations between genotype and medial orbitofrontal volumes with and without plasma homocysteine levels included as a mediator, respectively. $*P < .05$, $***P < .001$. (B) Partial mediation of the association between performance on the MMSE and scores on the GDS-15 by medial orbitofrontal volumes ($n = 640$). The *a*-path represents the association between MMSE scores and medial orbitofrontal volumes. The *b*-path denotes the relationship between medial orbitofrontal volumes and GDS-15 scores while also controlling for MMSE performance. The *c*′-path and the *c*-path represent the associations between MMSE and GDS-15 scores with and without medial orbital cortical volumes included as a mediator, respectively. $*P < .05$, $**P < .01$, $***P < .001$. Abbreviations: MMSE, Mini–Mental State Examination; GDS-15, 15-item version of Geriatric Depression Scale. Reproduced with permission from Roussotte et al. [32].

5. Origins: new evidence for the beginnings of AD

The earliest pathological changes in AD are thought to occur perhaps decades before the first clinical manifestation of the disease [33]. Using CN elders in ADNI, two studies used the discordance between CSF Aβ42 levels and florbetapir PET to investigate early stages of Aβ deposition. A discordant status (CSF+/PET−) may indicate early deposition of Aβ pathology [34], but even earlier deposition may be indicated by conversion of participants with no measurable signs of Aβ accumulation (CSF−/PET−) to an Aβ discordant status (CSF+/PET−) [35]. Comparison of CN participants stratified in this manner revealed that the earliest signs of Aβ cerebral accumulation were in regions of the DMN: the medial orbitofrontal cortex and PCC, followed by the precuneus and wider orbitofrontal cortex (Fig. 7) [35]. Furthermore, functional connectivity was increased within the DMN of CSF−/PET− CN subjects who converted to discordant status, consistent with AD disease progression models that propose very early functional connectivity changes as a result of increased metabolism in DMN hubs (Section 2). Intra-DMN connectivity and connectivity between the DMN and the frontoparietal network was subsequently decreased in Aβ discordant subjects, suggesting that cerebral Aβ accumulation then causes neuronal dysfunction [35]. This is supported by a metabolomics study that found changes in phospholipid metabolism in

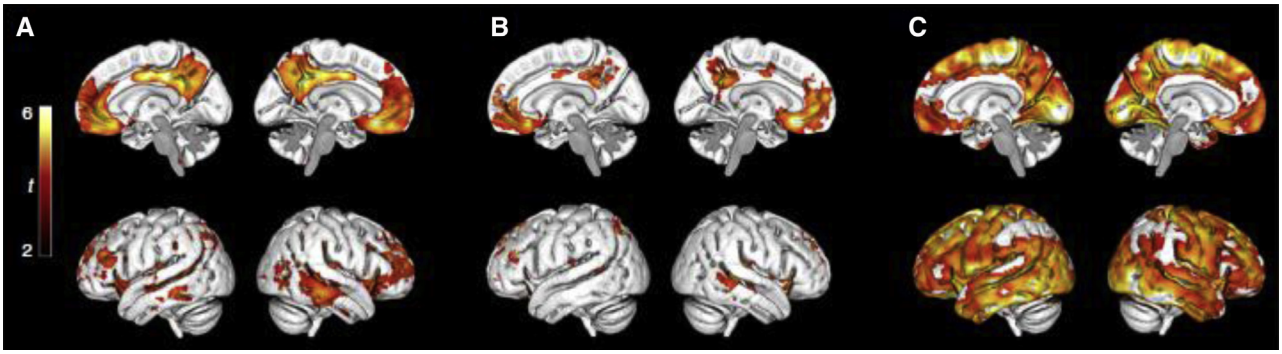

Fig. 7. Regions of Aβ accumulation from longitudinal voxel-wise analyses. (A) Comparison of annual florbetapir SUVR rate during 2 years between early-stage Aβ accumulators (CSF+/PET) and nonaccumulators (CSF−/PET−) showing regions where Aβ fibrils start to accumulate. The most significantly increased accumulation rate was in the posterior cingulate cortex, the precuneus, and the medial orbitofrontal cortex. (B) Voxelwise correlations between annual florbetapir SUVR rates and CSF Aβ42 levels in Aβ PET–negative individuals, confirming regions in A without biases from a specific CSF Aβ42 cut point. (C) Comparison of annual florbetapir SUVR rate during 2 years between late-stage Aβ accumulators (CSF+/PET+) and nonaccumulators (CSF−/PET−), showing a widespread pattern of Aβ accumulation. Voxelwise two-sample t-tests were used, and all analyses are adjusted for age and gender. The significant threshold was set at $P < .001$. The red and yellow colors illustrate significant t values according to the scale on the left. Abbreviations: Aβ, β-amyloid; SUVR, standardized uptake value ratio; CSF, cerebrospinal fluid; PET, positron emission tomography. Reproduced with permission from Palmqvist et al. [35].

CSF+ CN subjects that indicated early neurodegeneration and loss of membrane function [36].

CN elders with elevated baseline brain Aβ deposition had worse mean scores in a variety of cognitive tests at 4 years of follow-up [37]. How does increased Aβ deposition ultimately result in cognitive decline? There are several possibilities: Aβ deposition may have direct effects on neuronal function and viability. Aβ deposition may facilitate the spread of tau leading to neurodegeneration. Finally, factors (e.g., genetic, inflammation, diabetes) that cause Aβ deposition may be independently responsible for cognitive decline. ADNI CN subjects with declining CSF Aβ42 levels had an anticorrelated trajectory of CSF p-tau181, and these two biomarkers statistically interacted to have a significant effect on hippocampal atrophy. This implicates early pathogenic crosstalk between CSF Aβ42 and p-tau181 in downstream processes such as typical AD neurodegeneration, and by extension cognitive decline [38]. Similarly, increased cerebral blood flow in the hippocampus, posterior cingulate, and precuneus in these subjects was associated with poor memory performance [39]. Higher cerebral blood flow may be a vascular compensatory response to Aβ pathology [39]. These results suggest that early changes of CSF Aβ42 and p-tau181 and cerebral blood flow in response to Aβ deposition may mediate changes in cognition.

6. Differing pathways of neurodegeneration

Heterogeneity of MCI and CN subjects has been well established and is similar to many other human diseases. To some extent, the heterogeneity may reflect differing and possibly concurrent pathways leading to neurodegeneration [7]. Several ADNI studies have defined a set of remarkably consistent AD subtypes in these subjects determined using a wide variety of criteria [40–45]. A subgroup with little or no sign of abnormal AD biomarkers was consistently identified on the basis of neuroanatomical patterns [40], cortical atrophy [41], and neuropsychological variables [42]. These and other studies that included AD subjects also consistently identified two additional subgroups based on cortical atrophy patterns [43], whole-brain atrophy patterns [44], and the distribution of neurofibrillary tangles (NFTs) [45]. The

Table 2
Characteristics of probable AD subtypes

Characteristic	Typical AD	Dysexecutive/cortical
Cognitive impairment	Predominantly memory [40–42,47]	Predominantly executive function, also memory and other domains [40–43,45,47]
Atrophy	Hippocampal and medial temporal cortex [40,43,45,47]	Widespread cortical, particularly parietal [41,43,47]
Disease progression	Fast [41,42,45]	Fastest [41–43,45], earliest age of onset [40,43,45,47]
Glucose metabolism	Low [45]	Lowest [45]
WMH burden	High [40,44]	Lower [40,44]
CSF Aβ levels	Low [40–42,44,47]	Low [40–42,44,47]
CSF tau, p-tau181 levels	High [41,42,44]	High [40–42,44]
Neurofibrillary tangles	Typical AD cortical regions, hippocampal [45]	Widespread cortical, less hippocampal [45]
Genetics	Most carriers of risk allele in *CD2AP* [44]	Highly heritable executive prominent/memory prominent spectrum [46]

Abbreviations: Aβ, β-amyloid; AD, Alzheimer's disease; CSF, cerebrospinal fluid; WMH, white matter hyperintensity.

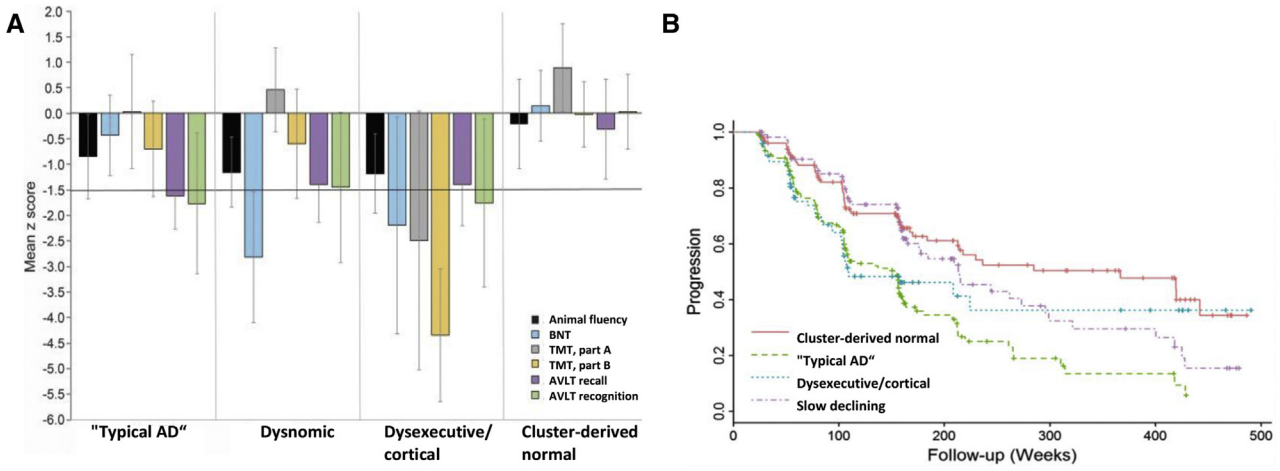

Fig. 8. Characteristics of cluster-derived MCI subgroups. (A) Neuropsychological performance for cluster-derived MCI groups based on cortical atrophy patterns. Mean Z scores for the cluster groups derived from cortical atrophy patterns on neuropsychological measures. Error bars denote standard deviations. The horizontal dotted line indicates the typical cutoff for impairment (−1.5 SDs). (B) Progression from MCI to Alzheimer's disease stratified by MRI-defined clusters. Abbreviations: AVLT, Rey Auditory Verbal Learning Test; BMT, Boston Naming Test; MCI, mild cognitive impairment; MRI, magnetic resonance imaging; TMT, trail making tests. Reproduced with permission from Dong et al. [40] and Edmonds et al. [41].

first appears to represent "typical AD" and is characterized by primarily memory impairment, and hippocampal and regional lateral temporal cortical atrophy (Table 2). The second group is characterized by predominantly executive function impairment and relatively spared hippocampal atrophy but widespread cortical atrophy particularly in the parietal lobe (Table 2). This "dysexecutive/mixed" subgroup is also characterized by impairment of multiple additional cognitive domains, more rapid decline, an earlier age of onset, lower white matter hyperintensity (WMH) burden, and lower glucose metabolism than the "typical AD" subgroup (Table 2) (Fig. 8). One study suggested that the high rate of decline in executive function of this subtype is not related to small vessel ischemic disease as this cluster had lower levels of WMH than the "typical AD" cluster [40]. However, individuals in this cluster may have different comorbidities, mixed pathology, or simply a more cortical representation of AD in which widespread cortical atrophy is commensurate with multiple cognitive impairments [45]. Despite having no significant differences in frequencies of the *APOE* ε4 allele, the subgroups were genetically differentiated by the levels of minor alleles in SNPs rs10948363 (*CD2AP*), rs11023139 (*SPON1*), and rs7245858 (*LOC 39095)* [44]. The dysexecutive/cortical subtype was found to have a different chromosomal pattern of SNPs explaining phenotypic variance [46].

Several additional subtypes have been less consistently reported. A dysnomic subtype of ADNI MCI subjects was characterized primarily by language impairment (Fig. 8) and a less severe pattern of cortical thinning and may represent an intermediate stage of cognitive decline [41]. A slower declining subtype was variously characterized by predominantly hippocampal atrophy and less cognitive impairment [45]; localized temporal atrophy and lower frequencies of abnormal CSF Aβ42 [40]; a pattern of diffuse cortical atrophy, lower frequencies of abnormal CSF Aβ42, the most carriers of the *APOE* ε2 allele, and a protective allele in *SPON1* [44]; and a pattern of diffuse cortical atrophy, lower memory and executive function impairment, and distinct age and gender distribution [43]. It is possible that these studies are identifying the same subgroup that has yet to be well characterized.

Characteristics of the "typical AD," "dysexecutive mixed," and "slow declining" subtypes were also identified in three latent atrophy factors using a Bayesian modeling approach [47]. A temporal atrophy factor was strongly associated with memory decline, a cortical atrophy factor was strongly associated with worse executive function and earlier age of onset, and a subcortical atrophy factor was associated with the slowest decline in memory and executive function and a high prevalence of the protective *APOE* ε2 allele. These atrophy factors appeared to differentially impact AD disease progression along the clinical spectrum. The temporal factor was the strongest predictor of memory decline in CN subjects but the cortical factor best predicted memory decline in AD subjects. Conversely, the cortical factor was not associated with either memory or executive function in CN participants but predicted executive function decline in MCI and AD subjects (Fig. 9A and B). Most AD patients (Fig. 9C) as well as Aβ+ MCI and CN participants expressed a mix of different atrophy factors, which may account for the wide range of heterogeneity observed. As these distinct atrophy factors were not directly linked to Aβ pathology, they may arise from different pathologies such as TDP-43, Lewy bodies, and hippocampal sclerosis that converge with AD pathology to influence AD disease progression.

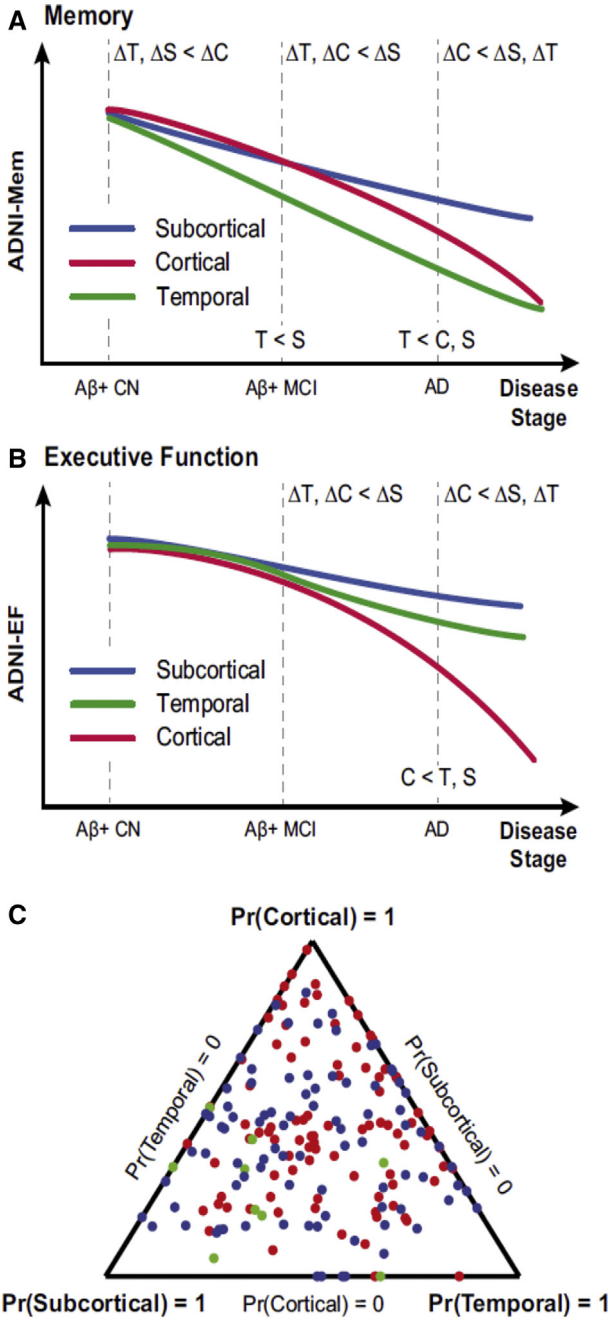

Fig. 9. Cognitive trajectories and factor compositions of temporal, subcortical, and cortical atrophy factors. Schematics of distinct memory (A) and executive function (B) trajectories. T, S, and C indicate temporal, subcortical, and cortical factors, respectively. Labels on the dotted lines indicate cross-sectional differences. Labels on the intervals indicate differences and longitudinal decline rates. (C) Factor compositions of 188 AD patients. Each patient corresponds to a dot, with location that represents the factor composition. Color indicates amyloid status: red for Aβ+, green for Aβ−, and blue for unknown. Corners of the triangle represent pure factors; closer distance to the respective corner indicates the probability for the respective factor. Abbreviations: AD, Alzheimer's disease; Aβ, β-amyloid. Reproduced with permission from Zhang et al. [47].

Taken together, these studies provide strong support for a consistent set of AD subtypes including a "normal" group, a "typical AD" group, a "dysexecutive/mixed group," and a slow declining group. The characteristics of these subtypes appeared to overlap with a set of co-occurring latent atrophy factors, suggesting that multiple differing pathways of neurodegeneration interact to influence AD disease progression and contribute to the observed heterogeneity of CN and MCI participants.

7. Amyloid-dependent neurodegeneration

What are the effects of very early Aβ deposition on AD disease progression? How does it influence neuronal injury, and functional and cognitive decline? To capture these relationships, two ADNI studies operationalized Aβ status as a continuous variable rather than dichotomizing participants as Aβ+ and Aβ− [48,49]. Insel et al. [49] investigated the points along the spectrum of Aβ pathology at which trajectories of measures of neuronal injury and cognitive decline began to accelerate. Rates of cognitive and functional decline, cortical Aβ deposition (florbetapir PET), temporal lobe atrophy, and neuronal injury (FDG-PET) all accelerated before the conventional threshold of CSF Aβ positivity (Fig. 10). Unexpectedly, the acceleration of atrophy rates occurred after the acceleration of cognitive and functional impairment, and worsening synaptic function (FDG-PET) occurred concomitantly with accelerating Aβ deposition (Fig. 10). In the second study, increasing Aβ deposition in preclinical CN subjects modulated glucose hypometabolism first in a globally synchronized manner, and later in a temporally and spatially divergent manner [48]. Initial global hypometabolism peaked when Aβ became measurable by florbetapir PET imaging. This was followed by regional hypometabolism within the DMN with increasing Aβ deposition in the gyrus and PCC [48]. In CN subjects, higher baseline brain Aβ was associated with greater longitudinal cognitive decline, and greater ventricular expansion and hippocampal atrophy [37]. Subregional measures of GM volume suggested that atrophy originates in the cholinergic cells of the basal forebrain in Aβ+ CN subjects and precedes atrophy in the entorhinal cortex in Aβ+ MCI nonprogressors [50]. Entorhinal cortex atrophy was found to be higher in MCI progressors and AD subjects supporting a link between atrophy in this region and memory impairment [50] (Fig. 11).

Aβ deposition has also been associated with changes in both functional and structural connectivity. Aβ+ early MCI subjects had a greater breakdown of DMN connectivity than Aβ− subjects, and this was correlated with decreased cognitive function [51]. Moreover, changes in functional connectivity are not limited to the DMN in Aβ+ subjects across the disease spectrum [52]. Intranetwork intrinsic functional connectivity declined gradually with AD disease progression and was associated with cognitive decline in multiple intrinsic brain networks [52] (Fig. 12). Changes in between-network functional connectivity were also observed [52], suggesting that Aβ deposition has deleterious effects on functional connectivity, perhaps arising from local

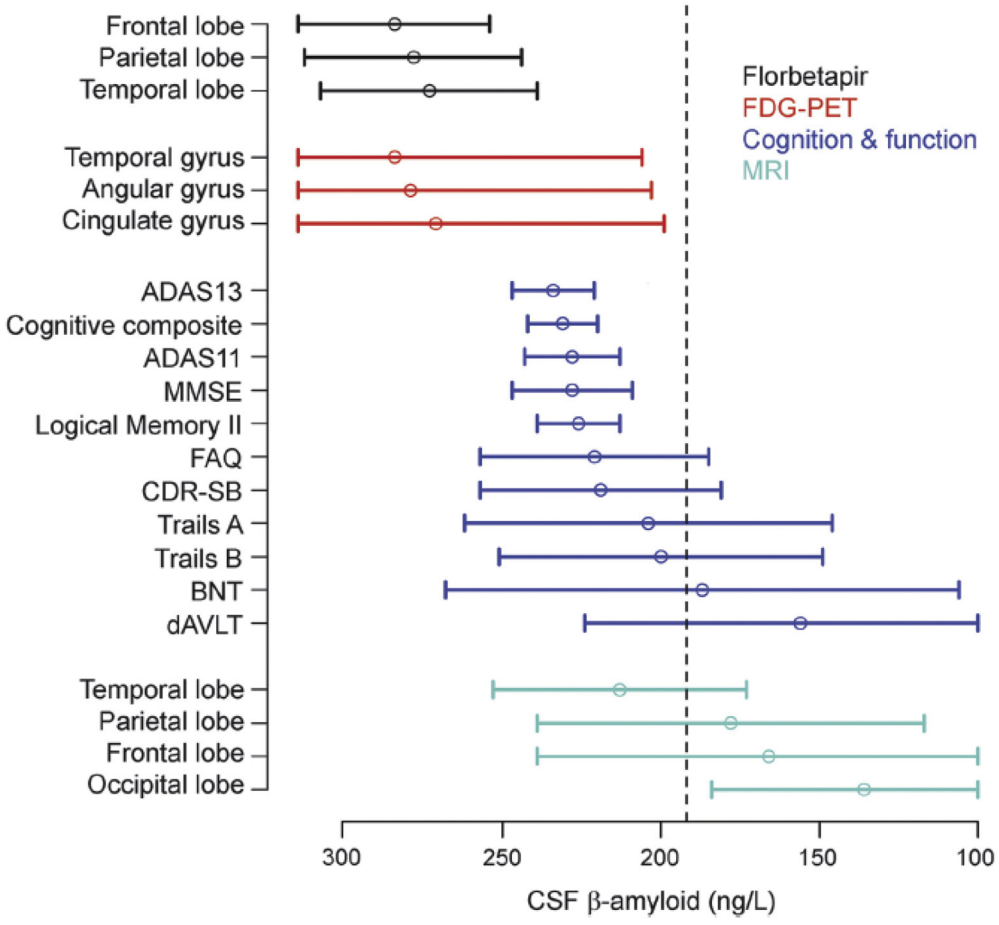

Fig. 10. Estimates of initial acceleration points for all outcomes in relation to CSF Aβ42 levels. Acceleration points are shown with 95% confidence intervals. Aβ pathology increases from left to right. The dashed black line is the conventional threshold for CSF Aβ42 levels (192 ng/mL). Abbreviations: Aβ, β-amyloid; ADAS, Alzheimer's Disease Assessment Scale; BNT, Boston Naming Test; CDR-SB, Clinical Dementia Rating Sum of Boxes; CSF, cerebrospinal fluid; dALVT, delayed Rey Auditory Verbal Learning Test; FAQ, Functional Assessment Questionnaire; FDG, ^{18}F-fluorodeoxyglucose; MMSE, Mini–Mental State Examination. Reproduced with permission from Insel et al. [49].

neural dysfunction. In addition, breakdown of subcortical WM causes a progressive anatomical disconnection of distant cortical regions [7]. Aβ+ MCI subjects displayed a progressively impaired connectome with increasing neurodegeneration, with initial alterations in the WM of the Papez circuit, followed by disconnection of the hippocampus and the amygdala from long-range subcortical brain regions [53].

CN and MCI Aβ+ subjects provide a powerful background for elucidating pathological events that occur in Aβ-dependent neurodegeneration. Consideration of CSF Aβ levels as a continuum rather than dichotomized by the 192 ng/mL cut point revealed that numerous markers appear to accelerate toward abnormality before the established cut point. Again, this sequence of events may be related to the sensitivity of the biomarkers used, and associations do not necessarily imply cause-effect relationships. However, one of the earliest events in this time frame appears to be first global then temporally and spatially divergent hypometabolism. Occurring around this time are the first changes in functional connectivity within the DMN in areas affected by Aβ deposition, implying a linkage between Aβ deposition, neuronal breakdown as measured by hypometabolism, and breakdown of functional connectivity networks. Later in the disease process, Aβ positivity is linked to successive breakdown of the connectome, along which Aβ may propagate according to some AD disease progression models (Section 2) [11,13,17,54]. The finding that changes in hypometabolism and cognition/function may occur before the Aβ42 cut point suggests that consideration of this marker as a continuous variable that can capture very early disease changes has potential in the selection of Aβ+ CN participants in clinical trials.

8. Recent insights into the role of tau in disease progression: Tau-PET imaging

Despite the associations of Aβ deposition with metabolic dysfunction, connectivity alterations, atrophy, and cognition, the exact role of tau has remained unclear. The amyloid

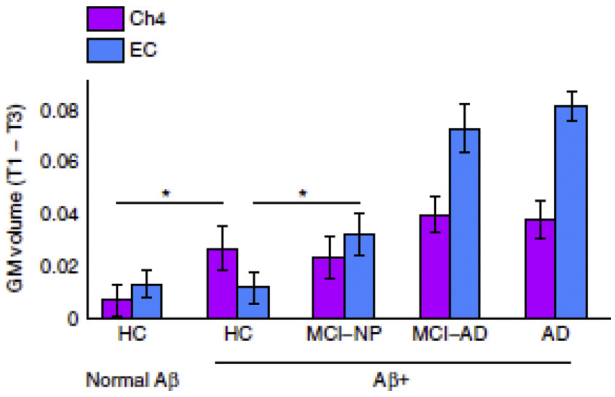

Fig. 11. Spread of atrophy from the basal forebrain to the entorhinal cortex with AD disease progression. Subgroups were delineated according to the CSF Aβ42 cut point for amyloid positivity (192 ng/mL) and then further delineated according to clinical diagnosis, yielding five subgroups: Aβ− and Aβ+ healthy controls (HC), and Aβ+ MCI nonprogressors (NP), MCI progressors (MCI-AD), and AD. Abnormal degeneration in the Aβ+ HC subgroup was isolated to the cholinergic CH4 cells of the basal forebrain. Abnormal degeneration in Aβ+ MCI nonprogressors was observed in both CH4 and the entorhinal cortex (EC). *One-tailed $P < .05$. Error bars are SEM. Abbreviations: Aβ, β-amyloid; AD, Alzheimer's disease; CSF, cerebrospinal fluid; MCI, mild cognitive impairment. Reproduced with permission from Schmitz et al. [50].

hypothesis [55,56] proposes that Aβ deposition leads to accumulation of NFTs that cause neurodegeneration. Alternatively, some evidence suggests that tau may accumulate independently of Aβ and may precede Aβ accumulation [57]. The incorporation of tau-PET imaging using flortaucipir into the ADNI-3 study has allowed investigation of this relationship and the interaction of tau with AD symptomatology. Consistent with previous pathology reports, greater binding of this ligand was observed in Aβ+ (by florbetapir PET) than Aβ− participants across the disease spectrum [58]. Moreover, flortaucipir retention in predominantly inferior parietal and lateral parietal regions was associated with antecedent longitudinal florbetapir retention in parietal and temporal regions [58] (Fig. 13). These regions significantly explained the variance in clinical outcome measures and cognitive performance, independent of the increased annualized change in florbetapir retention, suggesting that tau tangles and not Aβ plaques correlate with cognition [58]. However, regional cortical Aβ deposition mediated the effect of CSF p-tau181 on both hypometabolism [59,60] and cognitive decline and progression to dementia [61], suggesting a synergistic interaction between Aβ and tau. Similarly, a study of five different flortaucipir measures [62] found that while all measures were associated with florbetapir binding and global cognition (Mini–Mental State Examination [MMSE]), only regional flortaucipir binding in the medial temporal lobe was associated with memory (RAVLT), and hippocampal/entorhinal cortex volumes. A sharp decline in levels of CSF Aβ42 appeared to precede a rapid increase in t-tau after the onset of MCI, suggesting that tau accumulation is triggered once Aβ reaches a critical concentration [63].

The differential pattern of NFTs dependent on Aβ pathology [58] supports mechanism of transneuronal transmission of pathology along disease-specific networks. The pattern of flortaucipir binding overlapped primarily with higher order

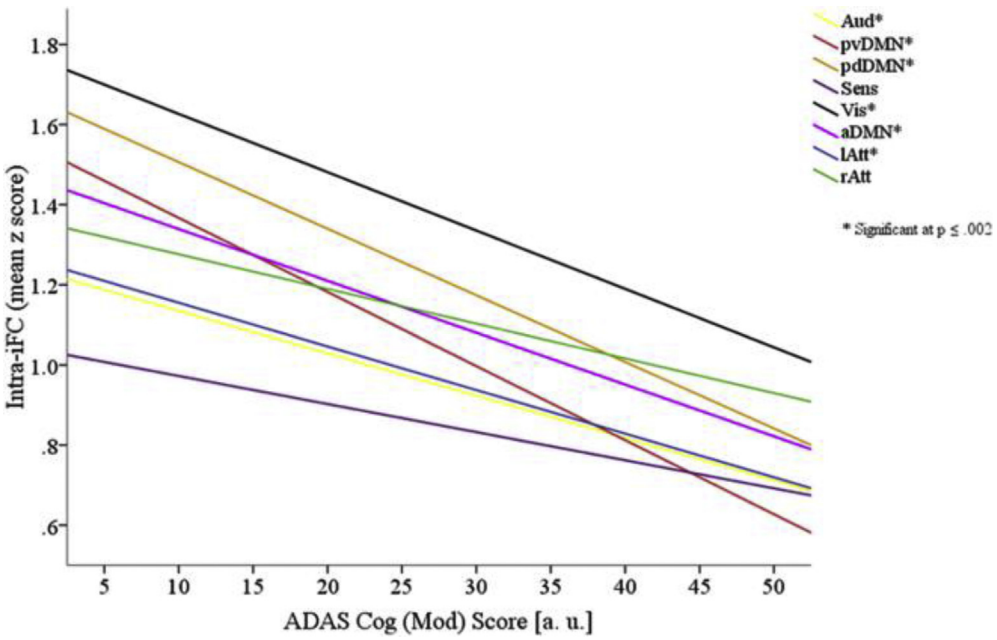

Fig. 12. Correlations of within-network intrinsic functional connectivity and cognitive impairment. Scatterplots with best-fitted linear regression lines showing intrinsic functional connectivity within each intrinsic brain network as a function of ADAS-cog (modified). Abbreviations: pvDMN, posterior-ventral default mode network; pdDMN, posterior dorsal default mode network; aDMN, anterior default mode network; Sens, sensory motor network; Vis, visual network; lAtt, left attention network; rAtt, right attention network; ADAS-cog, Alzheimer's Disease Assessment Scale–cognitive subscale. Reproduced with permission from Nuttall et al. [52].

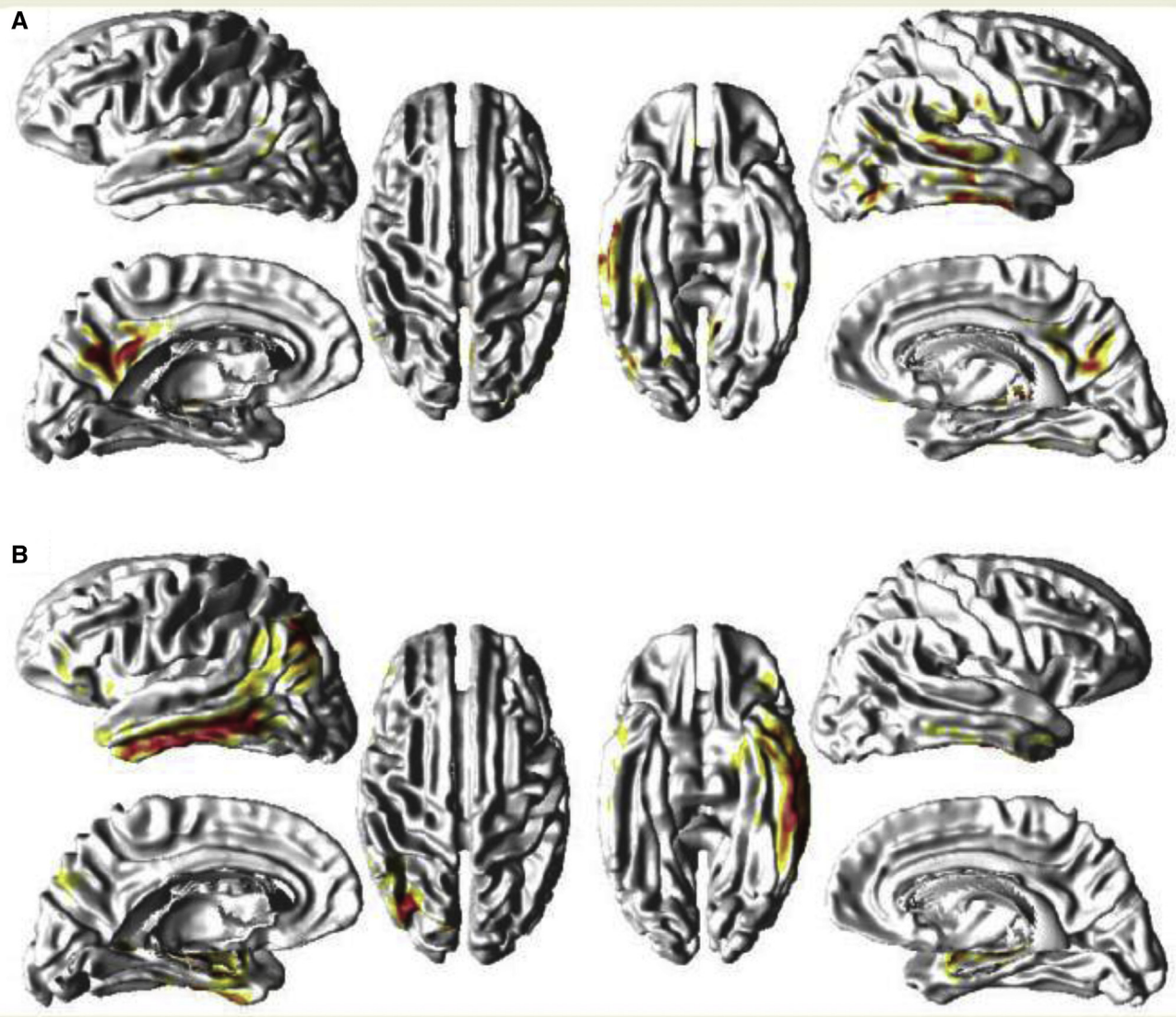

Fig. 13. Relationship between flortaucipir SUVR and antecedent annualized change in florbetapir SUVR. (A) Pattern of annualized changes in florbetapir antecedent to flortaucipir-PET scan. (B) Pattern of greater flortaucipir binding associated with greater annualized change in florbetapir pattern in panel A. Abbreviations: SUVR, standardized uptake value ratio; PET, positron emission tomography. Reproduced with permission from Tosun et al. [58].

functional cognitive rather than sensory motor networks but was not specific for the DMN or related limbic networks shown to be affected by Aβ deposition (Fig. 14) [64]. This disproportionate effect on specific subnetworks may reflect their differential vulnerability to tau accumulation and point to multiple seed points for tau deposition [62].

Tau-PET studies have shed some light on the temporal and spatial relationships between Aβ and NFT deposition. This appears to be a synergistic interaction that ultimately affects the spread of NFTs and subsequent cognitive decline.

9. Role of vascular burden

Numerous lines of evidence have pointed to the importance of disturbances to the vascular system in AD disease progression [7]. As hypertension, high cholesterol, and diabetes have long been recognized as AD risk factors [7], the question of how vascular burden affects AD disease progression is of paramount importance. Recent ADNI publications provide strong evidence for the enhancement of AD risk through cerebrovascular mechanisms and point to the potential of treating cerebrovascular disease in slowing AD disease progression.

Two statistically distinct factors of neurodegeneration in AD, one age- and vascular-related, and the other associated with "typical AD" neurodegeneration, were independently associated with CSF Aβ42, hippocampal atrophy, and cognitive decline [65]. The neurodegenerative factor was associated with cortical atrophy typical of AD, and with both CSF t-tau and p-tau181. By contrast, the age- and vascular-related factor was characterized by ventricular expansion strongly associated with age, and WM lesions of vascular origin. Cognitive decline in MCI converters was more highly associated with the age- and vascular-related factor than the neurodegenerative factor. These

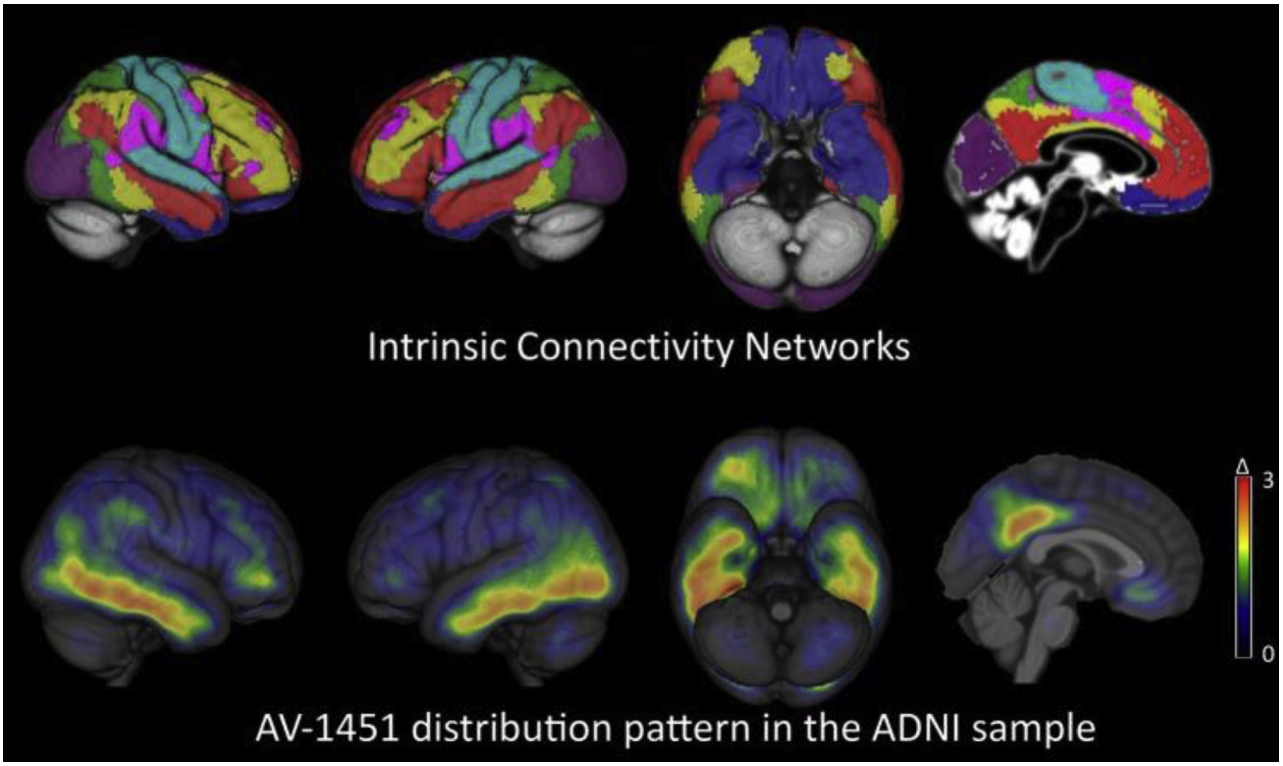

Fig. 14. Brain-wide patterns of increased tau deposition and illustration of standardized intrinsic connectivity networks. The bottom row images represent mean Z-score values. Intrinsic connectivity networks: red—default mode network; yellow—frontoparietal control network; pink—ventral attention network; green—dorsal attention network; purple—limbic network; aqua—somatomotor network; mauve—visual network. Abbreviation: ADNI, Alzheimer's Disease Neuroimaging Initiative. Reproduced with permission from Hansson et al. [64].

factors may represent two different pathologies that both affect the hippocampus, and which, in combination, may lead to a faster and more severe clinical manifestation [65]. As both these factors are Aβ related, these results imply that Aβ deposition cannot only precipitate the sequence of pathological events defined for "typical AD" neurodegeneration but may also be intertwined with vascular and age-induced changes in hippocampal atrophy and cognitive decline. Some support for these distinct factors of AD neurodegeneration comes from a study that used a vascular risk index comprising three risk factors, smoking, diabetes, and hypertension [66]. Higher scores on this index were associated with cortical thinning in temporal and frontal regions in CN and MCI subjects. These regions partially overlapped with characteristic AD cortical thinning, indicating the vulnerability of some regions to both AD-related and vascular risk factor–related neurodegeneration.

Cerebrovascular disease appears to impact many stages of AD disease progression, independently of or in concert with Aβ deposition. Vascular risk factors can impair function of cerebral small vessels and promote development of WMHs. CN subjects with both elevated Aβ burden and elevated blood pressure had proportionally greater WMH volume than accounted for by each factor alone (Fig. 15), which suggests that Aβ deposition and vascular burden interact synergistically to exacerbate WM disease in early disease stages [67]. In addition, of all AD biomarkers or cognitive tests, WMH volume best predicted Aβ deposition in Aβ+ CN subjects [68]. Both studies suggest the involvement of cerebrovascular disease very early in AD disease progression, either in the development of or as a result of Aβ deposition. Conversely, vascular burden may act independently of Aβ deposition. In CN and MCI subjects, greater baseline WMH volume was associated with greater hippocampal atrophy, after adjusting for CSF measures of AD pathology [69], and WMH volume appeared to affect DMN functional connectivity underlying cognition independently of Aβ deposition [70].

The effect of cerebral small vessel disease on brain Aβ deposition may be due to impairment of Aβ clearance via perivascular drainage of interstitial fluid into the CSF of the ventricular system [71]. One measure of cortical arterial disease is periventricular WMH load that reflects fluid accumulation in the periventricular space [71]. Parietal, occipital, and frontal periventricular WMH burden was associated with elevated cerebral Aβ, independent of age and *APOE* ε4 status, but only weakly associated with CSF t-tau and p-tau181 [72]. Moreover, both ventricular expansion and periventricular WMH burden were associated with cognitive impairment concomitantly with the replacement of functional ependymal cells with dense patches of astrocytes in which Aβ and tau accumulated abnormally [73]. As

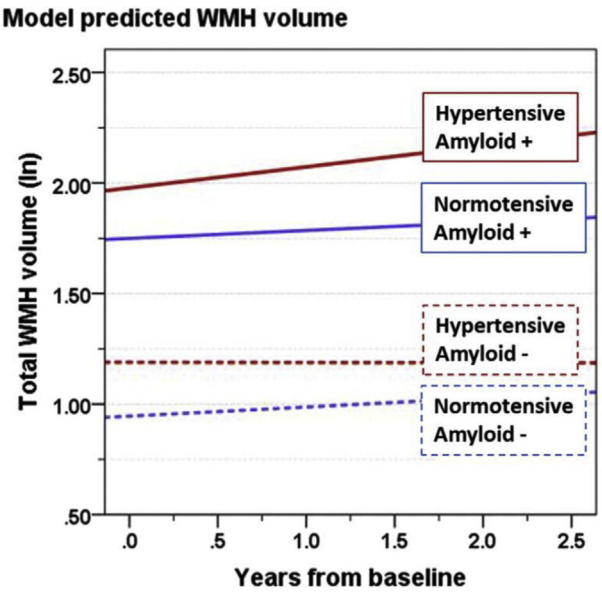

Fig. 15. The effect of blood pressure and amyloid on white matter hyperintensity volume. Estimated trends of white matter hyperintensity volume as a function of age are shown for prototype individuals dichotomized by BP and Aβ status using CSF Aβ42 cut point (192 ng/mL). Abbreviations: Aβ, β-amyloid; WMH, white matter hyperintensity; BP, blood pressure; CSF, cerebrospinal fluid. Reproduced with permission from Scott et al. [67].

ependymal cells mediate the movement of interstitial fluid into the ventricular system, and astrocytes impair the bulk flow mechanisms between interstitial fluid and CSF, these results support the putative role of WMHs in inhibiting clearance of both Aβ and tau.

The importance of vascular risk factors in cognitive decline has also been underscored by the association of gene variants underlying known vascular risk factors with cognitive decline. A risk variant for brain arteriosclerosis in *ACDC9* was associated with lower global cerebral blood flow and worse global cognition [74], and a risk variant for type 2 diabetes in *SRR* was associated with faster progression from MCI to AD [75]. A region encompassing three genes, *ICT1/KCTD2/ATP5H*, contributed to genetic risk for both ischemic stroke and AD [76].

The effect of vascular burden on AD disease progression is complex and appears to involve both Aβ-dependent and Aβ-independent pathways. Analysis of the effect of renal function on hippocampal volume and cognition provides a specific example of the complexity of the relationships between vascular burden and AD pathophysiology [77] (Fig. 16). Both vascular burden (Framingham scores) and brain Aβ deposition mediated the relationship between renal function (estimated glomerular filtration rate) and

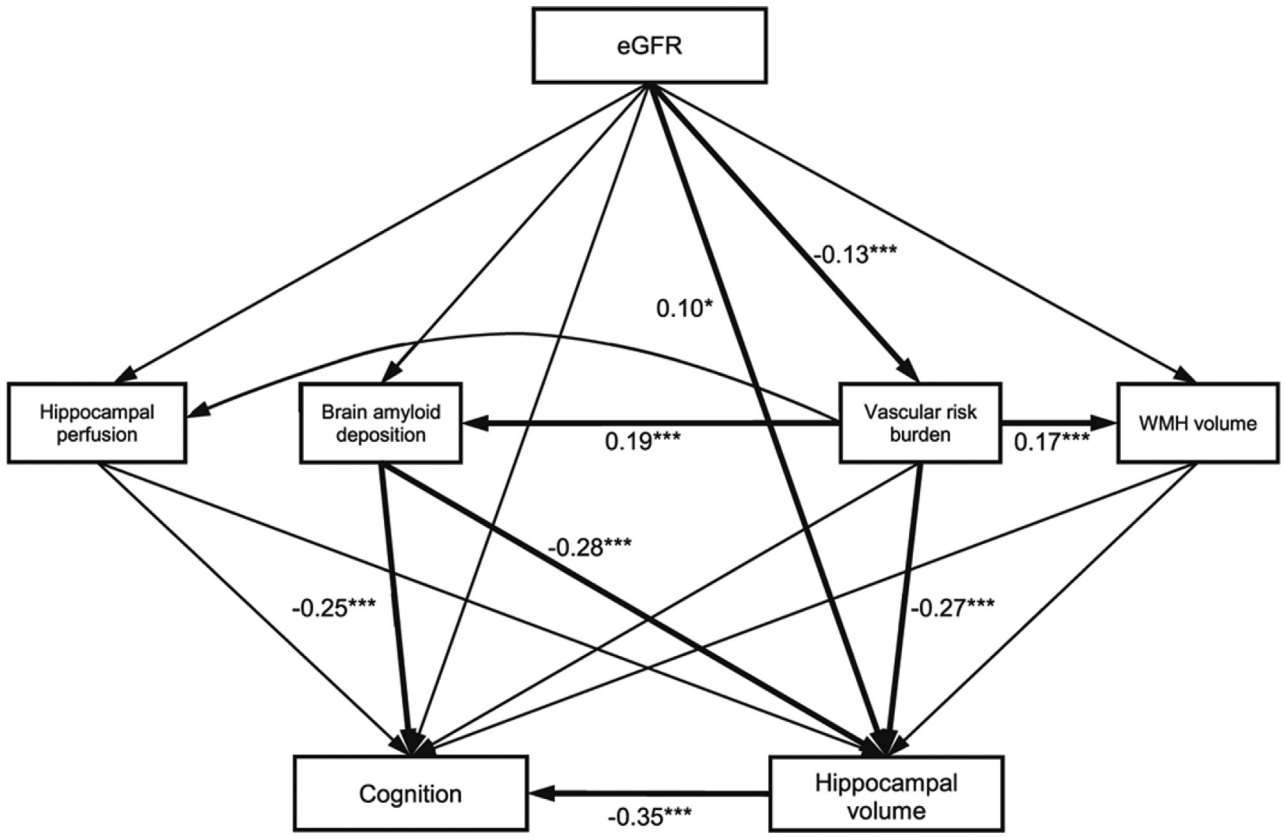

Fig. 16. Path analysis model of estimated glomerular filtration rate, hippocampal volume, and cognition. Baseline arterial spin labeling measurements of both hippocampi, amyloid PET SUVR, Framingham scores, and WMH volume measurements were entered as indicators of hippocampal perfusion, brain amyloid deposition, vascular burden, and WMH volume, respectively. All factors were entered as continuous variables. Bold arrows indicate significant associations, and numbers correspond to standardized regression weights.*$P < .05$, ***$P < .001$. Abbreviations: eGFR, estimated glomerular filtration rate; SUVR, standardized uptake value ratio; WMH, white matter hyperintensity; PET, positron emission tomography. Reproduced with permission from An et al. [77].

hippocampal volume and cognition, with vascular risk burden affecting hippocampal volume directly and via brain Aβ deposition. These studies are consistent with the "two-hit vascular hypothesis" [78] in which "hit one" is blood-brain barrier (BBB) dysfunction and reduced cerebral blood flow caused by vascular risk factors, and "hit two" is the accumulation of cerebral Aβ deposition due to both the disruption of clearance mechanisms via perivascular spaces and oligemia-induced APP processing changes. Aβ accumulation may then initiate a cascade of events involving tau, neuronal dysfunction, and cognitive decline [78] and also act synergistically with vascular risk factors to exacerbate WM disease [67]. Understanding the exact role of vascular burden in AD disease progression is of paramount importance for future AD clinical trials, as concurrent therapies targeting both "typical AD" and vascular contributions may be more effective than monotherapy.

10. Effects of insulin resistance and type II diabetes

Type 2 diabetes mellitus (T2DM), a common vascular risk factor, was previously shown to be associated with lower cortical thickness and CSF t-tau and p-tau181, but not Aβ deposition in the ADNI cohort [79]. Moreover, plasma levels of insulin-like growth factor binding protein 2 (IGFBP-2), a marker of insulin sensitivity correlated with T2DM, were associated with AD-like patterns of brain atrophy and with CSF p-tau181, suggesting that high levels of this marker may promote neurodegeneration independently of Aβ deposition [80]. Several recent ADNI papers have further investigated the role of T2DM in AD. Plasma proinsulin, the main insulin precursor, was found to be highly abnormal in MCI and AD subjects [11]. Alterations to BBB permeability may allow entrance of proinsulin to the brain where it can then induce changes in brain glucose, and in Aβ and p-tau181 regulation. A genetic study supported the influence of insulin signaling in AD disease progression [81]. A risk variant in *PPP4R3A*, a gene involved in gluconeogenesis whose increased risk expression has been linked to insulin resistance, was reported to be protective of glucose metabolism reduction in the PCC, suggesting that this variant may slow down the onset of AD pathology by the modification of insulin signaling pathways.

T2DM may act through both Aβ-dependent and Aβ-independent mechanisms. Nondemented T2DM elderly had lower global cognitive function, but no differences in Aβ deposition compared to controls [82], supporting an Aβ-independent mechanism for the effect of T2DM on cognitive decline. As the insulin growth factor (IGF) signaling pathway is implicated in the interaction between insulin and AD neuropathology, IGFBP may exacerbate IGF signaling defects in Aβ− subjects, blocking the neuroprotective effect of IGF1 and mediating neurodegeneration and cognitive decline through tau [83]. On the other hand, cognitive deficits in CN subjects with T2DM were independent of Aβ deposition [82] and high baseline levels of plasma IGFBP-2 were associated with low hippocampal volumes only among Aβ− participants (Fig. 17) [83]. MCI, but not CN or AD, patients with T2DM had lower whole-brain volume, and worse hypometabolism in the frontal lobe, sensory motor cortex, and striatum compared to MCI patients without T2DM (Fig. 18), suggesting that the additive effect of T2DM to accelerate cognitive decline in MCI patients is exerted via its effect on glucose metabolism [84].

Taken together, these results support a mechanism in which T2DM exacerbates neurodegeneration, possibly acting through its effects on glucose metabolism, and in which it acts additively with AD pathology. Mixed findings on the effect of T2DM in Aβ+ and Aβ− subjects are consistent with reported effects of other vascular factors (Section 9). Further studies will be required to untangle the complexities of the effects of T2DM on AD disease progression and to determine the contribution of Aβ-dependent and Aβ-independent mechanisms.

11. Effects of *APOE*

The ε4 allele of *APOE* is the major genetic risk factor in the development of late-onset AD and is thought to affect AD pathogenesis by both Aβ-dependent and Aβ-independent processes [85,86]. Differential affinities of *APOE* isoforms for Aβ can result in disturbance of Aβ clearance and subsequent Aβ accumulation and in the modulation of

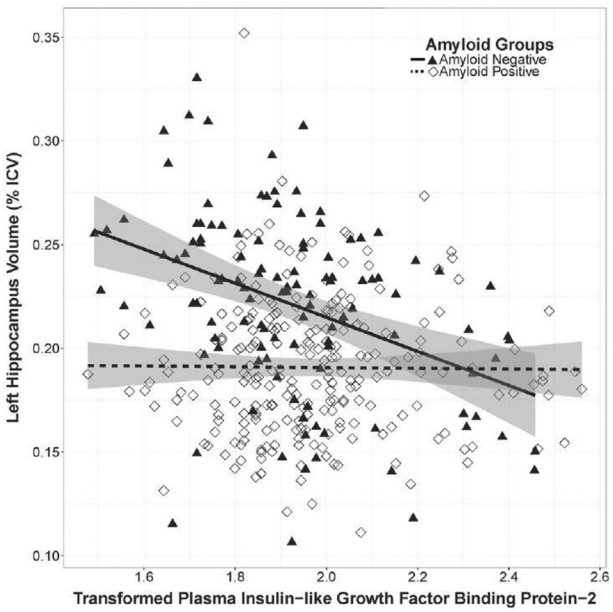

Fig. 17. Left hippocampal volume and plasma IGFBP-2 by Aβ42 biomarker status. Aβ− (dark triangle) and Aβ+ (clear diamond) participants were delineated by the threshold for Aβ positivity (CSF Aβ42 < 192 ng/mL). Gray shading represents the 95% confidence intervals. There is a negative association between increasing levels of IGFBP-2 and hippocampal volume among Aβ− individuals only. Abbreviations: Aβ, β-amyloid; ICV, intracranial volume; IGFBP-2, insulin growth factor binding protein 2; CSF, cerebrospinal fluid. Reproduced with permission from Lane et al. [83].

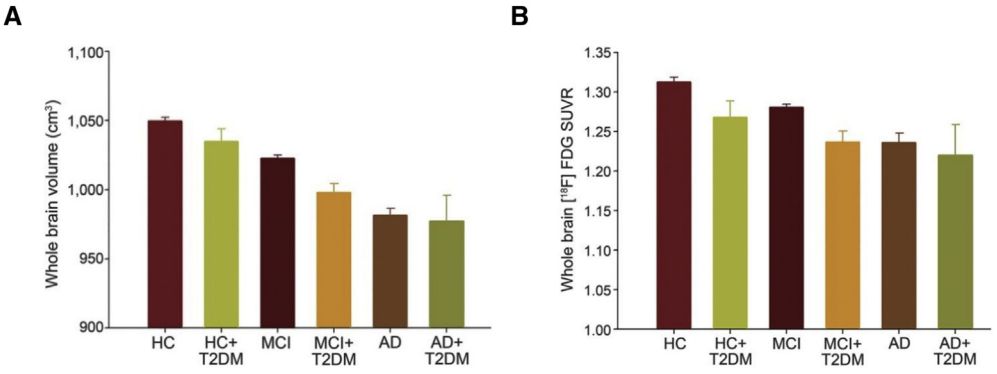

Fig. 18. Effect of type 2 diabetes on whole-brain volume and glucose metabolism. (A) Whole-brain volumes in subject groups with and without T2DM. The effects of T2DM were only seen in participants with MCI. The whole-brain volume in the MCI + T2DM group was lower than that in the MCI group ($P = .003$). (B) Whole-brain FDG SUVR in subject groups with and without T2DM. The effects of T2DM on the whole-brain FDG SUVR were only seen in participants with MCI. The MCI + T2DM group had a lower whole-brain FDG SUVR than the MCI group ($P = .04$). Abbreviations: AD, Alzheimer's disease; HC, healthy controls; MCI, mild cognitive impairment; T2DM, type 2 diabetes mellitus; SUVR, standardized uptake value ratio; FDG, fluorodeoxyglucose. Reproduced with permission from Li et al. [84].

glucose metabolism [86]. Aβ-independent aberrant proteolysis of ApoE may also generate neurotoxic fragments that stimulate tau phosphorylation, leading to cytoskeletal disruption and impairment of mitochondrial function [85]. Recent ADNI studies have shed light on both Aβ-dependent and Aβ-independent effects of the *APOE* ε4 allele.

Bozoki et al. [87] examined the effect of *APOE* ε4 status and cerebral Aβ on regional metabolism in brain regions known to be affected by p-tau181 deposition. *APOE4*+, but not *APOE4*−, Aβ+ CN individuals had increased metabolism in the entorhinal cortex and amygdala, the earliest known sites of NFT accumulation. These results suggest that the *APOE* ε4 genotype may cause the earlier emergence of clinical symptoms in AD by causing a more aggressive, compensatory metabolic response to Aβ deposition in NFT-evolving regions. Furthermore, MCI *APOE4*+/Aβ+ participants had decreased temporal lobe hypometabolism [88] and worse global cognition and memory [89,90], suggesting an interactive effect between the *APOE* ε4 allele and Aβ positivity. Aβ-independent effects of the *APOE* ε4 allele on cognition were also observed. *APOE4*+/Aβ− CN and MCI participants had reduced parietal and frontal hypometabolism [88], and in MCI participants, the *APOE* ε4 allele was independently associated with worse executive function [89]. *APOE* ε4 status was associated with cortical thinning in restricted brain regions (inferior temporal and medial orbitofrontal regions) in late MCI and AD participants, and with thickening in limbic regions vulnerable to AD pathology in CN and early MCI participants independent of Aβ status [90]. In CN and MCI participants, Aβ and *APOE* ε4 status were independently associated with cognitive impairment, but greatest impairment was observed in *APOE4*+/Aβ+ participants [90]. These results are suggestive of an *APOE* ε4-dependent mechanism of neurodegeneration that is distinct from Aβ status but also of a synergistic interaction between *APOE* ε4 and Aβ status that acts to exacerbate AD disease progression.

The *APOE* ε4 allele may enhance AD risk through cerebrovascular mechanisms. *APOE* ε4/ε4 homozygotes had a proportionally greater increase in an age- and vascular-related factor strongly related to WM damage than in a neurodegenerative factor, reflective of "typical" AD-related neurodegeneration [65]. These participants also accumulated WMHs at a faster rate than *APOE* ε3/ε4 heterozygotes or ε3/ε3 homozygotes [91], suggesting that the *APOE* ε4 allele is a major independent driver of WMH accrual. Moreover, parietal WMHs may mediate the reduction in information processing speed observed in carriers of the *APOE* ε4 allele [92].

Given that the *APOE* ε4 allele affects Aβ deposition and also interacts with cerebrovascular disease, what are the interactions between these three factors, and how do they affect cognition? In a longitudinal study of CN participants, Luo et al. [93] found that carriers of the *APOE* ε4 allele had greater baseline and faster progression of frontal WMH burden, and more abnormal levels of CSF Aβ42, which was negatively related to baseline and longitudinal total WMH burden. The interaction between frontal WMH burden, particularly in the anterior periventricular horn, and the *APOE* ε4 allele was associated with a trend in cognitive decline. These results are consistent with a mechanism in which *APOE* ε4-associated WMH damage in frontal regions leads to both impaired Aβ clearance and further accrual of WM damage especially in the hypoperfusion-vulnerable anterior periventricular horn, which in turn further impairs Aβ clearance eventually leading to cognitive decline [93].

The *APOE* ε4 allele may also exert its effect on cognition via modulation of immune response. The inflammation hypothesis of AD posits that the binding of misfolded and aggregated proteins to microglial and estrogen receptors can trigger an innate immune response characterized by the release of inflammatory factors that subsequently influence AD disease progression severity [94]. Recent ADNI papers have provided genetic [95,96] and biochemical [97,98]

evidence for the involvement of immune response in AD progression. Bonham et al. [99] reported a synergistic interaction between complement C3 of the inflammatory response and the *APOE* ε4 allele that increased Aβ and NFT pathology. They found that Aβ itself mediated the effect of C3 on p-tau181 and proposed a biological model for the interactions between C3, *APOE* ε4, and Aβ on p-tau181 (Fig. 19).

Overall, recent ADNI studies are consistent with distinct neurodegenerative pathways associated with *APOE* status. These pathways may be Aβ dependent, or Aβ independent, and some evidence supports a synergistic interaction between the *APOE* ε4 allele and Aβ that may act to influence downstream neurodegenerative processes. The effect of the *APOE* ε4 allele may be mediated by and in turn exacerbated by cerebrovascular disease, which appears to be mediated by impairment of Aβ clearance mechanisms. This suggests that the effect of the *APOE* ε4 allele is intertwined with both vascular burden and Aβ deposition. One further effect of the *APOE* ε4 allele may be in mediating the effect of inflammatory response. Clearly, this allele has far ranging effects, and recent ADNI studies have elucidated novel mechanisms of its action.

12. Amyloid-independent neurodegeneration

A total of 34% of clinically diagnosed MCI participants, and 15% of clinically diagnosed AD participants in the ADNI cohort, were reported to be Aβ− on florbetapir PET [100]. These participants were characterized as being generally less "AD-like" compared to Aβ+ participants: they had a very low frequency of the *APOE* ε4 allele (Fig. 20), higher metabolism in AD-typical temporoparietal regions, greater medial temporal volume, lower CSF p-tau181 and t-tau, and a slower decline on the MMSE and Alzheimer's Disease Assessment Scale–Cognitive subscale [100]. In addition, Aβ− MCI participants had lower rates of MCI to AD conversion, and Aβ− AD participants were more likely to be diagnosed as "possible" rather than "probable" AD. Clinically, these participants were characterized by high rates of hypertension, and a greater probability of depression medication use, which point to vascular disease and subclinical depression as potential contributors to cognitive decline in this group. As autopsy studies have found a wide variety of comorbidities in patients diagnosed with AD, it is possible that distinct neuropathologies such as TDP-43 proteinopathy, argyrophilic grain disease, hippocampal sclerosis, frontotemporal dementia, and vascular disease underlie the observed characteristics in Aβ− ADNI participants [100]. This is consistent with the well-established heterogeneity of the MCI cohort which several studies reported to contain a slow declining subgroup (Section 6).

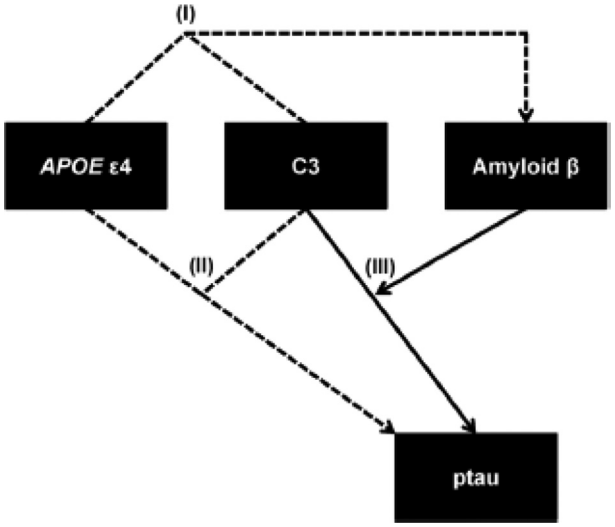

Fig. 19. Proposed biological model for the relationships between C3, *APOE* ε4, and Aβ on p-tau181. C3 and *APOE* ε4 work synergistically to elevate both Aβ and p-tau181. Aβ itself regulates the effect of the complement cascade on p-tau181. Solid arrows represent main effects of each variable, and dotted arrows represent the interaction effect of two variables, all assessed in multivariate linear models which included age, sex, and CDR-SB scores as covariates. (I) Interaction effect of C3 and *APOE* ε4 on Aβ, (II) interaction effect of C3 and *APOE* ε4 on ptau 181, and (III) the effect of C3 on p-tau181, which is mediated by Aβ. Abbreviations: C3, cerebrospinal fluid complement 3; CDR-SB, Clinical Dementia Rating–sum of boxes; *APOE* ε4, ε4 allele of apolipoprotein E. Reproduced with permission from Bonham et al. [99].

Further stratification of Aβ− ADNI MCI participants on the basis of biomarkers of neurodegeneration revealed that 25.4% of MCI patients were negative for both Aβ and neurodegeneration (A−N−), whereas 13.2% were positive for neurodegeneration alone (A−N+) [53]. The A−N− group was less impaired but had non–AD-specific short-range disconnections in structural connectivity compared to the MCI A−N+ group and CN A−N− controls [53]. The A−N+ group, previously termed as having suspected non-Alzheimer's pathology (SNAP) [7,101], had a more diffuse and weaker pattern of degeneration involving a wide cluster of structural network disconnections compared to the AD-like disconnection pattern observed in the A+N+ group (Fig. 21). This group had fewer *APOE* ε4 allele carriers than A + N + MCI subjects and was distinguished by an intermediate rate of progression to AD and hippocampal atrophy. Clinical misdiagnosis of MCI due to AD may account for some of the observed progression to AD. The wider and weaker pattern of structural network alterations may instead be indicative of multiple pathologies such as cerebrovascular disease, α-synucleinopathy, argyrophilic grain disease, TDP-43 proteinopathy, hippocampal sclerosis, or primary age-related tauopathy [53]. An alternative explanation is that many of the participants had Aβ levels close to the cutoff mark for abnormality and may in fact be A + N+ "typical AD".

Neurofilament light (NFL), a putative marker of subcortical large caliber axonal degeneration, was associated with cognitive decline and brain atrophy in Aβ− but not Aβ+ MCI and AD ADNI subjects [102]. Increased levels of CSF NFL have been observed in AD but also in other neurological conditions including subcortical vascular

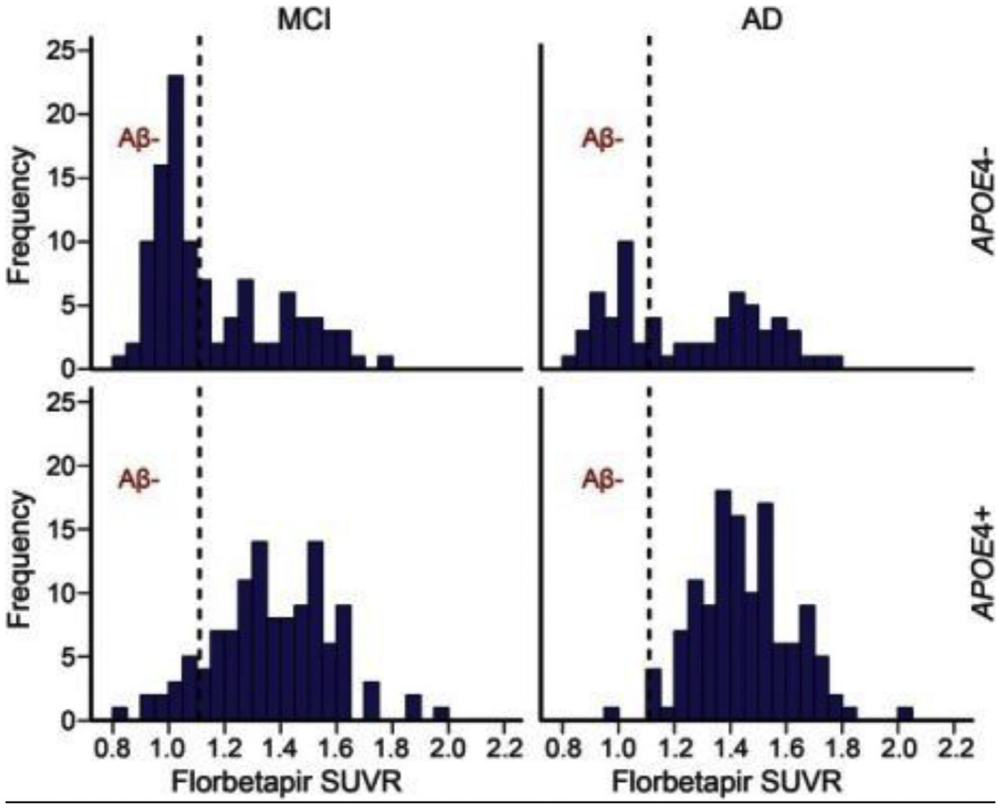

Fig. 20. Florbetapir standardized uptake value ratio distribution stratified by diagnosis and *APOE* ε4 status. The dotted lines represent the 1.11 positivity threshold for cortical summary florbetapir SUVRs. Aβ− subjects are more likely to be noncarriers of *APOE*ε4. Abbreviations: Aβ, β-amyloid; AD, Alzheimer's disease; *APOE*ε4, ε4 allele of apolipoprotein E; MCI, mild cognitive impairment; SUVR, standardized uptake value ratio. Reproduced with permission from Landau et al. [10].

dementia, frontotemporal lobe dementia, and inflammatory diseases [102]; clearly NFL is not specific for AD.

Taken together, these studies suggest that a multiplicity of etiologies may be responsible for the neurodegeneration-associated dementia in Aβ− ADNI participants. A−N− subjects may represent an earlier stage of progression to SNAP status or a separate slower declining as yet ill-defined group. A−N+ subjects may harbor a variety of underlying pathologies, may be "typical AD" with Aβ levels slightly below established cut points, or some combination of the two.

13. Role of networks in AD

The view of AD as a disconnection syndrome in which brain regions become successively disconnected both structurally and functionally during the course of AD disease progression is now well established with considerable evidence to support it [7]. Progressive alterations in brain functional networks were reported in a study, which used diffusion tensor imaging of 20 modules shown to have the best correspondence between structural and functional network modules [103]. Compared to CN participants, early MCI participants showed no significant differences in functional connectivity, but late MCI participants differed in the connectivity of a memory function subnetwork (module 18), and AD participants had widespread disconnection affecting the same memory subnetwork in addition to the DMN, medial visual network, sensorimotor network, subcortical networks, and others (Fig. 22) [103]. Increasing disconnection throughout AD disease progression was also observed using another measure of whole-brain functional network organization, eigenvector centrality, which was decreased in important nodes of the hippocampal network in progressive compared to stable MCI participants [104]. Moreover, eigenvector centrality in the left temporal pole was associated with memory function and CSF t-tau in progressive MCI participants, indicating that changes in functional network organization are associated with pathological changes [104].

Two longitudinal studies investigated changes in structural networks throughout AD disease progression. AD participants had substantially decreased fractional anisotropy and increased mean diffusivity across widespread WM tracts including the hippocampal cingulum, which likely represents AD-specific neurodegeneration [105]. Less extensive changes likely reflecting age-related deterioration were observed in CN participants [105]. Compared to CN participants, the structural network organization of stable MCI participants was characterized by longer path lengths and reduced nodal closeness centrality in the hippocampus and

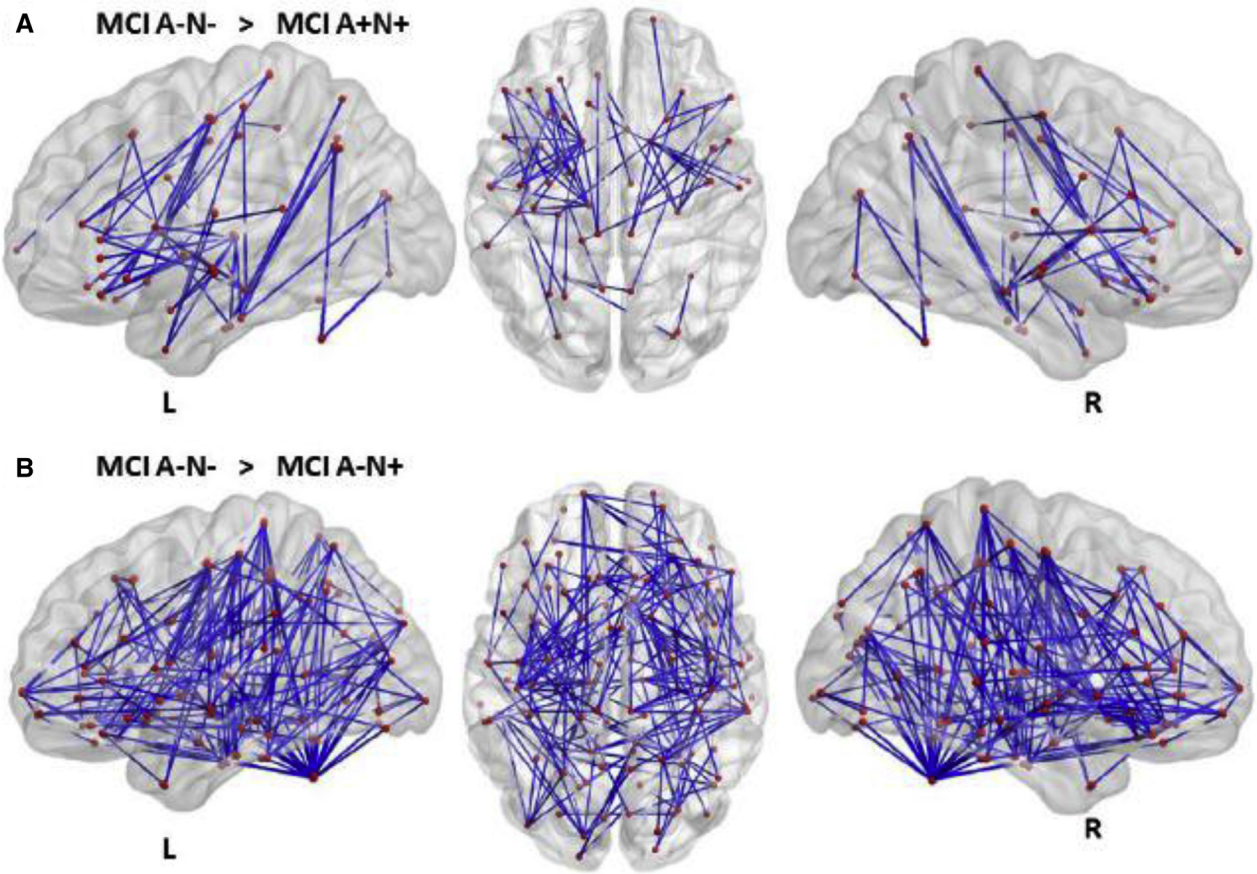

Fig. 21. Structural network-based analysis of MCI A+N+ and MCI A−N+ compared to MCI A−N−. Significant modules of impaired connection were found both in MCI A+N+ and MCI A−N+ compared to MCI A−N−. (A) A cluster of 63 disconnections and 56 modes were impaired in MCI A+N+ and compared to MCI A−N−. (B) A weaker pattern of alteration involved in a cluster of 216 disconnections and 131 nodes were impaired in MCI A−N+ compared to MCI A−N−. Abbreviations: A+/-, positive/negative for β-amyloid; MCI, mild cognitive impairment; N+/-, positive/negative for neurodegeneration. Reproduced with permission from Jacquemont et al. [53].

amygdala, indicative of reduced connections between distal brain regions [106]. In MCI participants who converted to AD within 1 or 3 years, and in AD participants, there was a progressive reduction in mean clustering coefficient and path length, suggesting a loss of connections between neighboring areas [106].

Structural covariance networks which consider the similarity between different anatomical patches and geometrically represent atrophy progression may also indicate anatomical connectivity although the biological significance of networks identified in this way is uncertain. Networks constructed from patterns of cortical thinning were more disorganized and less clustered with fewer hub regions and weaker connections in AD participants compared to CN participants (Fig. 23) [107]. A second study found the connections between 4, 290, and 74 regions were altered in stable MCI, progressive MCI, and AD participants, respectively [108]. The relative decrease in the number of altered connections in AD participants compared to those in stable MCI participants is likely due to the increased atrophy in the later stages of the disease; this yields a higher number of connected atrophic, instead of healthy, patches. Eight and seven nodes differed between AD and stable MCI, and AD and progressive MCI, respectively, of which six formed a connected brain region corresponding to the hippocampus, amygdala, parahippocampal gyrus, planum polare, frontal orbital cortex, temporal pole, and subcallosal cortex [108]. These results provide a measure of the location and quantity of atrophy in MCI and AD participants compared to healthy controls. These results support progressive disorganization of structural networks, particularly targeting the hippocampus, which reduces the ability to integrate information across distal brain regions and subsequently impairs communication between neighboring areas.

14. Effect of gender on AD disease progression

Of an estimated 5.7 million people in the United States with AD, approximately two thirds are women [109]. This is due in part to longer life expectancies, but even after accounting for the age effects, women appear to develop AD more often than men. Recent ADNI studies have investigated

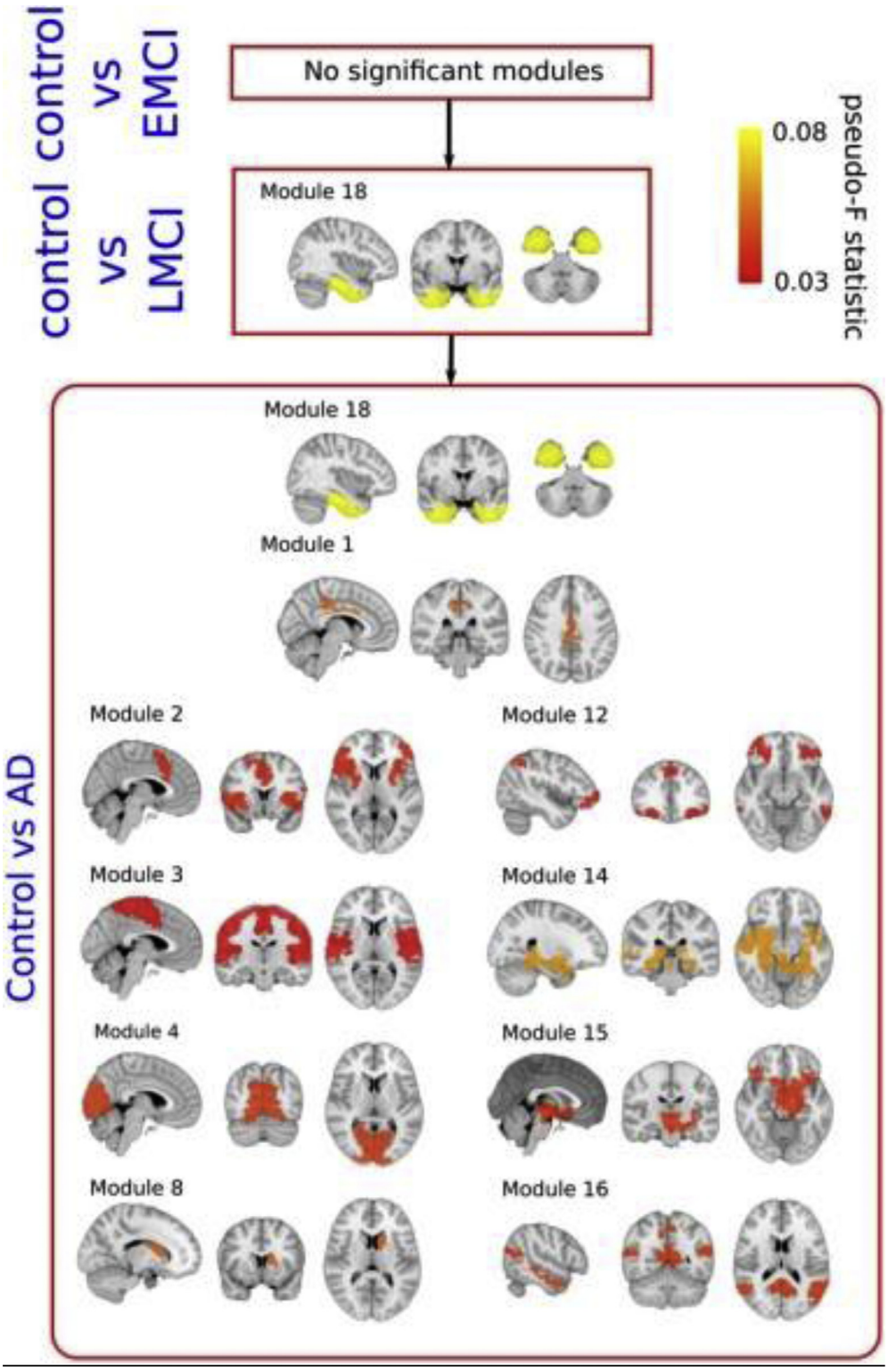

Fig. 22. Brain disconnection across AD disease progression measured by diffusion tensor imaging of 20 modules corresponding to functional networks. Brain disconnection as disease progresses is quantitatively addressed by looking at the pseudo F-statistic values of the modules. At first stages (control vs. EMCI, top), fiber deterioration is not sufficient to yield significant changes in modules connectivity patterns. In the following stage (control vs. LMCI, middle), the connectivity pattern of module 18, which involves parts of the hippocampus, entorhinal cortex, amygdala, and other memory-related areas, disconnects statistically with respect to control (P value = .007). Such connectivity differences are widely spread to the rest of the brain at the final stage (control vs. AD, bottom). Abbreviations: AD, Alzheimer's disease; EMCI, early mild cognitive impairment; LMCI, late mild cognitive impairment. Reproduced with permission from Rasero et al. [103].

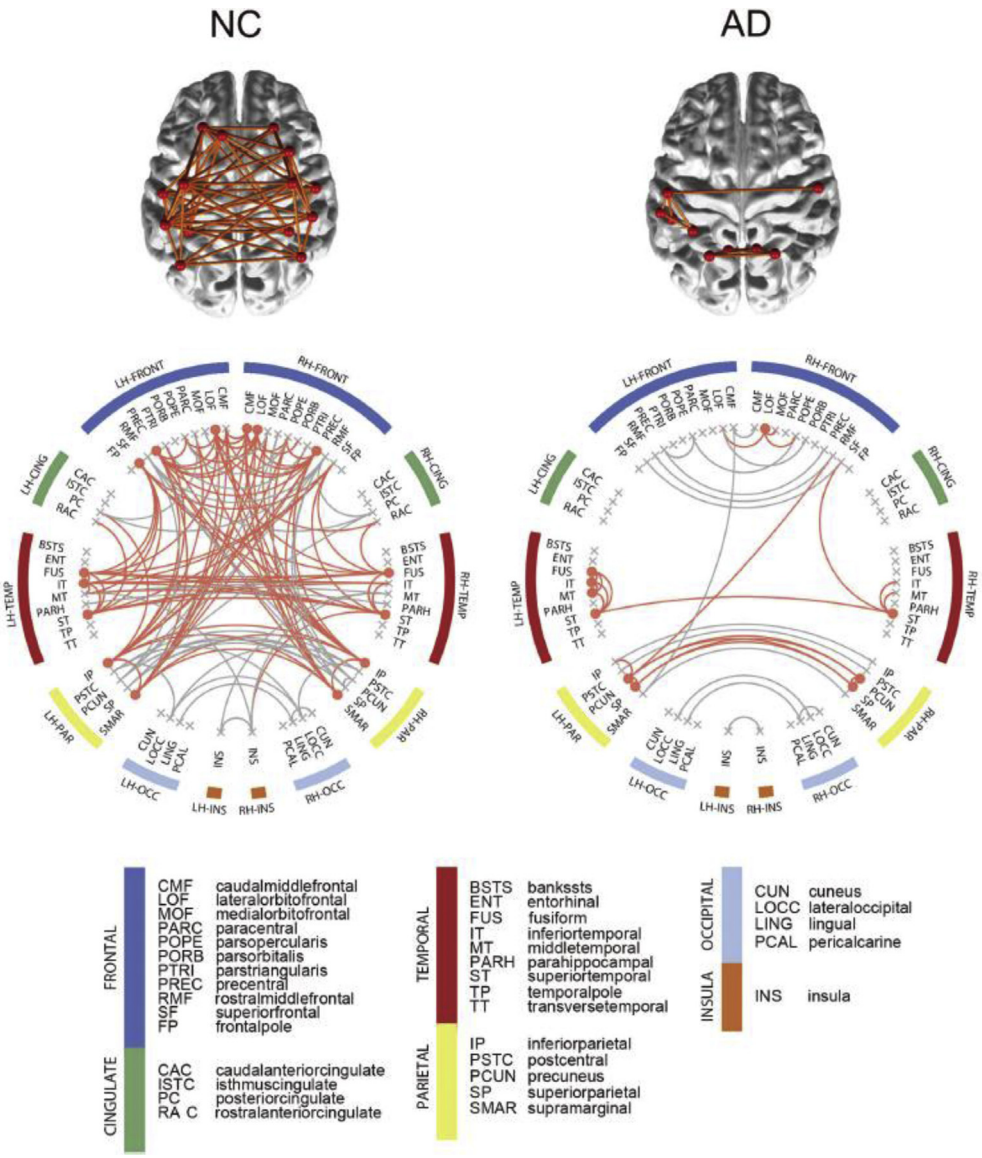

Fig. 23. Connectograms of anatomical connectivity from structural covariance networks. Group level network and its corresponding display of brain connectivity superimposed on the template brain surface. Hub regions and their connections are illustrated in orange. Connectivity is displayed only for identified hub regions. AD patients have fewer hubs, some of which are not major hubs in NC patients, and weaker connections between hubs. Abbreviations: AD, Alzheimer's disease; NC, cognitively normal controls. Reproduced with permission from Kim et al. [107].

whether gender interacts with biomarkers or *APOE* genotype to influence specific disease outcomes. Baseline hippocampal volume, but not entorhinal cortex thickness, and *APOE* ε4 status predicted MCI to AD progression in women, but not in men [110]. More rapid hippocampal atrophy and cognitive decline in women were driven by interactions between sex and Aβ42 (on hippocampal atrophy [110,111], memory [110,111], and executive function [110]), and between sex and t-tau (on hippocampal atrophy and executive function [110]), suggesting an increased susceptibility of women to the clinical effects of Aβ deposition and NFTs. An opposite sex bias was described for the contribution of WM disease to AD with the finding that male carriers of the *APOE* ε4 allele had doubled the risk of cerebral microbleeds than female carriers [112].

BDNF appears to play a role in AD disease progression [7]. A common genetic variant in *BDNF*, Val66Met (A allele of rs6265), was associated with AD in Han Chinese women and a subsequent meta-analysis found a significant association of Val66Met with AD in females only [113]. Val66Met was also associated with faster cognitive decline, lower CSF Aβ42 and higher CSF tau, and faster atrophy in females of the ADNI cohort (Fig. 24) [113]. These results suggest that *BDNF* may be a female-specific risk gene for AD. However, the sex-specific effect of the Val66Met is controversial, and a meta-analysis of case-control studies and high-

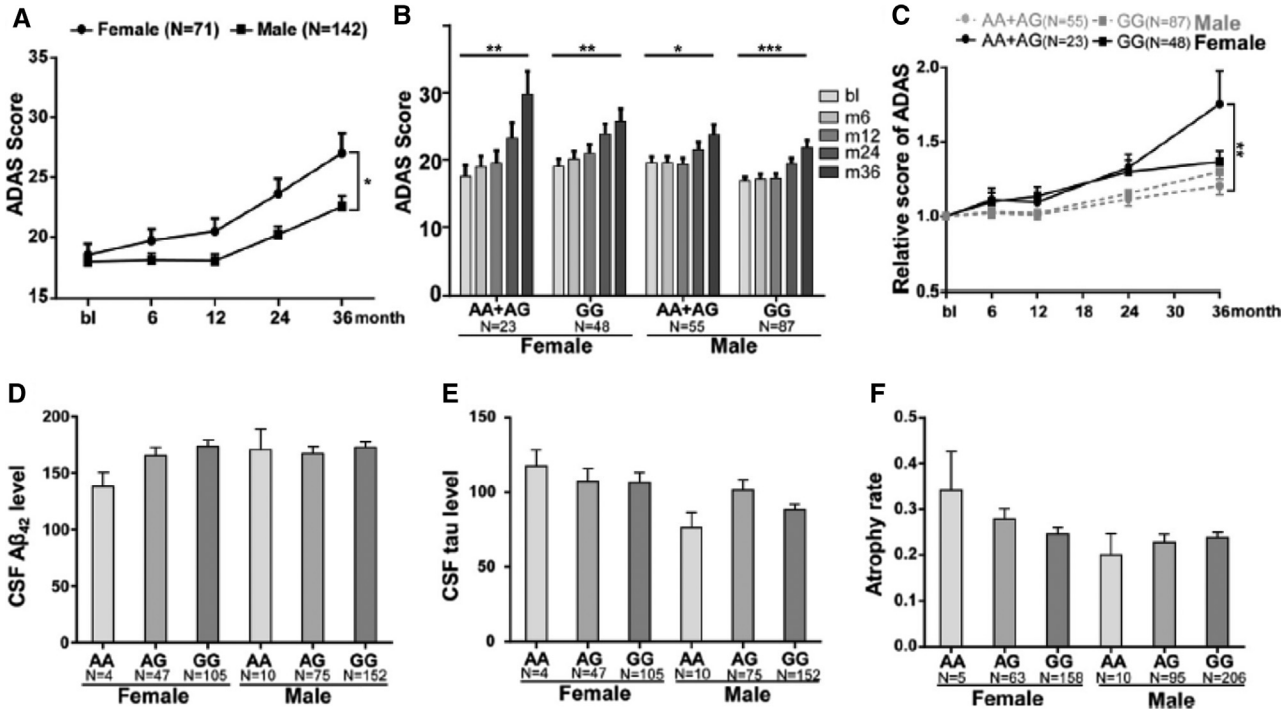

Fig. 24. Effect of BDNF Val66Met (rs6265) in males and females on AD endophenotypes in the ADNI cohort. (A) Longitudinal change in ADAS-cog scores stratified by sex. (B) Longitudinal change in ADAS-cog score was stratified by rs6265 genotype; A = risk allele (Val66Met polymorphism). (C) Cognitive decline stratified by sex and rs6265 genotype. (D) CSF Aβ42 levels stratified by sex and rs6265 genotype. (E) CSF tau levels stratified by sex and rs6265 genotype. (F) Whole-brain atrophy rate stratified by sex and rs6265 genotype. *$P < .05$; **$P < .01$; and ***$P < .001$. Abbreviations: AD, Alzheimer's disease; ADAS-cog, Alzheimer's Disease Assessment Scale–cognitive subscale; CSF, cerebrospinal fluid. Reproduced with permission from Li et al. [113].

throughput genotyping cohorts found no sexual dimorphic effects on AD susceptibility of this polymorphism [114].

15. Brain changes underlying neuropsychiatric symptoms

Neuropsychiatric symptoms (NPSs) are commonly found in AD and MCI and are thought to be associated with damage to brain regions affected in AD. David et al. [115] identified three trajectories of NPS in MCI—worsening, stable, and improving—and reported that worsening NPSs were associated with a greater risk of AD and more rapid cognitive and functional decline than stable NPSs (Fig. 25). Recent ADNI studies have sought to elucidate the neurobiology of these often devastating symptoms, with the aim of enabling more effective prevention and treatment. Anxiety and irritability were associated with regional increases in florbetapir uptake across diagnostic groups predominantly in frontal and cingulate regions, suggesting that NPS may accelerate AD disease progression by increasing deposition of Aβ [116]. Higher Neuropsychiatric Inventory scores in healthy elderly were associated with greater baseline hypometabolism in the limbic networks (PCC, ventromedial prefrontal cortex, and right anterior insula) and predicted PCC hypometabolism [117]. Sleep disorders, irritability, and lability were the main drivers of high Neuropsychiatric Inventory scores in this population and may represent an early clinical sign of AD pathophysiology [117]. Furthermore, apathy was associated with worse hypometabolism in the PCC and supramarginal gyrus [118], and depressive symptoms were associated with worse hypometabolism in the PCC and frontotemporal cortices, brain regions associated with mood [119]. Regional atrophy was also associated with NPS. Disinhibition was associated with reduced cortical thickness in the right frontopolar complex [120], delusions were associated with atrophy in the cerebellum and left posterior hemisphere [121], and apathy was associated with atrophy of medial and orbital prefrontal cortex networks [122]. Taken together, these studies indicate that NPSs are associated with regional changes to many aspects of AD progression, from Aβ deposition to hypometabolism to atrophy.

16. Mechanisms underlying resilience to AD

Asymptomatic AD is defined by having autopsy-confirmed AD neuropathology despite a lack of cognitive impairment [123]. These patients represent an extreme case of resilience to AD but other patients also have better-than-expected cognitive function for their level of neuropathology. Concepts underlying this advantage include cognitive reserve, the maintenance of function, and brain reserve, the maintenance of brain integrity, despite pathological brain changes. Cognitive reserve and brain reserve are

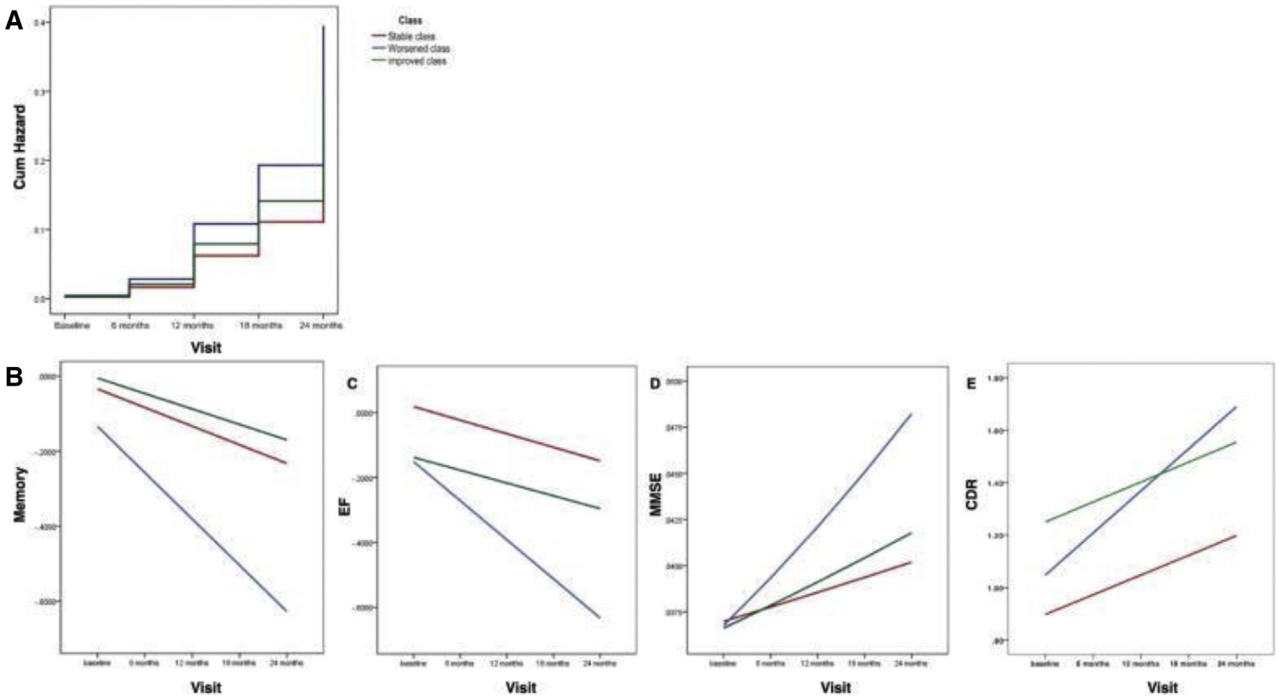

Fig. 25. Longitudinal changes of cognitive and functional outcomes by NPS trajectory. (A) Cumulative hazard of progression to AD of participants with stable (red), worsening (blue), and improving (green) NPI. Trajectories of composite memory (B), executive function (C), Mini–Mental State Examination (D), and Clinical Dementia Rating (E) in stable, worsening, and improving NPI classes. Abbreviations: AD, Alzheimer's disease; NPI, Neuropsychiatric Inventory; NPS, neuropsychiatric symptoms; EF, executive function; MMSE, Mini–Mental State Examination; CDR, Clinical Dementia Rating. Reproduced with permission from David et al. [115].

commonly operationalized by educational attainment or IQ, and intracranial volume, respectively. A higher composite global resilience factor, incorporating the disparity between CSF biomarkers and hippocampal atrophy or cognitive decline in addition to both cognitive reserve and brain reserve, was associated with slower cognitive decline [123]. The mechanisms that underlie resilience to AD, including in functional connectivity, and genetic factors have been investigated by further recent ADNI studies.

In Aβ+ MCI participants, a higher level of education was associated with higher global functional connectivity in the left frontal cortex, a region associated with IQ [124]. These participants were also better able to function with greater precuneus hypometabolism, suggesting that global frontal cortex connectivity may act to maintain episodic memory in the face of emerging temporoparietal hypometabolism [124]. In MCI participants, higher levels of education or IQ attenuated the anticorrelation between the lower anterior DMN and dorsal attention networks, alleviating the association between lower anticorrelation between these networks and lower episodic memory performance [124]. This suggests that cognitive reserve allows the maintenance of episodic memory performance by altering patterns of functional connectivity. This relationship may be maintained regardless of Aβ level. Older "supernormal" adults who maintain excellent memory were found to have increased functional connectivity within the cingulate cortex, and between the cingulate cortex and other regions involved in memory maintenance, regardless of the level of Aβ deposition [125].

Do genetic mechanisms also underlie resilience to AD? A gene interaction analysis of tissues in the brain and heart in Aβ+ participants identified genes that modified the association between Aβ and cognitive decline [126]. Imputed gene expression levels for three genes in heart tissues (*CNTLN, PROK1, PRSS50*) interacted with Aβ deposition to affect episodic memory performance, and expression levels of one gene expressed in basal ganglia (*TMC4*) and one expressed in the aorta (*HMBS*) interacted with Aβ deposition to affect executive function [126]. These candidate genes of resilience are involved in angiogenesis, heme biosynthesis, and cell cycle regulation, suggesting that these processes contribute to AD disease progression [126].

The amount of available neural substrate may also underlie the brain's ability to resist the accumulation of AD neuropathology. Variants in a major AD risk gene, *PICALM*, were associated with predominantly greater baseline thickness and slower atrophy rate of the posterior cingulate (Fig. 26) [28]. These variants may therefore act protectively against AD disease progression by increasing brain reserve in the posterior cingulate. A different mechanism was proposed for the action of the Val66Met polymorphism in *BDNF,* the protective activity of which is affected by variants in *SORL1*, an established AD risk allele [127]. In elderly

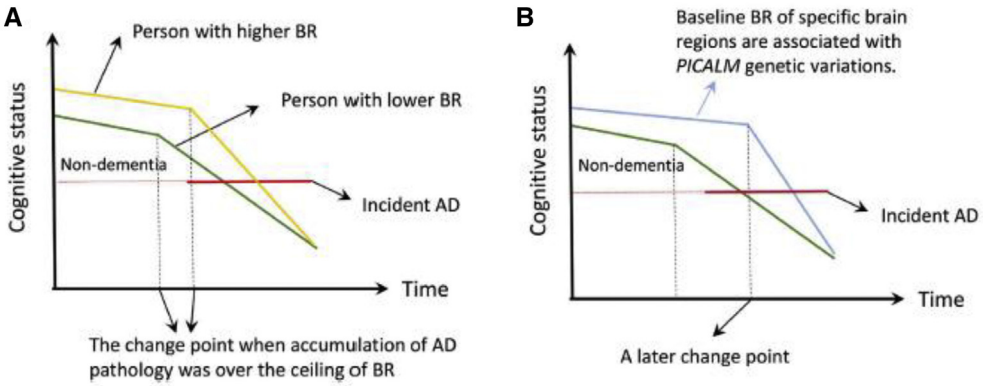

Fig. 26. Effect of *PICALM* genetic variants on the brain reserve. (A) Depiction of how brain reserve operates to protect the brain. Assuming that AD pathology accumulates at the same rate in two individuals with high and low brain reserve, the amount of pathology needed for an effect on cognitive function is greater for the individual with higher brain reserve, leading to a later point of time for change. Greater pathology will be needed for the person with higher BR to reach the clinical diagnostic criteria for AD, thus delaying the onset of the disease. Following this point, cognitive decline is faster in the individual with higher BR. (B) Hypothetical mechanism of the effect of *PICALM* genetic variants on BR. Individuals carrying specific *PICALM* genetic variants have greater baseline thickness and/or slower atrophy rate of specific brain regions for a given level of AD pathology. This allows individuals to maintain normal cognition and avoid clinically diagnosed AD for a longer period than others. Abbreviations: AD, Alzheimer's disease; BR, brain reserve. Reproduced with permission from Xu et al. [28].

without pathological AD, a *SORL1* RNA transcript that strongly regulated the interaction between *SORL1* and *BDNF* was strongly associated with diffuse rather than neuritic Aβ plaques and significantly influenced Aβ load [127]. These results implicate genetic epistasis affecting regulation of Aβ deposition as a mechanism of resilient aging.

Resilience to AD may also be gender specific. Greater educational attainment was associated with increased metabolism in posterior associative cortices and increased connectivity in the posterior DMN in men, but with increased metabolism in the anterior limbic affective and executive networks and increased connectivity in the anterior frontal executive network in women [128]. Women with MCI outperformed men with MCI in tests of verbal memory despite similar hippocampal volume: intracranial volume ratios [129], temporal lobe hypometabolism [130], and cortical Aβ load [131], suggesting that a female-specific form of resilience may delay declines in verbal memory until later in the disease process.

These studies are of great relevance to clinical trials of AD-modifying or AD-preventive therapies. The definition of resilience to AD [123] and a greater understanding of the mechanisms underlying this resilience can help select low-resilience participants with a greater likelihood of faster progression and cognitive decline, increasing power and reducing costs of these trials.

17. Defining the hippocampus

Measurement of the hippocampus is fundamental to tracking and predicting AD disease progression. Recent ADNI papers have refined and augmented our knowledge of hippocampal morphometry changes with AD disease progression and their genetic underpinnings. In CN elders, the majority of variability in hippocampal volume could be accounted for by the interaction of age and global brain atrophy with gender, education, and total intracranial volume [132], highlighting the difficulty in distinguishing between pathological effects and normal aging. The determination of normative morphometric data for subcortical brain regions [133,134] addresses this issue by allowing quantification of brain abnormalities that deviate from these norms. Accurate hippocampal segmentation is critical in determining pathological effects. Comparisons of automated hippocampal segmentation methods [135] demonstrated acceptable conformity with the gold standard HarP manual segmentation [136] but questioned their reliability for measuring longitudinal hippocampal volume changes [137].

Beyond hippocampal atrophy, the measurement of hippocampal subregions has become increasingly important in pinpointing specific disease effects in studies such as those conducted by the ENIGMA Consortium [134]. A postmortem high-resolution 7T MRI study of hippocampal subfields of CN and AD subjects revealed differential regional disease effects [138]. The CA1 and subiculum subfields were most strongly associated with AD diagnosis and neuronal loss, and the CA2 and CA3 subfields with tau burden and hippocampal volume. A second 7T MRI study in which CN participants were dichotomized by Aβ status as a proxy for normal aging (Aβ−) and preclinical AD (Aβ+) found that granular subregional morphometry outperformed whole hippocampal atrophy in detecting the very early stages of AD disease progression [139]. The CA1 region was the first hippocampal subfield to display NFT pathology (after Brodmann area 35 and the entorhinal cortex), recapitulating Braak and Braak staging [140].

ADNI genetics data have contributed to identifying novel loci underlying hippocampal volume and to identifying changes in hippocampal surface morphology associated with the *APOE* ε4 allele. Four novel genetic loci with

nonspecific (rs7020341 in *ASTN2*, rs11979341 upstream of *SHH*, and rs2289881 in *MAST4*) and/or specific (rs2268894 in *DPP4*) effects on hippocampal volume were associated with an increased risk for AD and were estimated to account for nearly 19% of hippocampal volume variance out of an estimated 70% heritability for hippocampal volume [141]. Targeting pathways related to hippocampal neurogenesis identified the minor allele of rs9608282 in *ADORA2A* as having a protective effect on hippocampal volume [142]. ADORA2A (adenosine A2a receptor) was highly expressed in the CA1 and CA2 subregions, both of which are sites of neurogenesis. Finally, the *APOE* ε4 allele has strong gene dose effects on hippocampal surface morphometry over 12 months, with deformations of the left hippocampus becoming progressively more pronounced in ε4 heterozygotes and homozygotes compared to noncarriers of the allele [143].

18. Determination of the sequence of biomarkers for multimodal classification

The efficacy of multimodal classification is well established [7], but the simultaneous measurement of all biomarkers required for this approach is time consuming, costly, and invasive. Two studies have focused on determining sequences of biomarkers to optimize cost and benefit in the clinical setting. Prediction of MCI to AD conversion is complicated by the heterogeneity of MCI participants. MCI participants were classified as high-risk converter, slowest converter, and inconclusive by an individualized sequence of a limited set of baseline biomarkers [144]. An optimal sequence of three biomarkers (hippocampal volume, CSF tau, and regional hypometabolism) in combination with age identified MCI participants at high risk for conversion while minimizing cost and time [144]. An alternative approach analyzed the benefit of the sequential addition of each biomarker beginning with the use of ADAS-13 to characterize cognitive status [145]. A combination of cognition, neurodegeneration, and amyloidosis status was highly effective at overall risk stratification (Fig. 27). ADAS-13 had the highest effect size in differentiating stable MCI from progressive MCI, and CSF p-tau181 had the highest incremental value of neurodegeneration markers (CSF p-tau181, hippocampal volume, regional hypometabolism) when added to ADAS-13. However, the incremental benefit from the next sequential biomarker was largely dependent on the preceding biomarker; FDG-PET only outperformed hippocampal volume in MCI subjects with relatively preserved cognition, and CSF Aβ42 only provided benefit in subjects with abnormal CSF p-tau181 (Fig. 27) [145]. Both studies highlight the potential of the use of sequential biomarker testing to optimize clinical approaches to AD diagnosis.

19. Novel blood- and CSF-based biomarkers

Much effort has been devoted to the identification of predictive biomarkers in blood instead of CSF given that the collection of CSF by lumbar puncture is invasive and not without risk. Previous papers have identified panels of blood-based biomarkers [7], but few have reached the level of accuracy required for clinical applications. ADNI papers from 2016 to 2017 have described a variety of approaches to make the use of blood biomarkers more viable in the clinical setting. Very promising results were reported from a small proof-of-concept study that identified a panel of autoantibodies in the serum of MCI Aβ+ participants [146]. The top 10 autoantibodies distinguished MCI from CN participants with an accuracy of 98%, a sensitivity of 96%, and a specificity of 100% and were also able to distinguish AD from other diseases such as Parkinson's disease, suggesting a specificity for AD [146]. A panel of six blood biomarkers (α−1 macroglobulin, α−1 antitrypsin, α−2 macroglobulin, ApoE, complement C3, pancreatic polypeptide) discriminated CN from AD participants with a sensitivity of 85.4% and a specificity of 78.6%, which was judged to be sufficiently high for use as a clinical screening tool for AD diagnosis from blood samples [147].

Another focus has been the identification of novel CSF biomarkers for the diagnosis of MCI and AD. Two CSF biomarkers, neurogranin and NFL, were associated with cognitive decline in Aβ+ participants and atrophy in Aβ− participants, and their addition to CSF t-tau increased the accuracy of CN versus AD classification [102]. However, plasma NFL was reported to be positively associated with age and negatively associated with global cognition, suggesting that this biomarker is not sufficiently specific for diagnosis of MCI and AD [148]. Levels of CSF autotaxin, a marker for metabolic syndrome, were found to be elevated in MCI and AD and associated with regional hypometabolism, executive function, memory, prefrontal cortical thinning, and levels of CSF t-tau [149]. Given the growing recognition of the importance of vascular factors in AD, CSF autotaxin may prove to be an important complementary addition to existing CSF biomarkers.

Many biochemical processes are affected in AD. These include not only APP metabolism, Aβ neurotoxicity, and tau protein phosphorylation but also mitochondrial dysfunction, inflammation, insulin resistance, and oxidative stress among others [36]. To investigate these biochemical processes, ADNI has partnered with the Alzheimer's Disease Metabolomics Consortium to create a standardized metabolomics data set [150]. This metabolomics approach, which can simultaneously measure thousands of metabolites in serum samples from ADNI participants, aims to discover metabolic failures correlated with AD disease progression by studying changes in networks of metabolites that reflect interconnected chemical reactions [150]. In CN participants, changes in types of sphingomyelins and phosphatidylcholines were associated with abnormal CSF Aβ42, which may indicate early neurodegeneration caused by disruption of specific membrane structures by Aβ and subsequent membrane dysregulation (Fig. 28) [36]. In MCI and AD participants, CSF tau was related to long-chain acylcarnitines

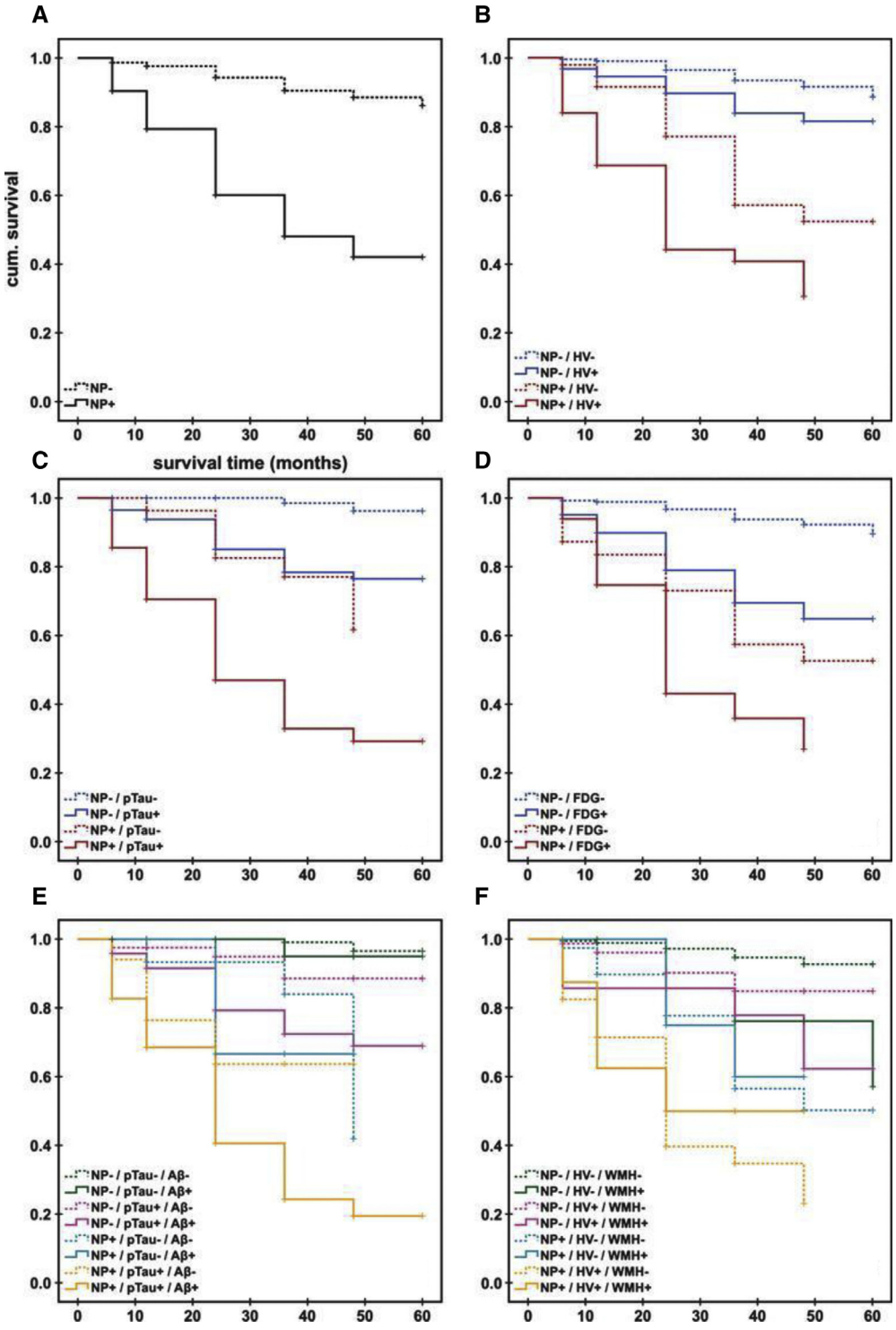

Fig. 27. Kaplan-Meier survival curves for the sequential addition of biomarkers in MCI participants. (A) Initial risk stratification based on neuropsychological performance (ADAS-13). Subsequent stratification with (B) hippocampal volume, (C) CSF p-tau181, or (D) regional hypometabolism (FDG-PET t-sum score). (E) Subsequent stratification with the combination of CSF Aβ42 and p-tau181. (F) The survival curves for the "medium cost" scenario were MRI (hippocampal volume and WMH load) but neither CSF nor FDG-PET. Survival time is given in months. "-"/"+" indicates negative/positive for AD characteristic alteration according to the corresponding cutoff. Abbreviations: ADAS-13, Alzheimer's Disease Assessment Scale–13-item subscale; CSF, cerebrospinal fluid; FDG-PET, fluorodeoxyglucose positron emission tomography; MCI, mild cognitive impairment; MRI, magnetic resonance imaging; WMH, white matter hyperintensity. Reproduced with permission from Lange et al. [145].

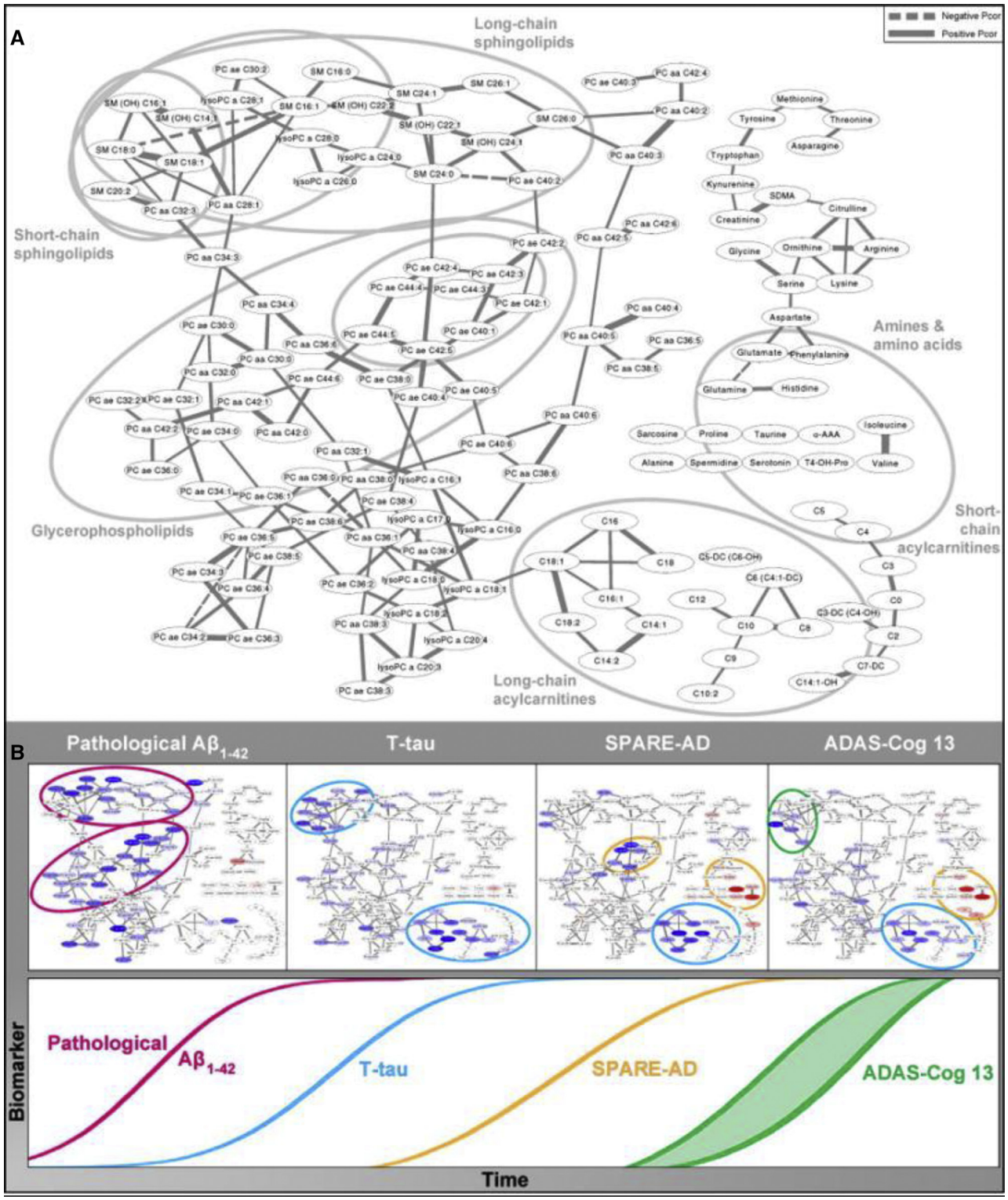

Fig. 28. Network model showing metabolic pathways correlated with the temporal evolution of biomarkers and clinical variables in AD. (A) Partial correlation network. Gaussian graphical model of metabolite concentrations showing reconstructed metabolic pathways and highlighting of the different modules involved in the steps along the temporal evolution of biomarkers and clinical variables in AD. Nodes in the network represent the metabolites, and edges (lines) illustrate the strength and direction of their partial correlations. Labels show the major classes of metabolites. Gray circles outline the modules highlighted in panel B. (B) Schematic diagram of the model of temporal evolution of biomarkers in AD, augmented with colored versions of the network from panel A. In these networks, nodes are highlighted according to the strength and direction of the metabolite's association with the respective clinical trait with blue as positive and red as negative. Significant associations are colored in dark blue/bright red, and weaker (but at least nominally significant at 0.05) associations are displayed in fainter colors. Modules of metabolites implicated in the respective trait are highlighted by circles colored by their first occurrence in the temporal order following the color scheme of the time sequence on the bottom. Abbreviations: AD, Alzheimer's disease; ADAS-Cog13, Alzheimer's Disease Assessment Scale–13-item cognitive subscale; BCAA, branched-chain amino acid; PC, glycero-phosphatidylcholines (*aa* = diacyl, *ae* = acyl–alkyl); SM, sphingomyelin; SPARE-AD, Spatial Pattern of Abnormalities for Recognition of Early Alzheimer's disease. Reproduced with permission from Toledo et al. [36].

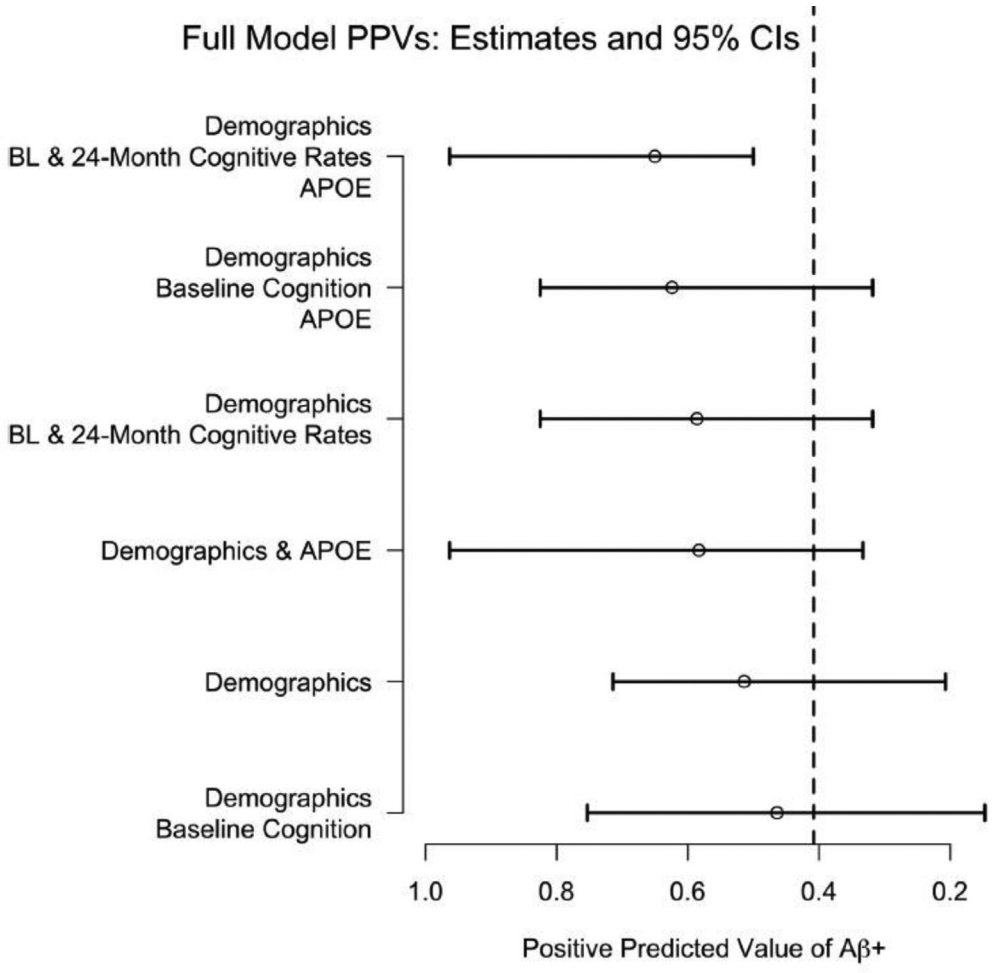

Fig. 29. Positive predicted value estimates of predictors of Aβ positivity. PPV estimates and 95% confidence intervals are shown for seven different groups of predictors. The vertical dashed black line is the reference PPV for the full cohort. Abbreviations: Aβ, β-amyloid; *APOE,* apolipoprotein E; BL, baseline; CI, confidence interval; PPV, positive predicted value. Reproduced with permission from Insel et al. [151].

and sphingomyelin which are implicated in mitochondrial function, energetics, and neurotransmission in the brain. In AD participants, brain volume changes were related to branched-chain amino acids and short-chain acylcarnitines indicative of a shift in utilization of fatty acids and amino acids instead of glucose as energy substrates (Fig. 28) [36]. The cause-effect nature of these associations is very unclear. The authors suggest that these results may indicate early changes in the lipid raft composition associated with Aβ abnormalities leading to altered mitochondrial membrane composition, subsequently resulting in loss of membrane potential and the requirement for alternative energy substrate utilization [36].

20. Novel predictors of amyloid burden

As clinical trials of AD-modifying treatments move toward preclinical populations, many, in particular those of antiamyloid drugs, require evidence of Aβ positivity for inclusion. This currently involves screening of large numbers of participants with costly, time consuming, and/or invasive tests of either cortical Aβ binding using florbetapir PET or CSF Aβ42 levels. Several recent ADNI papers have evaluated alternative approaches for predicting Aβ burden with the aim of developing a fast and cost-effective screening method. Insel et al. [151] reported that a combination of easily obtained demographic data comprising age, *APOE* ε4 status, baseline cognition, and 24-month rates of cognitive decline had a positive predictive value of 0.65 for Aβ burden, a 60% increase over the reference proportion of 0.41 (Fig. 29). Used as a prescreening tool in a clinical trial aiming to recruit 1000 Aβ+ participants, this method could reduce the number of people undergoing Aβ biomarker screening from 2451 to 1539, substantially reducing screen fails and therefore costs [151]. Aβ-PET imaging and CSF methods may be hard to implement in some global clinical trial sites, whereas MRI is more widely available. A multimodal classifier that used a structural MRI signature of Aβ positivity in addition to baseline demographics, baseline cognition, and *APOE* ε4 status was able to distinguish

florbetapir-positive from florbetapir-negative mild AD subjects from the global phase 3 EXPEDITION trials with an accuracy of 83%, a sensitivity of 94%, a specificity of 55%, a positive predictive value of 85%, and a negative predictive value of 78% [152]. Subjects who were imputed to be Aβ+ had more rapid cognitive and functional decline (Fig. 30). These results suggest that MRI may be useful globally in screening for Aβ positivity in the absence of conventional forms of Aβ measurement [152]. Finally, Voyle et al. [153] identified five blood metabolite markers (phosphatidylethanolamine, a phosphatidylcholine, and two isotopes of anandamide, and one unidentified metabolite) that predicted neocortical Aβ burden with an accuracy of 72% which was increased to 79% with the addition of fibrinogen gamma chain. These results suggest that a simple blood test for these metabolites could also function as a prescreening tool to identify Aβ+ participants. Overall, a variety of approaches show promise in reducing costs associated with selection of Aβ+ subjects in clinical trials and in the elimination of subjects unlikely to clinically progress on the desired trajectory.

21. Novel approaches for disease staging

Expanding knowledge of AD disease progression has guided the investigation of disease staging methods in heterogeneous CN and MCI groups with the aim of better predicting the likelihood of patients to progress to a later disease stage. Some recent ADNI papers have evaluated and extended the utility of the 2011 National Institute of Aging–Alzheimer Association (NIA-AA) criteria [154,155] and International Working Group-2 (IWG-2) [156] criteria while others have investigated novel staging methods.

A comparison of 2011 NIA-AA and IWG-2 criteria for MCI diagnosis and prognosis [157] found that application of the IWG-2 criteria resulted in the classification of a number of MCI subjects as not having prodromal AD, but then progressing to AD (Table 3). This may be due to the inclusion of subjects with SNAP or isolated Aβ pathology (IAP) that is likely either an early stage in which neuronal injury has not yet been seen or another amyloid-related disease. By contrast, NIA-AA criteria identified both these heterogeneous groups (Table 3). A second study considered the effect of conflicting CSF biomarkers on progression risk in ADNI MCI participants classified using NIA-AA criteria [158]. Subjects positive for CSF Aβ42 but positive or negative for CSF p-tau181 or t-tau had an intermediate rate of conversion to AD, whereas subjects negative for CSF Aβ42 but positive for CSF p-tau181 or t-tau had the second slowest rate of conversion to AD after those subjects negative for all CSF biomarkers (Fig. 31). Approximately half

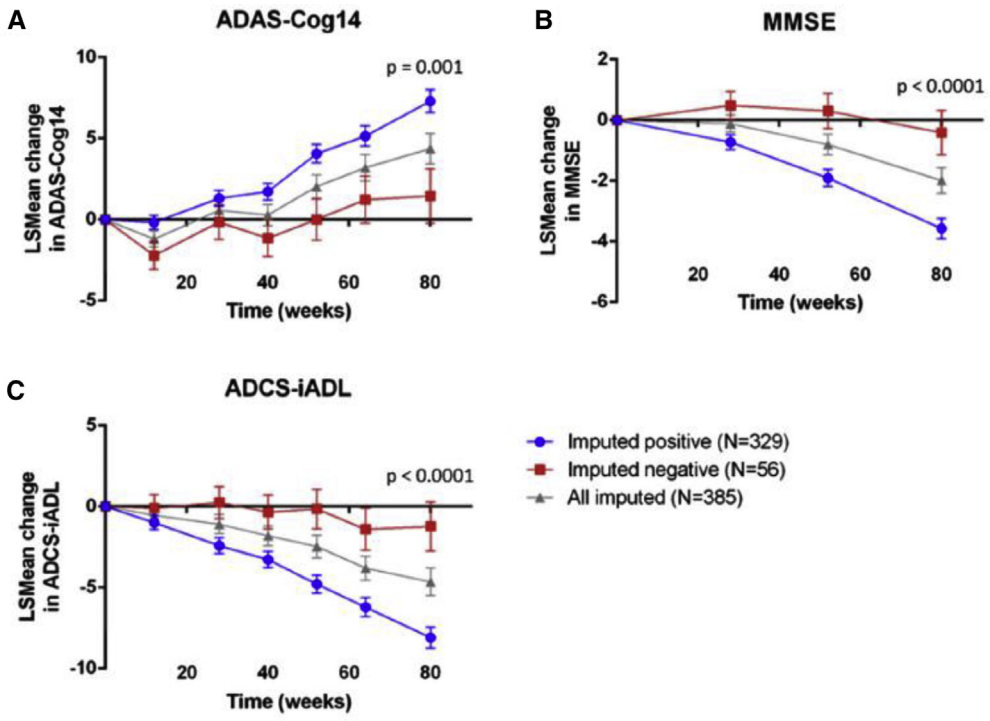

Fig. 30. Trajectories of cognition for imputed Aβ-positive and imputed Aβ-negative mild AD subjects. Change from baseline in (A) ADAS-Cog14, (B) MMSE, and (C) ADCS-iADL over 80 weeks for placebo-treated subjects from the EXPEDITION trials imputed as Aβ negative (red squares) or Aβ positive (blue circles), and the full test mild AD population (gray triangles). *P* values referred to the comparison between the imputed positive and imputed negative subgroups, shown for the 80-week time point. Abbreviations: Aβ, β-amyloid; AD, Alzheimer's disease; ADAS-Cog14, Alzheimer's Disease Assessment Scale–14-item cognitive subscale; ADCS-iADL, Alzheimer's Disease Cooperative Study–Instrumental Activities of Daily Living; MMSE, Mini–Mental State Examination. Reproduced with permission from Tosun et al. [152].

Table 3
Classification of MCI cohort according to NIA-AA and IWG-2 criteria

Criteria	Classification	Defining features in addition to any cognitive impairment	Classification of MCI subjects (%)	Progression to AD (%)*
NIA-AA [155]	Low AD likelihood group	Normal amyloid and neuronal injury markers	19	5
	High AD likelihood group	Abnormal amyloid and abnormal neuronal injury markers	46	59
	Conflicting—isolated amyloid pathology group	Abnormal amyloid and normal neuronal injury marker	6	22
	Conflicting—suspected non-Alzheimer's pathology group	Normal amyloid and abnormal neuronal injury marker	29	24
IWG-2 [156]	No prodromal AD	Normal CSF Aβ42 and/or tau or normal amyloid PET scan	47	21
	Prodromal AD	Abnormal CSF Aβ42 and tau or abnormal amyloid PET scan	53	50

Abbreviations: AD, Alzheimer's disease; CSF, cerebrospinal fluid; MCI, mild cognitive impairment; PET, positron emission tomography; NIA-AA, National Institute of Aging–Alzheimer Association; IWG-2, International Working Group-2.

NOTE. Amyloid marker = CSF Aβ42, neuronal injury marker = CSF tau/medial temporal lobe atrophy score/hippocampal volume/FDG PET.

*Over 3 years.Adapted from [157].

of MCI subjects had conflicting CSF biomarker constellations, including the SNAP and IAP groups [158]. Reclassification of ADNI CN, MCI, and AD subjects using IWG-2 criteria (memory scores and at least one of CSF Aβ42, CSF tau, or Aβ PET) identified 41% of CN participants as having asymptomatic AD, and 37% of MCI subjects and 84% of AD subjects as having "typical" AD [159]. These studies suggest that although NIA-AA and IWG-2 criteria appear able to select MCI participants with the highest probability of conversion for clinical trials, and the IWG-2 criteria appear able to select CN participants with asymptomatic AD, further refinements may improve disease staging and the ability to detect atypical groups such as SNAP and IAP. In 2018, the NIA-AA updated their criteria, emphasizing the importance of biomarkers in a biological definition of AD [160]. This "A/T/N" classification scheme includes evidence of both Aβ and tau deposition in addition to evidence of neurodegeneration, as proposed by previous studies [161,162]. Analyses of these criteria will be described in future reviews.

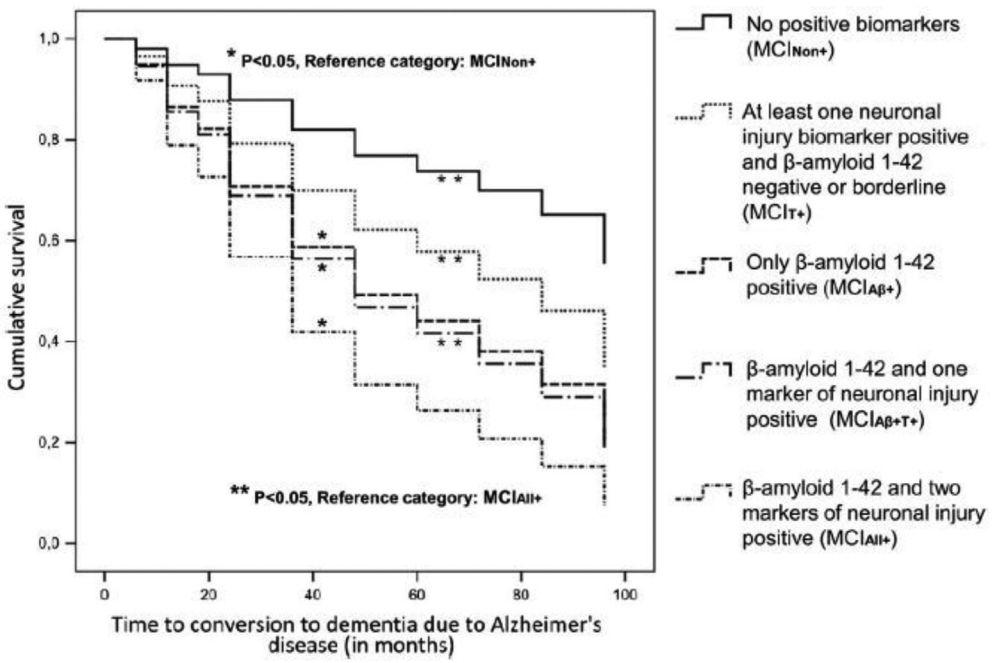

Fig. 31. Cox regression survival curves for MCI patients staged using CSF biomarkers of amyloid deposition and neuronal injury. Abbreviations: MCI_{Non+}, MCI without positive CSF biomarkers; $MCI_{A\beta+}$, MCI with positive Aβ42 and negative or borderline p-tau181 and t-tau; $MCI_{A\beta+T+}$, MCI with positive Aβ42 and positive p-tau181 or t-tau; MCI_{All+}, MCI positive for Aβ42, p-tau181, and t-tau; MCI_{T+}, MCI with negative or borderline Aβ42 and at least p-tau181 or t-tau positive; Aβ, β-amyloid; CSF, cerebrospinal fluid; MCI, mild cognitive impairment. Reproduced with permission from Alexopoulos et al. [158].

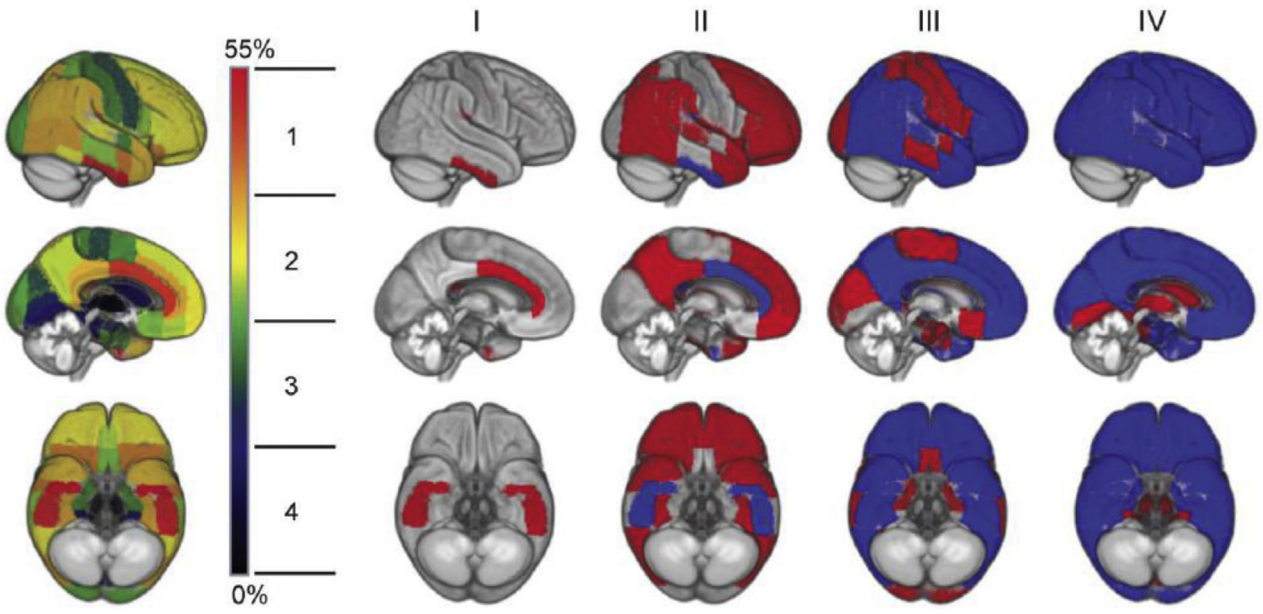

Fig. 32. Progression of regional amyloid deposition defined by in vivo amyloid imaging by stage. (Left) Brain renderings illustrating the frequency of regional amyloid positivity across individuals on a color scale from blue/black (lowest) to yellow/red (highest). (Right) Four-stage model of regional amyloid progression (I–IV) defined by involvement of unique anatomic divisions affected by stage (in red) in addition to the affected areas of the previous stage (blue). Reproduced with permission from Grothe et al. [165].

As clinical trials move toward enrolling preclinical participants, staging of CN subjects to select those likely to progress has become of paramount importance. Three preclinical stages were defined by 2011 NIA-AA criteria [154] using evidence of amyloidosis (A) and neurodegeneration (N): stage 0 – A−N−, stage 1 – A + N−, stage 2 – A + N+, and stage 3 – A+N+ and very subtle cognitive impairment. A study investigating cortical thickness changes in relation to these NIA-AA stages found that diminished atrophy across the brain with the exception of medial temporal regions (stage 1) preceded increased atrophy in temporoparietal regions (stage 2/3) [163]. This suggested a biphasic model for pathological cortical changes in which regional Aβ accumulation–related thickening evolves to AD-typical patterns of cortical thinning as tau accumulates and becomes toxic. These results supported the ability of these NIA-AA criteria to distinguish clinically relevant stages on the basis of CSF biomarkers and underscore the importance of distinguishing between CSF Aβ and tau for disease staging. A second study staged preclinical participants on the basis of the number, not order, of abnormal biomarkers (1, 2, or 3 of CSF Aβ42, CSF tau, and very subtle cognitive impairment) [164]. Cerebral Aβ deposition increased, but subcortical Aβ deposition in the hippocampus, pallidum, and thalamus did not differ across these preclinical disease stages, suggesting that Aβ accumulation is a very early event in AD disease progression that may not be captured by either the 2011 NIA-AA criteria or these alternative criteria [164].

A novel staging approach used florbetapir PET data from across the full ADNI cohort to define a four-stage model of Aβ pathology progression [165]. Aβ deposition was observed initially in temporobasal and frontomedial areas (stage I) and subsequently spread to the rest of the associative neocortex and primary sensory motor cortex (stage II), the medial temporal lobe (stage III), and the striatum (stage IV) (Fig. 32), a progression pattern similar to that reported in neuropathological studies. Successive stages were associated with progressively lower CSF Aβ42 levels and with more severe diagnostic classes (Fig. 33). Unlike dichotomous systems of defining Aβ positivity, stage I captured the earliest signs of Aβ deposition, suggesting that the system may aid the selection of participants for clinical trials of Aβ-modifying therapies [165].

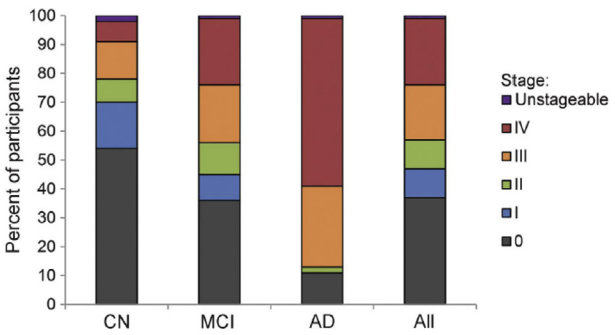

Fig. 33. Proportions of stages defined by in vivo amyloid imaging by clinical diagnosis. Relative proportions of in vivo amyloid stages for each diagnostic group separately and across all participants. Abbreviations: AD, Alzheimer's disease; CN, cognitively normal; MCI, mild cognitive impairment. Reproduced with permission from Grothe et al. [165].

22. Novel approaches to the prediction of future decline

Recent ADNI papers have detailed the development of prognostic biomarkers that identify subjects at a high risk of future progression to AD for use in clinical settings and in the selection of participants for clinical trials. Use of a single modality has become preferential to multimodal approaches due to cost and consideration of the burden of multiple tests to patients and their families. Structural MRI, a cornerstone of ADNI, is widely available and less invasive than other modalities such as collection of CSF. Consideration of subcortical shape changes revealed a significant increase in the longitudinal hemispheric asymmetry of the hippocampus, amygdala, and chordate across diagnostic groups above and beyond normal aging [166]. This asymmetry was significantly associated with both cognitive test scores and progression to AD, and bilateral temporal and left superior frontal cortical atrophy. Moreover, longitudinal shape asymmetry of the hippocampus and amygdala outperformed longitudinal volumetric measurements in predicting MCI to AD progression [166]. Diffusion-weighted imaging was used to investigate the potential of changes in microstructural WM integrity as AD prognostic biomarkers [167]. A classifier based on microstructural WM differences between CN and AD subjects primarily in the hippocampal formation (hippocampal alveus and parahippocampus), posterior cingulate, and optic tract achieved high classification accuracy, particularly in the early MCI versus AD challenge [167].

A genetic biomarker is a desirable alternative to MRI-based biomarkers as blood is easily collected and analysis is inexpensive and robust. A genetic biomarker risk algorithm that combines *APOE* status (ε2, ε3, ε4), *TOMM40* rs10524523 variable length poly T repeat polymorphism ('523) and age, predicted 5-year conversion from CN to MCI or AD with an AUC of 0.72 and was comparable to CSF and functional MRI biomarkers [168]. In addition, risk categorization using this algorithm correlated closely with pathological CSF biomarkers and neurocognitive scores, indicating its utility in identifying clinical trial participants with a high likelihood of cognitive decline. This genetic-based biomarker algorithm was used for stratification of participants in a delay of disease onset clinical trial of elderly CN participants (TOMORROW trial) [168].

A novel clustering approach identified groups of rapid and slow declining MCI subjects on the basis of all available ADNI-1 and ADNI-2 longitudinal biomarker data [169]. The groups differed in their rates of conversion to AD and reversion to CN; within 5 years, 13% of slow decliners but 64% of rapid decliners converted to AD, and 10% of slow decliners but 0% of fast decliners reverted to CN. Gender affected the rate of cognitive decline in both groups, with women more likely to progress to AD and less likely to revert to CN (Fig. 34). Finally, a baseline classifier combining ADAS-11 and ADAS-13 was able to discriminate between rapid and slow declining groups with high

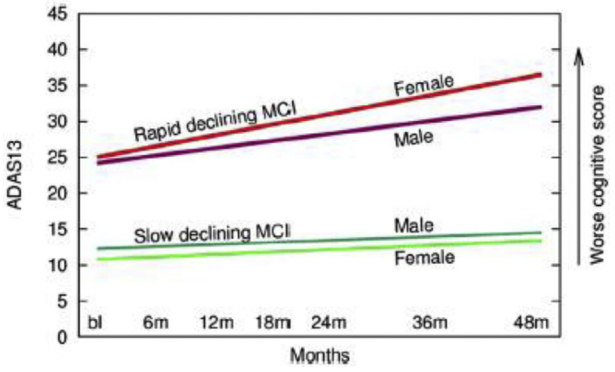

Fig. 34. Sex-specific longitudinal cognitive trajectories for rapid and slow declining MCI. Sex-specific decline in ADAS-Cog13 total scores over 4 years for slow versus rapid declining subpopulations of MCI subjects. Higher scores depict greater worsening of cognition. Abbreviations: ADAS-Cog13, Alzheimer's Disease Assessment Scale–13-item cognitive subscale; MCI, mild cognitive impairment. Reproduced with permission from Gamberger et al. [169].

sensitivity and specificity, suggesting that selection of clinical trial subjects with a high probability of rapid decline is possible on the basis of clinical tests alone.

Functional connectivity changes occur very early in AD disease progression (Sections 2 and 5) and thus have potential as biomarkers for CN to MCI progression. Chen et al. [12] used an event-based probabilistic model to estimate the optimum temporal order of 10 AD biomarkers and to develop a composite biomarker, the Characterizing AD Risk Events (CARE) index. The first two AD biomarkers estimated to become abnormal in this study were the hippocampal and PCC functional connectivity indices that preceded CSF Aβ42 and CSF p-tau181, suggesting the importance of functional impairment in these regions very early in AD disease progression. This index has potential for subject selection and patient staging in clinical trials. Similarly, large-scale failure of DMN functional networks is an early event in the cascading network failure model of AD pathophysiology [170]. Wiepert et al. [171] developed a biomarker of this large-scale network failure based on the ratio of increases over decreases in functional connectivity, termed the network failure quotient (NFQ). This measure was designed to reflect both the progressive disconnection of the DMN and compensatory increases in connectivity in the medial temporal lobe. NFQ was associated with age, tau deposition in the entorhinal cortex, global cortical Aβ deposition, hypometabolism, cortical thickness in AD signature regions, and cognition (Fig. 35), indicating its utility as a biomarker of AD pathophysiological changes in CN subjects. NFQ was also associated with changes in nodal centrality, consistent with the disconnection of the posterior DMN in conjunction with Aβ deposition in highly connected hubs posited by the cascading network failure model [171].

CSF and MRI biomarkers outlined in the 2011 NIA-AA criteria are commonly used for the diagnosis of MCI due to AD (Section 21) [155]. However, these criteria do not

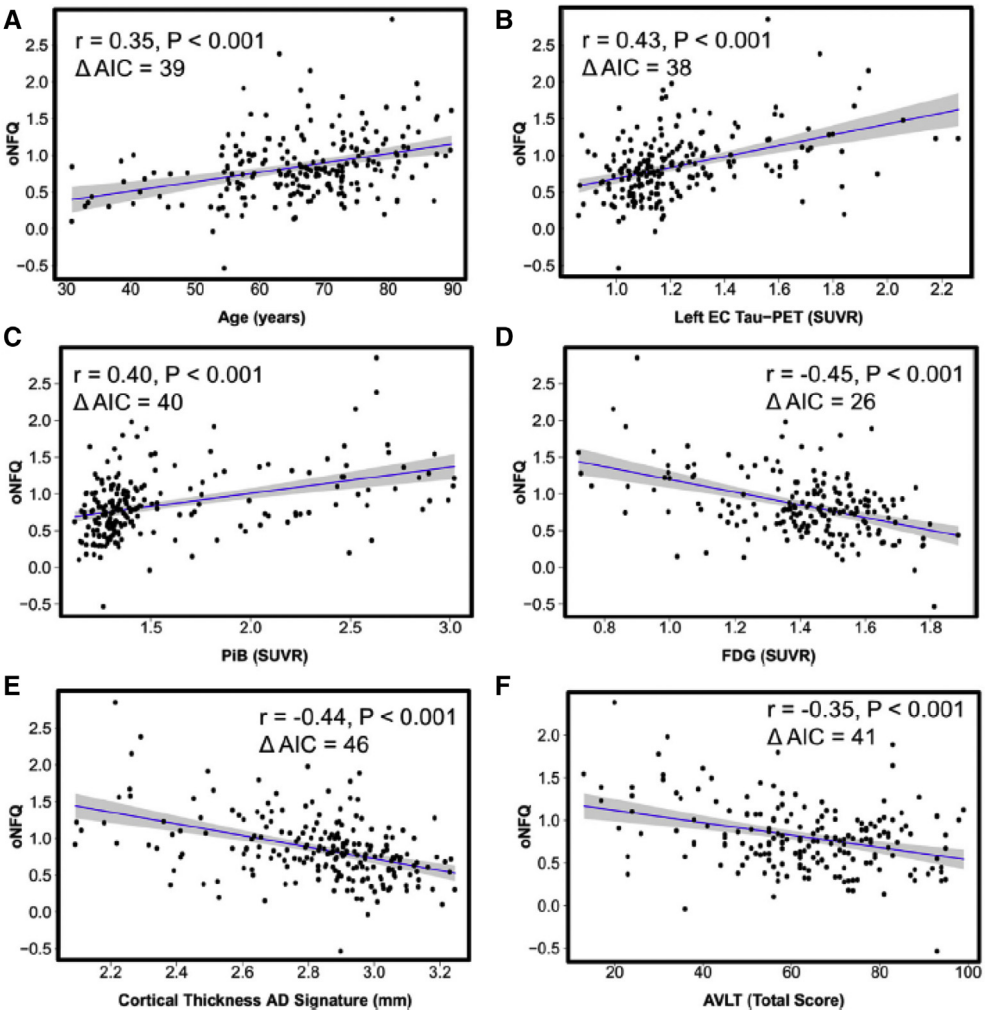

Fig. 35. Association of the network failure quotient with established AD biomarkers. The network failure quotient, a summary measure of large-scale brain network failure, plotted against (A) age, (B) tau PET SUVR in the entorhinal cortex, (C) amyloid PET SUVR, (D) FDG PET SUVR in AD signature regions, (E) cortical thickness in AD signature regions, (F) total score on the auditory verbal learning test. The blue lines indicate the linear fit, and the gray band indicates 95% confidence intervals. The correlation coefficient r, *P* value, and relative reduction in Akaike information criteria (ΔAIC) are given in the inset. Abbreviations: AD, Alzheimer's disease; FDG, fluorodeoxyglucose; NFQ, network failure quotient; PET, positron emission tomography; SUVR, standardized uptake value ratio. Reproduced with permission from Wiepert et al. [171].

take into account conflicting biomarkers or individual patient characteristics. Van Maurik et al. [172] described individualized biomarker-based prognostic models that combined two MRI biomarkers and CSF Aβ and tau with age, sex, and MMSE scores. These models predicted probabilities of MCI to AD conversion within 3 years ranging from 4% in patients with an MMSE score of 29 and no abnormal biomarkers to 89% in patients with an MMSE score of 24 and all abnormal biomarkers and provided individualized risk estimates for any given value of its components. This personalized medicine approach was designed to provide guidance for clinical decision making [172].

Many of these studies have used increasing knowledge of AD disease progression to target prognostic biomarkers such as changes in functional connectivity, microstructural WM integrity, and subcortical shape rather than volumetric changes. Others have explored the potential of a low-cost genetic blood test and provided guidance for clinical decision making by establishing guidelines for the individualized use of biomarkers, intended to support a personalized medicine approach.

23. Improvements to AD clinical trials

The failure of AD clinical trials involving primarily amnestic MCI participants to show treatment efficacy is of great concern. Placebo participants in seven randomized controlled trials over the past decade were found to have highly variable trajectories of cognitive change in a recent study (Fig. 36) [173]. Only participants in ADNI (as a simulated clinical trial) and the Alzheimer's Disease Cooperative Study MCI trial had the expected decline in

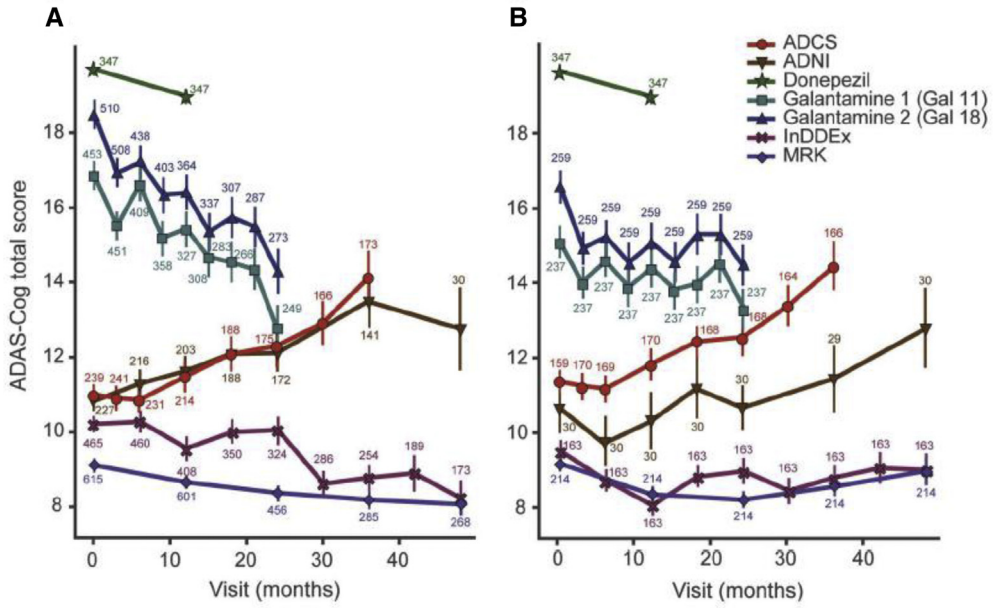

Fig. 36. Clinical trial cognitive performance of mild cognitive impairment placebo participants. (A) Mean performance on the ADAS-Cog for all participants. (B) Mean performance on the ADAS-Cog for participants who completed the trial. Bars denote 95% confidence intervals. Abbreviations: ADAS-Cog, Alzheimer's Disease Assessment Scale–cognitive subscale; ADCS, Alzheimer's Disease Cooperative Study; InDDEx, Investigation into Delay to Diagnosis of Alzheimer's Disease with Exelon; MRK, Merck rofecoxib trial. Reproduced with permission from Petersen et al. [173].

cognition; in all other trials, MCI placebo groups showed stable or even improved cognition (suggesting a placebo effect), despite the use of the same entry criteria for amnestic MCI participants. These results may explain the failures of these trials as the detection of a treatment effect against such placebo groups is extremely difficult. These discrepancies may be due to a combination of subtle differences in entry criteria, variations in *APOE* ε4 status, comorbidities, and outcome measures, and language and culture differences [173]. The study highlights the need for stringent attention to selection of MCI participants from this heterogeneous group and the subsequent use of standardized and sensitive outcome measures if MCI randomized controlled trials are to be successful. By extension, the same observations are perhaps even more applicable to early intervention trials of CN participants in whom detection of AD pathology and measurement of cognitive deterioration poses a greater challenge.

Wolz et al. [174] operationalized the 2011 NIA-AA diagnostic criteria for MCI due to AD [155]—namely Aβ positivity (florbetapir PET) plus a marker of neurodegeneration (in this case hippocampal volume)—as inclusion criteria for clinical trials. A combination of hippocampal volume and Aβ positivity, defined by explicit cut points, reduced required sample sizes by 45%–60% over no enrichment depending on the outcome measure used and outperformed hippocampal volume or Aβ enrichment alone (Fig. 37). Enrichment with hippocampal volume followed by Aβ positivity combined with the use of ADAS-Cog13 as an outcome measure reduced the sample size required to detect a 30% treatment effect with 80% power from 908 to 363, the estimated trial cost from $83 million to $45 million, and the estimated trial time from 5.2 years to 4.3 years. When hippocampal volume was measured before Aβ deposition, there was a further reduction in sample size of around 20%, and in estimated trial cost of around 25%, as fewer participants then required expensive PET imaging. However, Insel et al. [49] reported that the use of established cut points in determining Aβ positivity may lead to the exclusion of MCI participants although they are already experiencing cognitive/functional decline. Therefore, consideration of prethreshold levels of CSF Aβ42 may identify participants with the first signs of accelerating rates of decline.

The finding by Wolz et al. [174] that ADAS-Cog outperformed MMSE points to the potential benefits of improving outcome measures. Wang et al. [175] developed a composite clinical outcome measure, ADCOMS, comprising four ADAS-Cog subscale items, two MMSE subscale items, and all six Clinical Dementia Rating–Sum of Boxes subscale items. ADCOMS had improved sensitivity over individual tests to detect clinical decline in prodromal AD, amnestic MCI, and mild AD and reduced required sample sizes across all combinations of enrichment and outcome measures tested. For example, in amnestic MCI participants enriched using Aβ positivity, use of ADCOMS instead of ADAS-Cog as an outcome measure reduced the predicted sample size required from 1957 to 396. Furthermore, ADCOMS detected treatment effects of donepezil and vitamin E compared to placebo. These results led to the promotion of this composite test for qualification as a primary outcome measure in trials of prodromal AD/amnestic MCI by the Coalition Against Major Diseases.

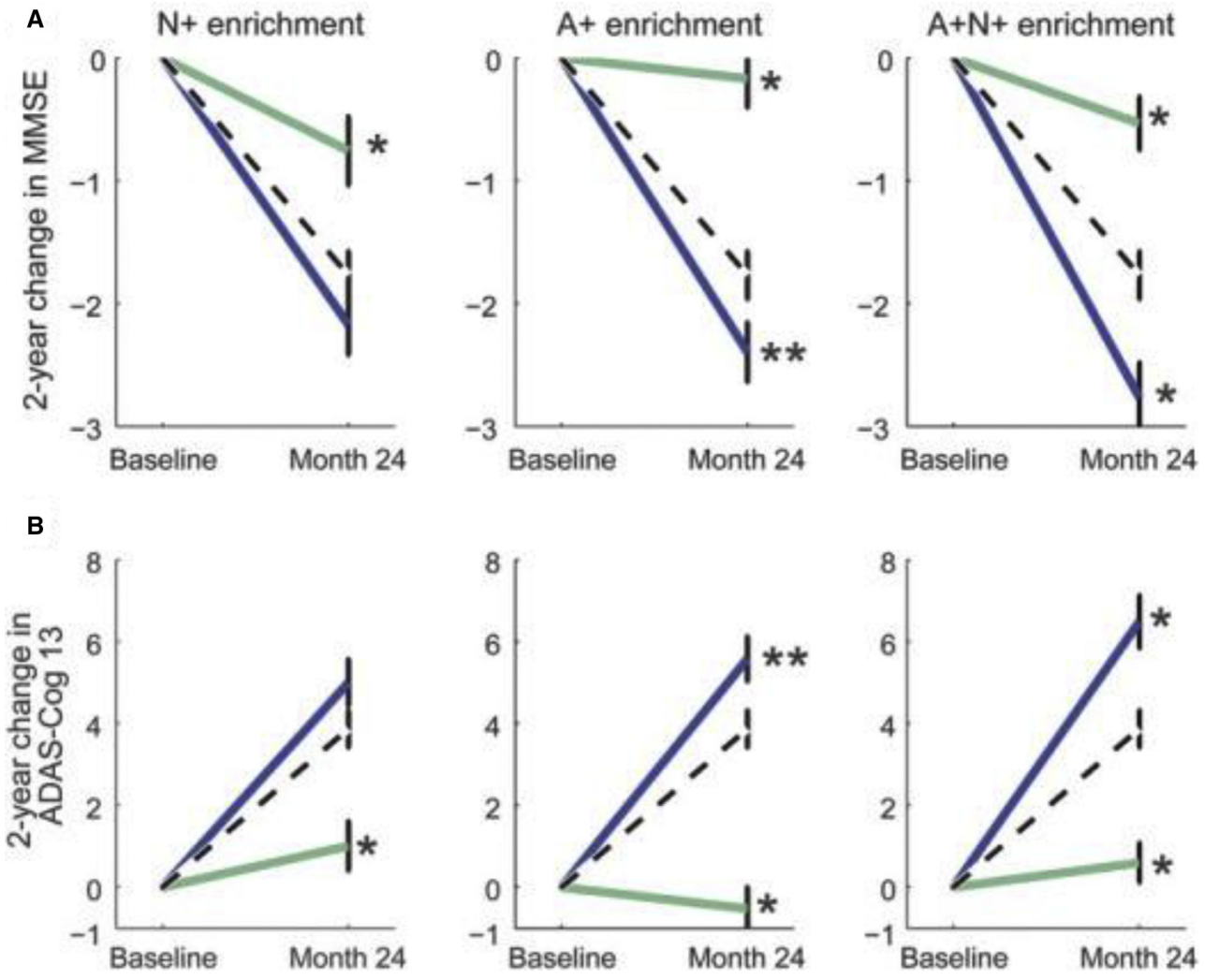

Fig. 37. Effect of enrichment of MCI participants with Aβ positivity and/or hippocampal atrophy on cognition over 2 years. Change in MMSE (A), and ADAS-Cog13 (B) with standard error for the unenriched sample (dashed black line), enriched sample (solid blue line), and excluded sample (solid green line). Significance of the difference between included and excluded groups and the unenriched sample is shown as $^{**}P < .05$ and $^{*}p < .01$. Abbreviations: Aβ, β-amyloid; ADAS-Cog13, Alzheimer's Disease Assessment Scale–13-item cognitive subscale; A+, amyloid positive; MCI, mild cognitive impairment; MMSE, Mini–Mental State Examination; N+, neurodegeneration positive (hippocampal atrophy). Reproduced with permission from Wolz et al. [174].

Early intervention clinical trials that enroll CN participants require selection criteria and outcome measures that reflect AD disease progression in this population. Selection of CN subjects likely to progress to MCI on the basis of both Aβ positivity, baseline cognitive/functional assessments, and demographic and *APOE* information improved power estimates over selection with Aβ positivity alone (Fig. 38) [176]. Furthermore, a composite clinical outcome measure that included a measure of function in addition to cognition measures improved power estimates over cognitive measures alone (Fig. 38). This methodical study calculated that optimum combination of subject selection criteria and outcome measures, namely selection of CN participants likely to convert using Aβ positivity and evidence of subtle cognitive impairment combined with an outcome measure incorporating both cognition and function, would require 375 participants per arm in a 30-month trial to detect a 30% slowing of decline at 80% power. Careful studies such as these will undoubtedly aid in rectifying the issues identified by Petersen et al. [173].

24. Multiple concurrent therapies for AD

Accumulating evidence suggests that vascular factors are important contributors to AD disease progression (Section 9). Treatments targeting vascular health may complement those targeting neurodegenerative aspects of the disease [65]. Antihypertensive treatment associated with angiotensin receptor blockers was associated with larger hippocampal volumes and less whole-brain atrophy in CN and MCI subjects, with lower WMH volume in AD subjects, and with better performance on tests of memory, language,

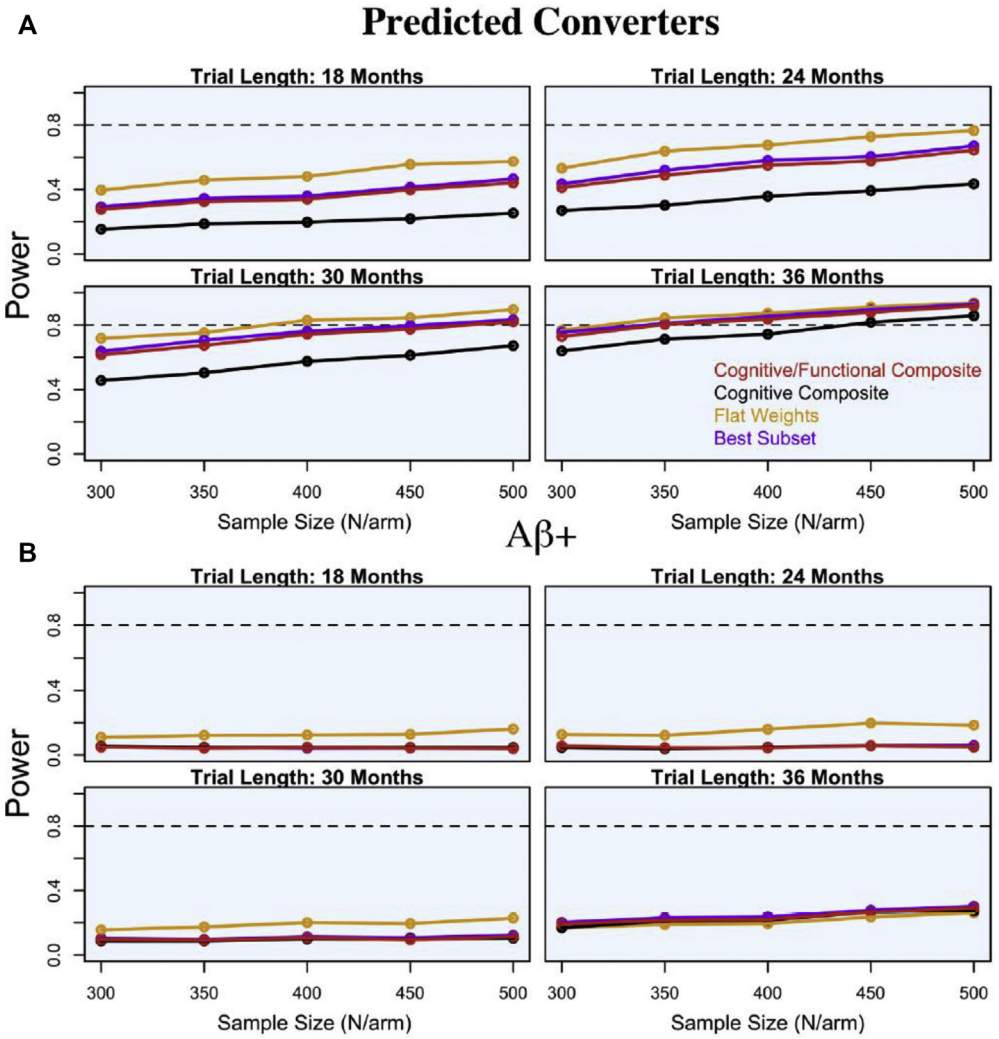

Fig. 38. Plots of power estimates at different sample sizes of completers per arm for clinical trials of CN participants. (A) Power estimates for Aβ+ subjects predicted using baseline data to convert to MCI for trials ranging from 18 to 36 months with 300 to 500 subjects per arm for four types of end points. (B) Power estimates for Aβ+ subjects over the same links trials and sample sizes for four types of end points. Abbreviations: Aβ+, β-amyloid positive; CN, cognitively normal; MCI, mild cognitive impairment. Reproduced with permission from Insel et al. [176].

and executive function [177]. Multiple concurrent therapies targeting vascular health, Aβ deposition, and AD-related neurodegeneration may be more likely to halt or reverse AD disease progression than targeting one aspect alone. An evaluation of hypothetical therapeutic interventions [13] found that combinatorial approaches outperformed single therapies both for modifying an individual's cognitive state without necessarily restoring all affected brain properties (output control strategy) and for restoring all biological properties to the clinically normal range (Fig. 39). The study assessed theoretical cost-energy of hypothetical therapeutic strategies, which reflected the degree of alteration to the brain system required to reach a desired final state. Notably, the cost-energy of therapies targeting Aβ alone was relatively high (Fig. 39), which may in part explain recent failures of anti-amyloid clinical trials. These studies support a combinatorial approach to therapeutic intervention that includes a vascular target in addition to Aβ and other AD-specific neurodegenerative changes.

25. Conclusions

ADNI papers from 2016 and 2017 (see Supplementary Material for entire list) have contributed to a better understanding of the complexities of late-onset AD. Data-driven models of AD disease progression paint a complex picture of multifactorial interactions rather than the linear cascade of events described by the amyloid cascade hypothesis [11–13,17]. Early events preceding deposition may include functional changes in areas of high metabolic demand such as the highly connected PCC hub, and vascular dysregulation that may cause disturbances to the BBB and negatively impact Aβ clearance, in turn negatively impacting vascular integrity in a feedback loop. Various studies support the concurrent

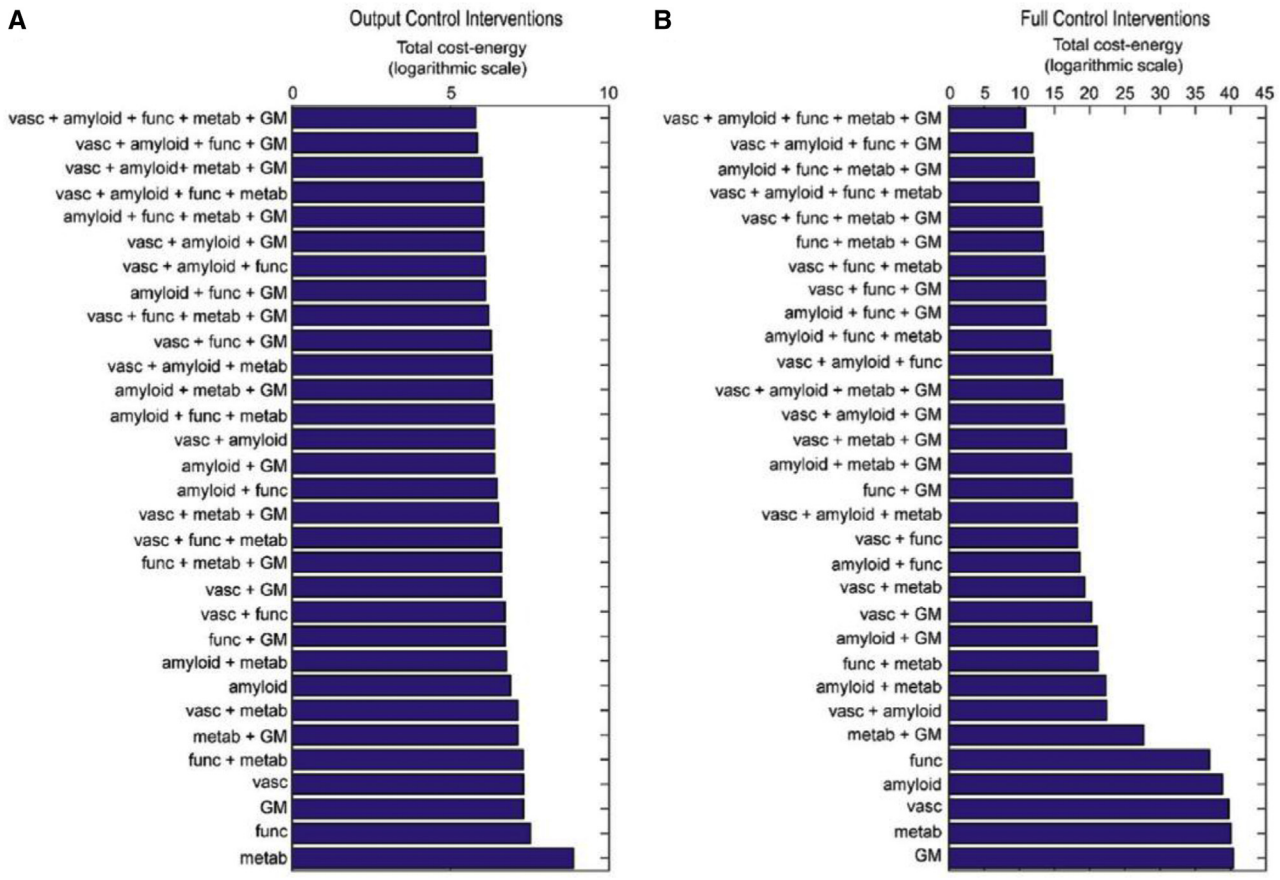

Fig. 39. Optimum cost-energies for hypothetical AD therapeutic strategies. Single target and combinatorial (up to a maximum of five target factors) therapies were sorted from minimum to maximum energy required to reverse disease progression from an advanced AD state to a normal CN state. (A) Costs of output control strategy requiring a return to normal cognition, but not normal levels of all biomarkers. (B) Costs of full control strategy requiring a return to normal cognition and normal levels of all biomarkers. Abbreviations: AD, Alzheimer's disease; CN, cognitively normal; GM, gray matter. Reproduced with permission from Iturria-Medina et al. [13].

deposition of Aβ and functional connectivity changes within the DMN [51,52,178] and suggest that Aβ may then spread along the structural connectome guided by metabolic load in remote regions [53]. Early pathogenic crosstalk between CSF Aβ42 and tau may induce intracellular NFT deposition causing neuronal death, atrophy, and cognitive changes [38]. Network analyses suggest a specific and progressive disconnection of functional and anatomical networks over the course of the disease [103–106]. Interestingly, some evidence suggests that subtle cognitive impairment occurs before detectable atrophy [164], and this is an area yet to be fully explored.

Consistent identification of several AD subtypes using a wide range of criteria [40–45] suggests that multiple interacting pathways of neurodegeneration may account for CN and MCI heterogeneity. The "typical AD" group is typified by neurodegenerative changes typical of AD, as well as those of vascular origin; however, pathology underlying the dysexecutive/mixed subtype found in Aβ+ participants is not yet clear. A less well-defined slow-declining group may have additional pathologies such as vascular dementia, TDP-43 proteinopathy, Lewy bodies, and hippocampal sclerosis underlying Aβ-independent neurodegeneration or may include subjects with prethreshold levels of Aβ who are yet to decline. Early pathological changes may occur at subthreshold levels of Aβ positivity [48,49], suggesting that operationalizing Aβ positivity as a continuous rather than dichotomous variable will aid in detecting early changes in AD disease progression, with the potential to identify participants at a high risk of future AD-related decline. Early results from flortaucipir tau PET imaging incorporated into the ADNI-3 study found a defined pattern of spread linked to prior Aβ deposition, in specific subnetworks vulnerable to tau accumulation, supporting a synergistic relationship between these two pathological markers [58,64].

The identification of statistically distinct vascular- and age-related factors of AD neurodegeneration [65] points to an important contribution of vascular burden to AD disease progression. This appears to be complex having both Aβ-dependent [67,68] and Aβ-independent [69,70] effects. Synergistic interaction between vascular risk factors and Aβ may exacerbate WMH volume and induce Aβ

deposition by affecting clearance mechanisms. However, vascular burden may also act independently of Aβ to affect functional connectivity changes, glucose metabolism, and hippocampal atrophy. The *APOE* ε4 allele may interact with cerebrovascular disease to affect Aβ clearance mechanisms, adding yet another layer of complexity to the system [65,91,93].

Systems biology studies supported the biological complexity of AD, identifying multiple contributing genetic factors including genes involved not only in tau phosphorylation and Aβ production but also in other neurodegenerative orders, cancers, calcium signaling, and oxidative stress [19–22,26]. Established AD risk alleles were associated with pathological changes in specific brain areas and differed in their effect at different stages in AD. Interestingly, genetic risk for AD included risk alleles for vascular disorders implicating a vascular contribution to AD [74–76].

A wide range of neuropsychiatric symptoms were associated with increased Aβ deposition, limbic hypometabolism, and regional atrophy in CN participants, suggesting that they may represent an easily measurable first clinical sign of AD pathophysiology [115–118,120–122]. Novel prognostic biomarkers for CN participants included changes in functional connectivity [171] and microstructural WM integrity [167] as well as the use of subcortical shape rather than volumetric changes [166]. These biomarkers are clearly based on our improved understanding of the biology of AD disease progression.

The highly variable trajectories of cognitive change in placebo populations of randomized controlled clinical trials [173] suggest that more stringent attention must be paid to the selection and monitoring of participants if clinical trials are to detect a measurable treatment effect. Selection with a variety of criteria such as hippocampal volume, Aβ positivity (perhaps even at prethreshold levels), baseline cognitive/functional assessments, and *APOE* ε4 status combined with improved cognitive outcome measures may hold the key to increase the power to detect a treatment effect in clinical trials of MCI and CN participants and to decrease trial duration and cost [151,174,175]. Entry criteria may differ between CN and MCI participants reflecting changing biomarkers in these different stages of AD disease progression. Finally, the view of AD as a multifactorial disease suggests that multiple concurrent therapies that target Aβ, vascular health, and other AD pathology may be more likely to reverse AD disease progression.

In sum, data-driven models of AD disease progression, which posit the influence of multifactorial interactions, have found considerable support in evidence presented by recent ADNI studies. Concurrently, application of important features of these models to better defining AD subtypes and to selecting participants for AD clinical trials at risk of imminent decline offers clear strategies for implementing future successful AD clinical trials. It is hoped that the incorporation of new approaches including flortaucipir tau-PET imaging into the ADNI-3 study will shed further light on the complexities of AD disease progression and allow further progress to achieving overarching goal of ADNI, for the improvement of AD clinical trials. All ADNI publications can be searched online at http://adni.loni.usc.edu/news-publications/publications/.

Acknowledgments

This work was supported by NIH grant U19-AG024904 funded by the National Institute on Aging to Dr. Michael Weiner. The following organizations are contributors to ADNI through the Foundation for NIH: AbbVie, ACT-AD, Alector, Alzheimer's Association, Araclon Biotech, BioClinica, Biogen Idec, Cogstate, Denali, Diami, Eisai Inc., Euroimmun, Eli Lilly and Company, GE Healthcare, Genentech, Janssen Alzheimer Immunotherapy, Lundbeck, Magou, Merck and Co., PeopleBio, Pfizer, Inc., Piramal Imaging, Roche, Saladax Biomedical, Servier, Takeda.

Supplementary data

Supplementary data to this article can be found online at https://doi.org/10.1016/j.jalz.2018.08.005.

RESEARCH IN CONTEXT

1. Systematic review: The authors selected publications using data from the Alzheimer's Disease Neuroimaging Initiative by traditional means (PubMed and Google Scholar).
2. Interpretation: Data-driven models of Alzheimer's disease (AD) progression that suggest multifactorial interactions were supported by multiple studies. Functional connectivity changes occur concurrently with early β-amyloid (Aβ) deposition. There is a progressive disconnection of functional and anatomical networks with AD progression. Vascular pathology may contribute to early vascular dysregulation affecting Aβ clearance in conjunction with *APOE4* or exacerbate AD progression through Aβ independent mechanisms. The spread of tau is dependent on antecedent Aβ deposition. Executive function–impaired and "typical AD" subgroups are consistently identified in Aβ+ participants. Genetic studies identified new risk factors and explored effects of established risk alleles. Clinical trials subject selection on the basis of multiple criteria may improve trial power.
3. Future directions: This knowledge will inform and improve clinical trial design.

References

[1] Weiner MW, Veitch DP, Aisen PS, Beckett LA, Cairns NJ, Cedarbaum J, et al. Impact of the Alzheimer's Disease Neuroimaging Initiative, 2004 to 2014. Alzheimer's Demen : J Alzheimer's Assoc 2015;11:865–884.

[2] Weiner MW, Veitch DP, Aisen PS, Beckett LA, Cairns NJ, Green RC, et al. The Alzheimer's Disease Neuroimaging Initiative 3: Continued innovation for clinical trial improvement. Alzheimers Dement 2017; 13:561–571.

[3] Yao X, Yan J, Ginda M, Borner K, Saykin AJ, Shen L, et al. Mapping longitudinal scientific progress, collaboration and impact of the Alzheimer's disease neuroimaging initiative. PLoS One 2017; 12:e0186095.

[4] Weiner MW, Veitch DP, Aisen PS, Beckett LA, Cairns NJ, Cedarbaum J, et al. 2014 Update of the Alzheimer's Disease Neuroimaging Initiative: A review of papers published since its inception. Alzheimer's Demen: J Alzheimer's Assoc 2015;11:e1–120.

[5] Weiner MW, Veitch DP, Aisen PS, Beckett LA, Cairns NJ, Green RC, et al. The Alzheimer's Disease Neuroimaging Initiative: a review of papers published since its inception. Alzheimer's Demen : J Alzheimer's Assoc 2013;9:e111–94.

[6] Weiner MW, Veitch DP, Aisen PS, Beckett LA, Cairns NJ, Green RC, et al. The Alzheimer's Disease Neuroimaging Initiative: a review of papers published since its inception. Alzheimer's Demen : J Alzheimer's Assoc 2012;8:S1–68.

[7] Weiner MW, Veitch DP, Aisen PS, Beckett LA, Cairns NJ, Green RC, et al. Recent publications from the Alzheimer's Disease Neuroimaging Initiative: Reviewing progress toward improved AD clinical trials. Alzheimers Dement 2017;13:e1–85.

[8] Jack CR Jr, Knopman DS, Jagust WJ, Petersen RC, Weiner MW, Aisen PS, et al. Tracking pathophysiological processes in Alzheimer's disease: an updated hypothetical model of dynamic biomarkers. Lancet Neurol 2013;12:207–16.

[9] Jack CR Jr, Knopman DS, Jagust WJ, Shaw LM, Aisen PS, Weiner MW, et al. Hypothetical model of dynamic biomarkers of the Alzheimer's pathological cascade. Lancet Neurol 2010;9:119–28.

[10] Young AL, Oxtoby NP, Daga P, Cash DM, Fox NC, Ourselin S, et al. A data-driven model of biomarker changes in sporadic Alzheimer's disease. Brain 2014;137:2564–77.

[11] Iturria-Medina Y, Sotero RC, Toussaint PJ, Mateos-Perez JM, Evans ACAlzheimer's Disease Neuroimaging I. Early role of vascular dysregulation on late-onset Alzheimer's disease based on multifactorial data-driven analysis. Nat Commun 2016;7:11934.

[12] Chen G, Shu H, Chen G, Ward DB, Antuono PG, Zhang Z, et al. Staging Alzheimer's Disease Risk by Sequencing Brain Function and Structure, Cerebrospinal Fluid, and Cognition Biomarkers. J Alzheimer's Dis 2016;54:983–93.

[13] Iturria-Medina Y, Carbonell FM, Sotero RC, Chouinard-Decorte F, Evans AC. Initiative AsDN. Multifactorial causal model of brain (dis) organization and therapeutic intervention: Application to Alzheimer's disease. NeuroImage 2017;152:60–77.

[14] Raj A, Kuceyeski A, Weiner M. A network diffusion model of disease progression in dementia. Neuron 2012;73:1204–15.

[15] Raj A, LoCastro E, Kuceyeski A, Tosun D, Relkin N, Weiner M, et al. Network Diffusion Model of Progression Predicts Longitudinal Patterns of Atrophy and Metabolism in Alzheimer's Disease. Cell Rep 2015;10:359–69.

[16] Iturria-Medina Y, Sotero RC, Toussaint PJ, Evans AC. Epidemic spreading model to characterize misfolded proteins propagation in aging and associated neurodegenerative disorders. PLoS Comput Biol 2014;10:e1003956.

[17] Pandya S, Kuceyeski A, Raj A. Alzheimer's Disease Neuroimaging, Initiative. The Brain's Structural Connectome Mediates the Relationship between Regional Neuroimaging Biomarkers in Alzheimer's Disease. J Alzheimers Dis 2017;55:1639–57.

[18] Buckner RL, Snyder AZ, Shannon BJ, LaRossa G, Sachs R, Fotenos AF, et al. Molecular, structural, and functional characterization of Alzheimer's disease: evidence for a relationship between default activity, amyloid, and memory. J Neurosci 2005;25:7709–17.

[19] Chapuis J, Flaig A, Grenier-Boley B, Eysert F, Pottiez V, Deloison G, et al. Genome-wide, high-content siRNA screening identifies the Alzheimer's genetic risk factor FERMT2 as a major modulator of APP metabolism. Acta Neuropathol 2017;133:955–66.

[20] Cong W, Meng X, Li J, Zhang Q, Chen F, Liu W, et al. Genome-wide network-based pathway analysis of CSF t-tau/Abeta1-42 ratio in the ADNI cohort. BMC Genomics 2017;18:421.

[21] Yao X, Yan J, Kim S, Nho K, Risacher SL, Inlow M, et al. Two-dimensional enrichment analysis for mining high-level imaging genetic associations. Brain Inform 2017;4:27–37.

[22] Hohman TJ, Bush WS, Jiang L, Brown-Gentry KD, Torstenson ES, Dudek SM, et al. Discovery of gene-gene interactions across multiple independent data sets of late onset Alzheimer disease from the Alzheimer Disease Genetics Consortium. Neurobiol Aging 2016; 38:141–50.

[23] Nho K, Horgusluoglu E, Kim S, Risacher SL, Kim D, Foroud T, et al. Integration of bioinformatics and imaging informatics for identifying rare PSEN1 variants in Alzheimer's disease. BMC Med Genomics 2016;9:30.

[24] Nho K, Kim S, Horgusluoglu E, Risacher SL, Shen L, Kim D, et al. Association analysis of rare variants near the APOE region with CSF and neuroimaging biomarkers of Alzheimer's disease. BMC Med Genomics 2017;10:29.

[25] Li J, Zhang Q, Chen F, Meng X, Liu W, Chen D, et al. Genome-wide association and interaction studies of CSF T-tau/Abeta42 ratio in ADNI cohort. Neurobiol Aging 2017;57:247.e1–247.e8.

[26] Caceres A, Vargas JE, Gonzalez JR. APOE and MS4A6A interact with GnRH signaling in Alzheimer's disease: Enrichment of epistatic effects. Alzheimers Dement 2017;13:493–7.

[27] Tan L, Wang HF, Tan MS, Tan CC, Zhu XC, Miao D, et al. Effect of CLU genetic variants on cerebrospinal fluid and neuroimaging markers in healthy, mild cognitive impairment and Alzheimer's disease cohorts. Sci Rep 2016;6:26027.

[28] Xu W, Wang HF, Tan L, Tan MS, Tan CC, Zhu XC, et al. The impact of PICALM genetic variations on reserve capacity of posterior cingulate in AD continuum. Sci Rep 2016;6:24480.

[29] Stage E, Duran T, Risacher SL, Goukasian N, Do TM, West JD, et al. The effect of the top 20 Alzheimer disease risk genes on gray-matter density and FDG PET brain metabolism. Alzheimers Dement (Amst) 2016;5:53–66.

[30] Gomar JJ, Conejero-Goldberg C, Huey ED, Davies P, Goldberg TE, Alzheimer's Disease Neuroimaging I. Lack of neural compensatory mechanisms of BDNF val66met met carriers and APOE E4 carriers in healthy aging, mild cognitive impairment, and Alzheimer's disease. Neurobiol Aging 2016;39:165–73.

[31] Zhang C, Lu J, Liu B, Cui Q, Wang Y. Primate-specific miR-603 is implicated in the risk and pathogenesis of Alzheimer's disease. Aging (Albany NY) 2016;8:272.

[32] Roussotte FF, Hua X, Narr KL, Small GW, Thompson PM. Alzheimer's Disease Neuroimaging I. The C677T variant in MTHFR modulates associations between brain integrity, mood, and cognitive functioning in old age. Biol Psychiatry : Cogn Neurosci Neuroimaging 2017;2:280–8.

[33] Vickers JC, Mitew S, Woodhouse A, Fernandez-Martos CM, Kirkcaldie MT, Canty AJ, et al. Defining the earliest pathological changes of Alzheimer's disease. Curr Alzheimer Res 2016;13:281–7.

[34] Palmqvist S, Mattsson N, Hansson OAlzheimer's Disease Neuroimaging I. Cerebrospinal fluid analysis detects cerebral amyloid-beta accumulation earlier than positron emission tomography. Brain 2016;139:1226–36.

[35] Palmqvist S, Scholl M, Strandberg O, Mattsson N, Stomrud E, Zetterberg H, et al. Earliest accumulation of beta-amyloid occurs

within the default-mode network and concurrently affects brain connectivity. Nat Commun 2017;8:1214.
[36] Toledo JB, Arnold M, Kastenmuller G, Chang R, Baillie RA, Han X, et al. Metabolic network failures in Alzheimer's disease: A biochemical road map. Alzheimers Dement 2017;13:965–84.
[37] Donohue MC, Sperling RA, Petersen R, Sun CK, Weiner MW, Aisen PS, et al. Association Between Elevated Brain Amyloid and Subsequent Cognitive Decline Among Cognitively Normal Persons. Jama 2017;317:2305–16.
[38] Gomar JJ, Conejero-Goldberg C, Davies P, Goldberg TE, Alzheimer's Disease Neuroimaging I. Anti-Correlated Cerebrospinal Fluid Biomarker Trajectories in Preclinical Alzheimer's Disease. J Alzheimers Dis 2016;51:1085–97.
[39] Bangen KJ, Clark AL, Edmonds EC, Evangelista ND, Werhane ML, Thomas KR, et al. Cerebral Blood Flow and Amyloid-beta Interact to Affect Memory Performance in Cognitively Normal Older Adults. Front Aging Neurosci 2017;9:181.
[40] Dong A, Toledo JB, Honnorat N, Doshi J, Varol E, Sotiras A, et al. Heterogeneity of neuroanatomical patterns in prodromal Alzheimer's disease: links to cognition, progression and biomarkers. Brain 2017; 140:735–47.
[41] Edmonds EC, Eppig J, Bondi MW, Leyden KM, Goodwin B, Delano-Wood L, et al. Heterogeneous cortical atrophy patterns in MCI not captured by conventional diagnostic criteria. Neurology 2016; 87:2108–16.
[42] Eppig JS, Edmonds EC, Campbell L, Sanderson-Cimino M, Delano-Wood L, Bondi MW, et al. Statistically Derived Subtypes and Associations with Cerebrospinal Fluid and Genetic Biomarkers in Mild Cognitive Impairment: A Latent Profile Analysis. J Int Neuropsychological Soc : JINS 2017;23:564–76.
[43] Park JY, Na HK, Kim S, Kim H, Kim HJ, Seo SW, et al. Robust Identification of Alzheimer's Disease subtypes based on cortical atrophy patterns. Sci Rep 2017;7:43270.
[44] Varol E, Sotiras A, Davatzikos C, Alzheimer's Disease Neuroimaging I. HYDRA: Revealing heterogeneity of imaging and genetic patterns through a multiple max-margin discriminative analysis framework. Neuroimage 2017;145:346–64.
[45] Risacher SL, Anderson WH, Charil A, Castelluccio PF, Shcherbinin S, Saykin AJ, et al. Alzheimer disease brain atrophy subtypes are associated with cognition and rate of decline. Neurology 2017;89:2176–86.
[46] Mez J, Mukherjee S, Thornton T, Fardo DW, Trittschuh E, Sutti S, et al. The executive prominent/memory prominent spectrum in Alzheimer's disease is highly heritable. Neurobiol Aging 2016; 41:115–21.
[47] Zhang X, Mormino EC, Sun N, Sperling RA, Sabuncu MR, Yeo BT, et al. Bayesian model reveals latent atrophy factors with dissociable cognitive trajectories in Alzheimer's disease. Proc Natl Acad Sci U S A 2016;113:E6535–44.
[48] Carbonell F, Zijdenbos AP, McLaren DG, Iturria-Medina Y, Bedell BJAlzheimer's Disease Neuroimaging I. Modulation of glucose metabolism and metabolic connectivity by beta-amyloid. J Cereb Blood Flow Metab 2016;36:2058–71.
[49] Insel PS, Mattsson N, Mackin RS, Scholl M, Nosheny RL, Tosun D, et al. Accelerating rates of cognitive decline and imaging markers associated with beta-amyloid pathology. Neurology 2016; 86:1887–96.
[50] Schmitz TW, Nathan Spreng R. Alzheimer's Disease Neuroimaging I. Basal forebrain degeneration precedes and predicts the cortical spread of Alzheimer's pathology. Nat Commun 2016;7:13249.
[51] Lee ES, Yoo K, Lee YB, Chung J, Lim JE, Yoon B, et al. Default Mode Network Functional Connectivity in Early and Late Mild Cognitive Impairment: Results From the Alzheimer's Disease Neuroimaging Initiative. Alzheimer Dis Assoc Disord 2016;30:289–96.
[52] Nuttall R, Pasquini L, Scherr M, Sorg C. Degradation in intrinsic connectivity networks across the Alzheimer's disease spectrum. Alzheimers Dement (Amst) 2016;5:35–42.
[53] Jacquemont T, De Vico Fallani F, Bertrand A, Epelbaum S, Routier A, Dubois B, et al. Amyloidosis and neurodegeneration result in distinct structural connectivity patterns in mild cognitive impairment. Neurobiol Aging 2017;55:177–89.
[54] Dyrba M, Grothe MJ, Mohammadi A, Binder H, Kirste T, Teipel SJ. Comparison of Different Hypotheses Regarding the Spread of Alzheimer's Disease Using Markov Random Fields and Multimodal Imaging. J Alzheimer's Dis 2017:1–16.
[55] Hardy J. Alzheimer's disease: the amyloid cascade hypothesis: an update and reappraisal. J Alzheimer's Dis : JAD 2006;9:151–3.
[56] Hardy J, Selkoe DJ. The amyloid hypothesis of Alzheimer's disease: progress and problems on the road to therapeutics. Science 2002; 297:353–6.
[57] Braak H, Zetterberg H, Del Tredici K, Blennow K. Intraneuronal tau aggregation precedes diffuse plaque deposition, but amyloid-beta changes occur before increases of tau in cerebrospinal fluid. Acta Neuropathologica 2013;126:631–41.
[58] Tosun D, Landau S, Aisen PS, Petersen RC, Mintun M, Jagust W, et al. Association between tau deposition and antecedent amyloid-beta accumulation rates in normal and early symptomatic individuals. Brain 2017;140:1499–512.
[59] Andriuta D, Moullart V, Schraen S, Devendeville A, Meyer ME, Godefroy O, et al. What are the Most Frequently Impaired Markers of Neurodegeneration in ADNI Subjects? J Alzheimers Dis 2016; 51:793–800.
[60] Pascoal TA, Mathotaarachchi S, Mohades S, Benedet AL, Chung CO, Shin M, et al. Amyloid-β and hyperphosphorylated tau synergy drives metabolic decline in preclinical Alzheimer's disease. Mol Psychiatry 2016;22:306.
[61] Pascoal TA, Mathotaarachchi S, Shin M, Benedet AL, Mohades S, Wang S, et al. Synergistic interaction between amyloid and tau predicts the progression to dementia. Alzheimers Dement 2017; 13:644–53.
[62] Maass A, Landau S, Baker SL, Horng A, Lockhart SN, La Joie R, et al. Comparison of multiple tau-PET measures as biomarkers in aging and Alzheimer's disease. Neuroimage 2017;157:448–63.
[63] Ower AK, Hadjichrysanthou C, Gras L, Goudsmit J, Anderson RM, de Wolf F, et al. Temporal association patterns and dynamics of amyloid-beta and tau in Alzheimer's disease. Eur J Epidemiol 2017:1–10.
[64] Hansson O, Grothe MJ, Strandberg TO, Ohlsson T, Hagerstrom D, Jogi J, et al. Tau Pathology Distribution in Alzheimer's disease Corresponds Differentially to Cognition-Relevant Functional Brain Networks. Front Neurosci 2017;11:167.
[65] Coutu JP, Lindemer ER, Konukoglu E, Salat DHAlzheimer's Disease Neuroimaging I. Two distinct classes of degenerative change are independently linked to clinical progression in mild cognitive impairment. Neurobiol Aging 2017;54:1–9.
[66] Tchistiakova E, MacIntosh BJAlzheimer's Disease Neuroimaging I. Summative effects of vascular risk factors on cortical thickness in mild cognitive impairment. Neurobiol Aging 2016;45:98–106.
[67] Scott JA, Braskie MN, Tosun D, Maillard P, Thompson PM, Weiner M, et al. Cerebral amyloid is associated with greater white-matter hyperintensity accrual in cognitively normal older adults. Neurobiol Aging 2016;48:48–52.
[68] Kandel BM, Avants BB, Gee JC, McMillan CT, Erus G, Doshi J, et al. White matter hyperintensities are more highly associated with preclinical Alzheimer's disease than imaging and cognitive markers of neurodegeneration. Alzheimers Dement (Amst) 2016;4:18–27.
[69] Fiford CM, Manning EN, Bartlett JW, Cash DM, Malone IB, Ridgway GR, et al. White matter hyperintensities are associated with disproportionate progressive hippocampal atrophy. Hippocampus 2017;27:249–62.
[70] Taylor ANW, Kambeitz-Ilankovic L, Gesierich B, Simon-Vermot L, Franzmeier N, Araque Caballero MA, et al. Tract-specific white matter hyperintensities disrupt neural network function in Alzheimer's disease. Alzheimers Dement 2017;13:225–35.

[71] Weller RO, Hawkes CA, Kalaria RN, Werring DJ, Carare RO. White matter changes in dementia: role of impaired drainage of interstitial fluid. Brain Pathol 2015;25:63–78.
[72] Marnane M, Al-Jawadi OO, Mortazavi S, Pogorzelec KJ, Wang BW, Feldman HH, et al. Periventricular hyperintensities are associated with elevated cerebral amyloid. Neurology 2016;86:535–43.
[73] Todd KL, Brighton T, Norton ES, Schick S, Elkins W, Pletnikova O, et al. Ventricular and Periventricular Anomalies in the Aging and Cognitively Impaired Brain. Front Aging Neurosci 2017;9:445.
[74] Ighodaro ET, Abner EL, Fardo DW, Lin AL, Katsumata Y, Schmitt FA, et al. Risk factors and global cognitive status related to brain arteriolosclerosis in elderly individuals. J Cereb Blood Flow Metab 2017;37:201–16.
[75] Girard H, Potvin O, Nugent S, Dallaire-Theroux C, Cunnane S, Duchesne S, et al. Faster progression from MCI to probable AD for carriers of a single-nucleotide polymorphism associated with type 2 diabetes. Neurobiol Aging 2018;64:157.e11–157.e17.
[76] Traylor M, Adib-Samii P, Harold D, Dichgans M, Williams J, Lewis CM, et al. Shared genetic contribution to ischemic stroke and Alzheimer's disease. Ann Neurol 2016;79:739–47.
[77] An H, Choi B, Son SJ, Cho EY, Kim SO, Cho S, et al. Renal function affects hippocampal volume and cognition: The role of vascular burden and amyloid deposition. Geriatr Gerontol Int 2017; 17:1899–906.
[78] Zlokovic BV. Neurovascular pathways to neurodegeneration in Alzheimer's disease and other disorders. Nat Rev Neurosci 2011; 12:723–38.
[79] Moran C, Beare R, Phan TG, Bruce DG, Callisaya ML, Srikanth V, et al. Type 2 diabetes mellitus and biomarkers of neurodegeneration. Neurology 2015;85:1123–30.
[80] Toledo JB, Da X, Bhatt P, Wolk DA, Arnold SE, Shaw LM, et al. Relationship between plasma analytes and SPARE-AD defined brain atrophy patterns in ADNI. PloS One 2013;8:e55531.
[81] Christopher L, Napolioni V, Khan RR, Han SS, Greicius MDAlzheimer's Disease Neuroimaging I. A variant in PPP4R3A protects against alzheimer-related metabolic decline. Ann Neurol 2017;82:900–11.
[82] Chiang GC, Chang E, Pandya S, Kuceyeski A, Hu J, Isaacson R, et al. Cognitive deficits in non-demented diabetic elderly appear independent of brain amyloidosis. J Neurol Sci 2017;372:85–91.
[83] Lane EM, Hohman TJ, Jefferson AL. Alzheimer's Disease Neuroimaging I. Insulin-like growth factor binding protein-2 interactions with Alzheimer's disease biomarkers. Brain Imaging Behav 2017; 11:1779–86.
[84] Li W, Risacher SL, Huang E, Saykin AJ. Alzheimer's Disease Neuroimaging I. Type 2 diabetes mellitus is associated with brain atrophy and hypometabolism in the ADNI cohort. Neurology 2016; 87:595–600.
[85] Huang Y. Abeta-independent roles of apolipoprotein E4 in the pathogenesis of Alzheimer's disease. Trends Molecular Medicine 2010; 16:287–94.
[86] Kanekiyo T, Xu H, Bu G. ApoE and Abeta in Alzheimer's disease: accidental encounters or partners? Neuron 2014;81:740–54.
[87] Bozoki AC, Zdanukiewicz M, Zhu DCAlzheimer's Disease Neuroimaging I. The effect of beta-amyloid positivity on cerebral metabolism in cognitively normal seniors. Alzheimers Dement 2016; 12:1250–8.
[88] Seo H, Kim SH, Park H, Kang S-H, Choo IL. Topographical APOE ε4 Genotype Influence on Cerebral Metabolism in the Continuum of Alzheimer's Disease: Amyloid Burden Adjusted Analysis. J Alzheimer's Dis 2016;54:559–68.
[89] Seo EH, Kim SH, Park SH, Kang SH, Choo IH, Alzheimer's Disease Neuroimaging I. Independent and Interactive Influences of the APOE Genotype and Beta-Amyloid Burden on Cognitive Function in Mild Cognitive Impairment. J Korean Med Sci 2016;31:286–95.
[90] Li C, Loewenstein DA, Duara R, Cabrerizo M, Barker W, Adjouadi M, et al. The Relationship of Brain Amyloid Load and APOE Status to Regional Cortical Thinning and Cognition in the ADNI Cohort. J Alzheimers Dis 2017;59:1269–82.
[91] Sudre CH, Cardoso MJ, Frost C, Barnes J, Barkhof F, Fox N, et al. APOE ε4 status is associated with white matter hyperintensities volume accumulation rate independent of AD diagnosis. Neurobiol Aging 2017;53:67–75.
[92] Luo X, Jiaerken Y, Yu X, Huang P, Qiu T, Jia Y, et al. Affect of APOE on information processing speed in non-demented elderly population: a preliminary structural MRI study. Brain Imaging Behav 2017;11:977–85.
[93] Luo X, Jiaerken Y, Yu X, Huang P, Qiu T, Jia Y, et al. Associations between APOE genotype and cerebral small-vessel disease: a longitudinal study. Oncotarget 2017;8:44477–89.
[94] Heneka MT, Carson MJ, El Khoury J, Landreth GE, Brosseron F, Feinstein DL, et al. Neuroinflammation in Alzheimer's disease. Lancet Neurol 2015;14:388–405.
[95] Peng Q, Schork A, Bartsch H, Lo MT, Panizzon MS, Pediatric Imaging N, et al. Conservation of Distinct Genetically-Mediated Human Cortical Pattern. PLos Genet 2016;12:e1006143.
[96] Zhang DF, Li J, Wu H, Cui Y, Bi R, Zhou HJ, et al. CFH Variants Affect Structural and Functional Brain Changes and Genetic Risk of Alzheimer's Disease. Neuropsychopharmacology 2016; 41:1034–45.
[97] Deming Y, Xia J, Cai Y, Lord J, Holmans P, Bertelsen S, et al. A potential endophenotype for Alzheimer's disease: cerebrospinal fluid clusterin. Neurobiol Aging 2016;37:208.e1–208.e9.
[98] Varma VR, Varma S, An Y, Hohman TJ, Seddighi S, Casanova R, et al. Alpha-2 macroglobulin in Alzheimer's disease: a marker of neuronal injury through the RCAN1 pathway. Mol Psychiatry 2017;22:13–23.
[99] Bonham LW, Desikan RS, Yokoyama JS. The relationship between complement factor C3, APOE ε4, amyloid and tau in Alzheimer's disease. Acta neuropathologica Commun 2016;4:65.
[100] Landau SM, Horng A, Fero A, Jagust WJ. Alzheimer's Disease Neuroimaging I. Amyloid negativity in patients with clinically diagnosed Alzheimer disease and MCI. Neurology 2016;86:1377–85.
[101] Jack CR Jr, Knopman DS, Chetelat G, Dickson D, Fagan AM, Frisoni GB, et al. Suspected non-Alzheimer disease pathophysiology–concept and controversy. Nat Rev Neurol 2016;12:117–24.
[102] Mattsson N, Insel PS, Palmqvist S, Portelius E, Zetterberg H, Weiner M, et al. Cerebrospinal fluid tau, neurogranin, and neurofilament light in Alzheimer's disease. EMBO Mol Med 2016;8:1184–96.
[103] Rasero J, Alonso-Montes C, Diez I, Olabarrieta-Landa L, Remaki L, Escudero I, et al. Group-Level Progressive Alterations in Brain Connectivity Patterns Revealed by Diffusion-Tensor Brain Networks across Severity Stages in Alzheimer's Disease. Front Aging Neurosci 2017;9:215.
[104] Qiu T, Luo X, Shen Z, Huang P, Xu X, Zhou J, et al. Disrupted Brain Network in Progressive Mild Cognitive Impairment Measured by Eigenvector Centrality Mapping is Linked to Cognition and Cerebrospinal Fluid Biomarkers. J Alzheimers Dis 2016;54:1483–93.
[105] Mayo CD, Mazerolle EL, Ritchie L, Fisk JD, Gawryluk JRAlzheimer's Disease Neuroimaging I. Longitudinal changes in microstructural white matter metrics in Alzheimer's disease. Neuroimage Clin 2017;13:330–8.
[106] Pereira JB, Mijalkov M, Kakaei E, Mecocci P, Vellas B, Tsolaki M, et al. Disrupted Network Topology in Patients with Stable and Progressive Mild Cognitive Impairment and Alzheimer's Disease. Cereb Cortex 2016;26:3476–93.
[107] Kim HJ, Shin JH, Han CE, Kim HJ, Na DL, Seo SW, et al. Using Individualized Brain Network for Analyzing Structural Covariance of the Cerebral Cortex in Alzheimer's Patients. Front Neurosci 2016; 10:394.
[108] Rasero J, Amoroso N, La Rocca M, Tangaro S, Bellotti R, Stramaglia S, et al. Multivariate regression analysis of structural MRI connectivity matrices in Alzheimer's disease. PLoS One 2017;12:e0187281.

[109] Association As. Alzheimer's disease facts and figures 2018, https://wwwalzorg/facts/#prevalence/2018 2018. Accessed 3/21/18.
[110] Spampinato MV, Langdon BR, Patrick KE, Parker RO, Collins H, Pravata E, et al. Gender, apolipoprotein E genotype, and mesial temporal atrophy: 2-year follow-up in patients with stable mild cognitive impairment and with progression from mild cognitive impairment to Alzheimer's disease. Neuroradiology 2016;58:1143–51.
[111] Caldwell JZK, Berg JL, Cummings JL, Banks SJ, AsDN Initiative. Moderating effects of sex on the impact of diagnosis and amyloid positivity on verbal memory and hippocampal volume. Alzheimer's Res Ther 2017;9:72–82.
[112] Cacciottolo M, Christensen A, Moser A, Liu J, Pike CJ, Smith C, et al. The APOE4 allele shows opposite sex bias in microbleeds and Alzheimer's disease of humans and mice. Neurobiol Aging 2016;37:47–57.
[113] Li GD, Bi R, Zhang DF, Xu M, Luo R, Wang D, et al. Female-specific effect of the BDNF gene on Alzheimer's disease. Neurobiol Aging 2017;53:192 e11–e19.
[114] Zhao Q, Shen Y, Zhao Y, Si L, Jiang S, Qiu Y, et al. Val66Met Polymorphism in BDNF Has No Sexual and APOE ε4 Status-Based Dimorphic Effects on Susceptibility to Alzheimer's Disease: Evidence From an Updated Meta-Analysis of Case–Control Studies and High-Throughput Genotyping Cohorts. Am J Alzheimer's Dis Other Demen 2017;33:55–63.
[115] David ND, Lin F, Porsteinsson AP, Alzheimer's Disease Neuroimaging I. Trajectories of Neuropsychiatric Symptoms and Cognitive Decline in Mild Cognitive Impairment. Am J Geriatr Psychiatry 2016;24:70–80.
[116] Bensamoun D, Guignard R, Furst AJ, Derreumaux A, Manera V, Darcourt J, et al. Associations between Neuropsychiatric Symptoms and Cerebral Amyloid Deposition in Cognitively Impaired Elderly People. J Alzheimers Dis 2016;49:387–398.
[117] Ng KP, Pascoal TA, Mathotaarachchi S, Chung CO, Benedet AL, Shin M, et al. Neuropsychiatric symptoms predict hypometabolism in preclinical Alzheimer disease. Neurology 2017;88:1814–1821.
[118] Gatchel JR, Donovan J, Locascio J, Becker JA, Rentz M, Sperling A, et al. Regional 18F-Fluorodeoxyglucose Hypometabolism is Associated with Higher Apathy Scores Over Time in Early Alzheimer's Disease. Am J Geriatr Psychiatry 2017;25:683–693.
[119] Brendel M, Reinisch V, Kalinowski E, Levin J, Delker A, Därr S, et al. Hypometabolism in Brain of Cognitively Normal Patients with Depressive Symptoms is Accompanied by Atrophy-Related Partial Volume Effects. Curr Alzheimer Res 2016;13:475–486.
[120] Finger E, Zhang J, Dickerson B, Bureau Y, Masellis M. Disinhibition in Alzheimer's Disease is Associated with Reduced Right Frontal Pole Cortical Thickness. J Alzheimer's Dis 2017;60:1161–1170.
[121] Fischer CE, Ting WK, Millikin CP, Ismail Z, Schweizer TA, Alzheimer Disease Neuroimaging I. Gray matter atrophy in patients with mild cognitive impairment/Alzheimer's disease over the course of developing delusions. Int J Geriatr Psychiatry 2016;31:76–82.
[122] Huey ED, Lee S, Cheran G, Grafman J, Devanand DP, Alzheimer's Disease Neuroimaging I. Brain Regions Involved in Arousal and Reward Processing are Associated with Apathy in Alzheimer's Disease and Frontotemporal Dementia. J Alzheimers Dis 2017;55:551–558.
[123] Hohman TJ, McLaren DG, Mormino EC, Gifford KA, Libon DJ, Jefferson AL, et al. Asymptomatic Alzheimer disease: Defining resilience. Neurology 2016;87:2443–2450.
[124] Franzmeier N, Duering M, Weiner M, Dichgans M, Ewers MAlzheimer's Disease Neuroimaging I. Left frontal cortex connectivity underlies cognitive reserve in prodromal Alzheimer disease. Neurology 2017;88:1054–1061.
[125] Lin F, Ren P, Mapstone M, Meyers SP, Porsteinsson A, Baran TM, et al. The cingulate cortex of older adults with excellent memory capacity. Cortex 2017;86:83–92.
[126] Hohman TJ, Dumitrescu L, Cox NJ, Jefferson ALAlzheimer's Neuroimaging I. Genetic resilience to amyloid related cognitive decline. Brain Imaging Behav 2017;11:401–409.
[127] Felsky D, Xu J, Chibnik LB, Schneider JA, Knight J, Kennedy JL, et al. Genetic epistasis regulates amyloid deposition in resilient aging. Alzheimers Dement 2017;13:1107–1116.
[128] Malpetti M, Ballarini T, Presotto L, Garibotto V, Tettamanti M, Perani D, et al. Gender differences in healthy aging and Alzheimer's Dementia: A (18) F-FDG-PET study of brain and cognitive reserve. Hum Brain Mapp 2017;38:4212–4227.
[129] Sundermann EE, Biegon A, Rubin LH, Lipton RB, Mowrey W, Landau S, et al. Better verbal memory in women than men in MCI despite similar levels of hippocampal atrophy. Neurology 2016;86:1368–1376.
[130] Sundermann EE, Maki PM, Rubin LH, Lipton RB, Landau S, Biegon A, et al. Female advantage in verbal memory: Evidence of sex-specific cognitive reserve. Neurology 2016;87:1916–1924.
[131] Sundermann EE, Biegon A, Rubin LH, Lipton RB, Landau S, Maki PM, et al. Does the Female Advantage in Verbal Memory Contribute to Underestimating Alzheimer's Disease Pathology in Women versus Men? J Alzheimers Dis 2017;56:947–957.
[132] Ferreira D, Hansson O, Barroso J, Molina Y, Machado A, Hernandez-Cabrera JA, et al. The interactive effect of demographic and clinical factors on hippocampal volume: A multicohort study on 1958 cognitively normal individuals. Hippocampus 2017;27:653–667.
[133] Potvin O, Mouiha A, Dieumegarde L, Duchesne SAlzheimer's Disease Neuroimaging I. Normative data for subcortical regional volumes over the lifetime of the adult human brain. Neuroimage 2016;137:9–20.
[134] Thompson PM, Andreassen OA, Arias-Vasquez A, Bearden CE, Boedhoe PS, Brouwer RM, et al. ENIGMA and the individual: Predicting factors that affect the brain in 35 countries worldwide. Neuroimage 2017;145:389–408.
[135] Zandifar A, Fonov V, Coupe P, Pruessner J, Collins DLAlzheimer's Disease Neuroimaging I. A comparison of accurate automatic hippocampal segmentation methods. Neuroimage 2017;155:383–393.
[136] Bocchetta M, Boccardi M, Ganzola R, Apostolova LG, Preboske G, Wolf D, et al. Harmonized benchmark labels of the hippocampus on magnetic resonance: The EADC-ADNI project. Alzheimer's & dementia. J Alzheimer's Assoc 2015;11:151–160.e5.
[137] Sankar T, Park MTM, Jawa T, Patel R, Bhagwat N, Voineskos AN, et al. Your algorithm might think the hippocampus grows in Alzheimer's disease: Caveats of longitudinal automated hippocampal volumetry. Hum Brain Mapp 2017;38:2875–2896.
[138] Blanken AH, Hurtz S, Zarow C, Biado K, Honarpisheh H, Somme J, et al. Associations between hippocampal morphometry and neuropathologic markers of Alzheimer's disease using 7T MRI. NeuroImage: Clin 2017;15:56–61.
[139] Wolk DA, Das SR, Mueller SG, Weiner MW, Yushkevich PA, Alzheimer's Disease Neuroimaging I. Medial temporal lobe subregional morphometry using high resolution MRI in Alzheimer's disease. Neurobiol Aging 2017;49:204–213.
[140] Braak H, Braak E. Neuropathological stageing of Alzheimer-related changes. Acta Neuropathologica 1991;82:239–259.
[141] Hibar DP, Adams HHH, Jahanshad N, Chauhan G, Stein JL, Hofer E, et al. Novel genetic loci associated with hippocampal volume. Nat Commun 2017;8:13624.
[142] Horgusluoglu-Moloch E, Nho K, Risacher SL, Kim S, Foroud T, Shaw LM, et al. Targeted neurogenesis pathway-based gene analysis identifies ADORA2A associated with hippocampal volume in mild cognitive impairment and Alzheimer's disease. Neurobiol Aging 2017;60:92–103.
[143] Li B, Shi J, Gutman BA, Baxter LC, Thompson PM, Caselli RJ, et al. Influence of APOE Genotype on Hippocampal Atrophy over Time - An N=1925 Surface-Based ADNI Study. PLoS One 2016;11:e0152901.
[144] Si B, Yakushev I, Li JInitiative AsDN. A Sequential Tree-based Classifier for Personalized Biomarker Testing of Alzheimer's Disease Risk. IISE Trans Healthc Syst Eng 2017;4:248–260.
[145] Lange C, Suppa P, Pietrzyk U, Makowski MR, Spies L, Peters O, et al. Prediction of Alzheimer's Dementia in Patients with Amnestic Mild Cognitive Impairment in Clinical Routine: Incremental Value of

Biomarkers of Neurodegeneration and Brain Amyloidosis Added Stepwise to Cognitive Status. J Alzheimers Dis 2018;61:373–388.
[146] DeMarshall CA, Nagele EP, Sarkar A, Acharya NK, Godsey G, Goldwaser EL, et al. Detection of Alzheimer's disease at mild cognitive impairment and disease progression using autoantibodies as blood-based biomarkers. Alzheimer's & Dementia: Diagnosis. Assess Dis Monit 2016;3:51–62.
[147] Jammeh E, Zhao P, Carroll C, Pearson S, Ifeachor E. Identification of blood biomarkers for use in point of care diagnosis tool for Alzheimer's disease. Conf Proc IEEE Eng Med Biol Soc 2016; 2016:2415–2418.
[148] Zhou W, Zhang J, Ye F, Xu G, Su H, Su Y, et al. Plasma neurofilament light chain levels in Alzheimer's disease. Neurosci Lett 2017; 650:60–64.
[149] McLimans KE, Willette AAAlzheimer's Disease Neuroimaging I. Autotaxin is Related to Metabolic Dysfunction and Predicts Alzheimer's Disease Outcomes. J Alzheimers Dis 2017;56:403–413.
[150] St John-Williams L, Blach C, Toledo JB, Rotroff DM, Kim S, Klavins K, et al. Targeted metabolomics and medication classification data from participants in the ADNI1 cohort. Scientific Data 2017;4:170140.
[151] Insel PS, Palmqvist S, Mackin RS, Nosheny RL, Hansson O, Weiner MW, et al. Assessing risk for preclinical beta-amyloid pathology with APOE, cognitive, and demographic information. Alzheimers Dement (Amst) 2016;4:76–84.
[152] Tosun D, Chen YF, Yu P, Sundell KL, Suhy J, Siemers E, et al. Amyloid status imputed from a multimodal classifier including structural MRI distinguishes progressors from nonprogressors in a mild Alzheimer's disease clinical trial cohort. Alzheimers Dement 2016; 12:977–986.
[153] Voyle N, Kim M, Proitsi P, Ashton NJ, Baird AL, Bazenet C, et al. Blood metabolite markers of neocortical amyloid-β burden: discovery and enrichment using candidate proteins. Translational Psychiatry 2016;6:e719.
[154] Sperling RA, Aisen PS, Beckett LA, Bennett DA, Craft S, Fagan AM, et al. Toward defining the preclinical stages of Alzheimer's disease: Recommendations from the National Institute on Aging-Alzheimer's Association workgroups on diagnostic guidelines for Alzheimer's disease. Alzheimer's Demen : J Alzheimer's Assoc 2011;7:280–292.
[155] Albert MS, Dekosky ST, Dickson D, Dubois B, Feldman HH, Fox NC, et al. The diagnosis of mild cognitive impairment due to Alzheimer's disease: Recommendations from the National Institute on Aging-Alzheimer's Association workgroups on diagnostic guidelines for Alzheimer's disease. Alzheimer's Demen : J Alzheimer's Assoc 2011;7:270–279.
[156] Dubois B, Feldman HH, Jacova C, Hampel H, Molinuevo JL, Blennow K, et al. Advancing research diagnostic criteria for Alzheimer's disease: the IWG-2 criteria. The Lancet Neurol 2014; 13:614–629.
[157] Vos SJ, Verhey F, Frolich L, Kornhuber J, Wiltfang J, Maier W, et al. Prevalence and prognosis of Alzheimer's disease at the mild cognitive impairment stage. Brain 2015;138:1327–1338.
[158] Alexopoulos P, Werle L, Roesler J, Thierjung N, Gleixner LS, Yakushev I, et al. Conflicting cerebrospinal fluid biomarkers and progression to dementia due to Alzheimer's disease. Alzheimer's Res Ther 2016;8:51.
[159] Wang HF, Tan L, Cao L, Zhu XC, Jiang T, Tan MS, et al. Application of the IWG-2 Diagnostic Criteria for Alzheimer's Disease to the ADNI. J Alzheimers Dis 2016;51:227–236.
[160] Jack CR Jr, Bennett DA, Blennow K, Carrillo MC, Dunn B, Haeberlein SB, et al. NIA-AA Research Framework: Toward a biological definition of Alzheimer's disease. Alzheimer's Demen : J Alzheimer's Assoc 2018;14:535–562.
[161] Lewczuk P, Kornhuber J, Toledo JB, Trojanowski JQ, Knapik-Czajka M, Peters O, et al. Validation of the Erlangen Score Algorithm for the Prediction of the Development of Dementia due to Alzheimer's Disease in Pre-Dementia Subjects. J Alzheimer's Dis: JAD 2015;48:433–441.
[162] Jack CR Jr, Bennett DA, Blennow K, Carrillo MC, Feldman HH, Frisoni GB, et al. A/T/N: An unbiased descriptive classification scheme for Alzheimer disease biomarkers. Neurology 2016; 87:539–547.
[163] Pegueroles J, Vilaplana E, Montal V, Sampedro F, Alcolea D, Carmona-Iragui M, et al. Longitudinal brain structural changes in preclinical Alzheimer's disease. Alzheimers Dement 2017;13:499–509.
[164] Edmonds EC, Bangen KJ, Delano-Wood L, Nation DA, Furst AJ, Salmon DP, et al. Patterns of Cortical and Subcortical Amyloid Burden across Stages of Preclinical Alzheimer's Disease. J Int Neuropsychological Soc : JINS 2016;22:978–990.
[165] Grothe MJ, Barthel H, Sepulcre J, Dyrba M, Sabri O, Teipel SJ, et al. In vivo staging of regional amyloid deposition. Neurology 2017; 89:2031–2038.
[166] Wachinger C, Salat DH, Weiner M, Reuter MAlzheimer's Disease Neuroimaging I. Whole-brain analysis reveals increased neuroanatomical asymmetries in dementia for hippocampus and amygdala. Brain 2016;139:3253–3266.
[167] Kruggel F, Masaki F, Solodkin AAlzheimer's Disease Neuroimaging I. Analysis of longitudinal diffusion-weighted images in healthy and pathological aging: An ADNI study. J Neurosci Methods 2017; 278:101–115.
[168] Lutz MW, Sundseth SS, Burns DK, Saunders AM, Hayden KM, Burke JR, et al. A Genetics-based Biomarker Risk Algorithm for Predicting Risk of Alzheimer's Disease. Alzheimer's Dementia (New York, N Y) 2016;2:30–44.
[169] Gamberger D, Lavrac N, Srivatsa S, Tanzi RE, Doraiswamy PM. Identification of clusters of rapid and slow decliners among subjects at risk for Alzheimer's disease. Sci Rep 2017;7:6763.
[170] Jones DT, Knopman DS, Gunter JL, Graff-Radford J, Vemuri P, Boeve BF, et al. Cascading network failure across the Alzheimer's disease spectrum. Brain 2016;139:547–562.
[171] Wiepert DA, Lowe VJ, Knopman DS, Boeve BF, Graff-Radford J, Petersen RC, et al. A robust biomarker of large-scale network failure in Alzheimer's disease. Alzheimers Dement (Amst) 2017;6:152–161.
[172] van Maurik IS, Zwan MD, Tijms BM, Bouwman FH, Teunissen CE, Scheltens P, et al. Interpreting Biomarker Results in Individual Patients With Mild Cognitive Impairment in the Alzheimer's Biomarkers in Daily Practice (ABIDE) Project. JAMA Neurol 2017; 74:1481–1491.
[173] Petersen RC, Thomas RG, Aisen PS, Mohs RC, Carrillo MC, Albert MS, et al. Randomized controlled trials in mild cognitive impairment: Sources of variability. Neurology 2017;88:1751–1758.
[174] Wolz R, Schwarz AJ, Gray KR, Yu P, Hill DL, Alzheimer's Disease Neuroimaging I. Enrichment of clinical trials in MCI due to AD using markers of amyloid and neurodegeneration. Neurology 2016; 87:1235–1241.
[175] Wang J, Logovinsky V, Hendrix SB, Stanworth SH, Perdomo C, Xu L, et al. ADCOMS: a composite clinical outcome for prodromal Alzheimer's disease trials. J Neurol Neurosurg Psychiatry 2016; 87:993–999.
[176] Insel PS, Donohue MC, Mackin RS, Aisen PS, Hansson O, Weiner MW, et al. Cognitive and functional changes associated with Aβ pathology and the progression to mild cognitive impairment. Neurobiol Aging 2016;48:172–181.
[177] Edwards JD, Ramirez J, Callahan BL, Tobe SW, Oh P, Berezuk C, et al. Antihypertensive Treatment is associated with MRI-Derived Markers of Neurodegeneration and Impaired Cognition: A Propensity-Weighted Cohort Study. J Alzheimer's Dis 2017; 59:1113–1122.
[178] Elman JA, Madison CM, Baker SL, Vogel JW, Marks SM, Crowley S, et al. Effects of Beta-Amyloid on Resting State Functional Connectivity Within and Between Networks Reflect Known Patterns of Regional Vulnerability. Cereb Cortex 2016;26:695–707.

[179] Zhao QF, Wan Y, Wang HF, Sun FR, Hao XK, Tan MS, et al. ABCA7 Genotypes Confer Alzheimer's Disease Risk by Modulating Amyloid-beta Pathology. J Alzheimers Dis 2016;52:693–703.
[180] Wang HF, Wan Y, Hao XK, Cao L, Zhu XC, Jiang T, et al. Bridging Integrator 1 (BIN1) Genotypes Mediate Alzheimer's Disease Risk by Altering Neuronal Degeneration. J Alzheimers Dis 2016; 52:179–190.
[181] Li J-Q, Wang H-F, Zhu X-C, Sun F-R, Tan M-S, Tan C-C, et al. GWAS-linked loci and neuroimaging measures in Alzheimer's disease. Mol Neurobiol 2017;54:146–153.
[182] Wang WY, Liu Y, Wang HF, Tan L, Sun FR, Tan MS, et al. Impacts of CD33 Genetic Variations on the Atrophy Rates of Hippocampus and Parahippocampal Gyrus in Normal Aging and Mild Cognitive Impairment. Mol Neurobiol 2017;54:1111–1118.
[183] Zhu XC, Wang HF, Jiang T, Lu H, Tan MS, Tan CC, et al. Effect of CR1 Genetic Variants on Cerebrospinal Fluid and Neuroimaging Biomarkers in Healthy, Mild Cognitive Impairment and Alzheimer's Disease Cohorts. Mol Neurobiol 2017;54:551–562.
[184] Wang ZX, Wang HF, Tan L, Sun FR, Tan MS, Tan CC, et al. HLA-A2 Alleles Mediate Alzheimer's Disease by Altering Hippocampal Volume. Mol Neurobiol 2017;54:2469–2476.
[185] Wang ZX, Wang HF, Tan L, Liu J, Wan Y, Sun FR, et al. Effects of HLA-DRB1/DQB1 Genetic Variants on Neuroimaging in Healthy, Mild Cognitive Impairment, and Alzheimer's Disease Cohorts. Mol Neurobiol 2017;54:3181–3188.
[186] Wang ZX, Wan Y, Tan L, Liu J, Wang HF, Sun FR, et al. Genetic Association of HLA Gene Variants with MRI Brain Structure in Alzheimer's Disease. Mol Neurobiol 2017; 54:3195–3204.
[187] Cao L, Wang HF, Tan L, Sun FR, Tan MS, Tan CC, et al. Effect of HMGCR genetic variation on neuroimaging biomarkers in healthy, mild cognitive impairment and Alzheimer's disease cohorts. Oncotarget 2016;7:13319–13327.
[188] Haddick PC, Larson JL, Rathore N, Bhangale TR, Phung QT, Srinivasan K, et al. A Common Variant of IL-6R is Associated with Elevated IL-6 Pathway Activity in Alzheimer's Disease Brains. J Alzheimers Dis 2017;56:1037–1054.
[189] Ma J, Zhang W, Tan L, Wang HF, Wan Y, Sun FR, et al. MS4A6A genotypes are associated with the atrophy rates of Alzheimer's disease related brain structures. Oncotarget 2016;7:58779–58788.
[190] Yang X, Li J, Liu B, Li Y, Jiang T. Impact of PICALM and CLU on hippocampal degeneration. Hum Brain Mapp 2016; 37:2419–2430.
[191] Yin RH, Li J, Tan L, Wang HF, Tan MS, Yu WJ, et al. Impact of SORL1 genetic variations on MRI markers in non-demented elders. Oncotarget 2016;7:31689–31698.